Petrography and diagenesis of the Triassic and Jurassic sandstones, eastern part of the Norwegian-Danish Basin

Rikke Weibel, Mette Olivarius, Lars Henrik Nielsen, Tanni Abramovitz & Claus Kjøller

Petrography and diagenesis of the Triassic and Jurassic sandstones, eastern part of the Norwegian-Danish Basin

Rikke Weibel, Mette Olivarius, Lars Henrik Nielsen,
Tanni Abramovitz & Claus Kjøller

Summary

The most prominent clastic reservoir rocks in eastern part of the Norwegian-Danish Basin (onshore Denmark) are the Triassic-Jurassoc sediments comprising the Bunter Sandstone Formation, Skagerrak Formation, Gassum Formation and the Haldager Sand Formation. The Bunter Sandstone Formation is deposited by ephemeral streams, terminal fans or aeolian activity in an arid (hot) climate. The Skagerrak Formation comprises sediments from alluvial fans grading into braided streams. The lower part of the Skagerrak Formation is northern equivalent to the Bunter Sandstone Formation occurring mainly south of the Ringkøbing-Fyn High, whereas the upper part is contemporaneous with the Gassum Formation. The Gassum Formation and the Haldager Sand formations are deposited in fluvial, parallic and shallow marine environment under humid and vegetated conditions.

The petrography and the diagenetic evolution are investigated for each formation by the use of transmitted light (and reflected light) microscopy, scanning electron microscopy (SEM) and X-ray diffraction (XRD). The Skagerrak Formation has an immature detrital composition (lithic arkoses, arkoses and subarkoses). The Bunter Sandstone Formation is also characterised by a high feldspar content, and consists typically of arkoses and subarkoses. Some samples from the Bunter Sandstone Formation contain numerous ooids, carbonate clasts or clay intraclasts from overbank strata. The Gasssum Formation is typically subarkoses and arkoses. The feldspar abundance in the Gassum Formation varies across the basin and feldspar is relatively more abundant in the northwestern part than in the eastern part of the Danish Subbasin. The Haldager Sand Formation is characterized by quartz arenites and subordinate subarkoses and consequently the most mature sandstone of the investigated formations. The volumetrically important authigenic phases in the Bunter Sandstone Formation are carbonates (calcite and dolomite) and anhydrite. The dominating porosity reducing cements in the Skagerrak Formation are also carbonates (typically dolomite, but also calcite and ankerite) besides clays, which are typically smectite in the shallow wells, but mixed-layer illite/smectite and illite with increased burial depth. Changes in the porosity in the Gassum Formation are the result of precipitation of carbonate cement and clay minerals, quartz diagenesis and feldspar dissolution. Mechanical compaction is the major porosity reducing factor in the Haldager Sand Formation, which is due to its shallow burial. The authigenic phases are similar to those of the Gassum Formation, however their abundance is typically lower in the Haldager Sand Formation compared to the Gassum Formation.

Early diagenetic (eogenetic) changes are linked to the depositional environment and climate. Iron, liberated during alteration of unstable minerals, is precipitated as iron-oxide/hydroxides under oxidising conditions, which prevailed in the arid (hot) environments of the Bunter Sandstone Formation and main part of the Skagerrak Formation. In the humid (vegetated) deposits of the Gassum Formation and the Haldager Sand Formation, reducing conditions promote precipitation of Fe-rich phases, such as pyrite and siderite. Kaolin forms at the expense of feldspar grains, when these sediments are flushed by meteoric water. Kaolin forms locally in reduction spots in the arid (hot) deposits, whereas smectite and its transformation products, as mixed-layer illite/smectite and illite otherwise dominate these sediments. Intensive evaporation in the arid (hot) climate leads to calcrete formation and

gypsum precipitation. Gypsum transforms into anhydrite during increased burial. Anhdyrite is more abundant in the Bunter Sandstone Formation, and is probably associated with more gypsum precipitation in a more distal depositional environment closer to inlands seas compared to the proximal Skagerrak Formation.

During deeper burial the diagenetic alterations are defined by the pore fluid changes in respect to the mineral stability during increased temperature and pressure. The authigenic minerals forming at deep burial are similar for the investigated formations, though there is a high variance in the amounts of authigenic phases. Illite forms in all formations either precipitated directly or via transformations of smectite through mixed-layer illite/smectite. As the pore fluid becomes depleted in potassium, albite becomes more stable than K-feldspar and albitisation begins. Authigenic quartz forms in all investigated formations. Limited authigenic quartz is present as prismatic outgrowths where partly inhibited by iron-oxide/hydroxides or as quartz mountains at shallow burial depth. Pressure solution, stylolite formation and authigenic quartz form when the sandstones are dominated by detrital quartz despite being deposited in an arid or humid climate. Such quartz diagenesis leads to intensively cemented sandstones. Relatively late carbonate cement forms in all formations, though the chemical composition and abundance vary. Calcite is typical in the intermediately buried Bunter Sandstone Formation, whereas dolomite commonly forms in the deeper buried Skagerrak Formation. Ankerite is a characteristic pore filling cement in deposits containing organic matter (Gassum and Haldager Sand formations) and occasionally in reduced areas of the Skagerrak Formation.

The early diagenetic changes count for the main differences in the diagenetic evolution between the investigated formations. The climate and the depositional environment therefore strongly influence the alterations, and almost similar diagenetic changes occurs in the Bunter Sandstone Formation and the Skagerrak Formations; and the Haldager Sand Formation can diagentically be considered a shallow equivalent to the Gassum Formation.

Content

1. Introduction

In order to obtain a direct link between diagenesis and petrophysical logs a diagenesis study was initiated on five selected wells, from the Norwegian–Danish Basin, with coinciding cores and geophysical logs.

A general knowledge of the prevailing mineralogy and the most prominent diagnetic reactions is necessary to understand the influence of diagenesis on the seismic response and the petrophysical logs. Porosity and permeability are some of the petrophysical parameters that directly affect the log response and the acoustic impedance. When relating porosity and permeability variations to mineralogy and diagenetic changes, the porosity and permeability act as links between acoustic impedance and the detrital and authigenic mineralogical assemblage.

The majority of the deep onshore Danish wells were drilled, logged and cored during the early days of oil exploration in the 1950's, with the exception of a few new wells (1984, 2002-04 and 2010) drilled for other purposes such as exploitation of geothermal energy or natural gas storage. The major potential reservoir rocks in the eastern part of the Norwegian-Danish Basin comprise the Bunter Sandstone Formation, Skagerrak Formation, Gassum Formation and Haldager Sand Formation. The burial depths of the Skagerrak Formation vary from 600 to 5100 m and the burial depths of the Gassum Formation span from 550 to 3360 m. The differences in burial depths highlight the importance of a diagenetic understanding, as well as a mineralogical description, of these reservoir sandstones.

This report focus on the general detrital mineralogy, diagenetic evolution and porosity/permeability changes in the Triassic-Jurassic sandstones (Bunter Sandstone Formation, Skagerrak Formation, Gassum formation and Haldager Sand Formation) in the eastern part of the Norwegian-Danish Basin.

This report is one out of several contributions to the diagenesis project that has been financed by the Statoil-Hydro.

2. Geological setting

2.1 Structural setting

The Norwegian-Danish Basin is an intracratonic, Permian–Cenozoic structure that trends WNW–ESE and was formed by crustal stretching in Late Carboniferous-Early Permian times. It is bounded by shallow basement blocks of the Ringkøbing-Fyn High to the south and the stable Precambrian Baltic Shield to the north (Fig. 2.1). A fundamental tectonic feature, forming part of the basin is the 30–50 km wide and strongly block-faulted Sorgen-frei-Tornquist Zone (Fig. 2.1). The crustal extension phase was accompanied by deposition of alluvial conglomerates and sandstones and lacustrine mudstones in grabens and half-grabens during the Rootliegendes followed by regional subsidence governed by thermal cooling during the Mesozoic (Vejbæk 1989; Michelsen & Nielsen 1991, 1993). In the east-ern part of the Norwegian-Danish Basin and the Sorgenfrei-Tornquist Zone the top pre-Zechstein surface, which in many places is a pronounced unconformity defining the base of the post-rift basin-fill truncates tilted faults blocks in most of the area and is the deepest regional surface mapable by reflection seismic data. This mid Permian unconformity is overlain by a relatively complete succession of Upper Permian, Mesozoic and Cenozoic deposits that is ca. 5–6.5 km thick along the basin axis and more than 9 km locally in the Sorgenfrei-Tornquist Zone. Isocore maps of the Triassic and Jurassic–Lower Cretaceous successions show a relatively uniform regional thickness in most of the basin except for areas influenced by local faulting and halokinetic movements (Vejbæk 1989, Britze & Japsen 1991;). Thinning of the Zechstein–Lower Jurassic and Upper Jurassic–Lower Cre-taceous successions indicates a general shallowing of the basin toward the Ringkøbing-Fyn High. In early Middle Jurassic time the Ringkøbing-Fyn High, most of the Danish Basin and parts of Southern Sweden was uplifted and subjected to deep erosion. Only the Sorgenfrei-Tornquist Zone experienced slow continued subsidence. Southwest of this zone, the erosional unconformity, the "Base Middle Jurassic Unconformity" shows a pro-gressively deeper truncation toward the Ringkøbing-Fyn High where the Lower Jurassic is deeply truncated. On the high the truncation reach deep into the Triassic succession. In late Middle–early Late Jurassic time subsidence gradually took over again and became more widespread as shown by a progressively younger Upper Jurassic-Lower Cretaceous onlap to the unconformity toward the Ringkøbing-Fyn High (Michelsen et al. 2003; Nielsen 2003). During Late Cretaceous–Palaeogene times the Sorgenfrei-Tornquist Zone was characterized by inversion and erosion of the Chalk succession (Liboriussen *et al.*, 1987; Michelsen & Nielsen 1993). Substantial uplift and erosion occurred during the Neogene along the Northern and eastern basin margins (Japsen et al. 2007).
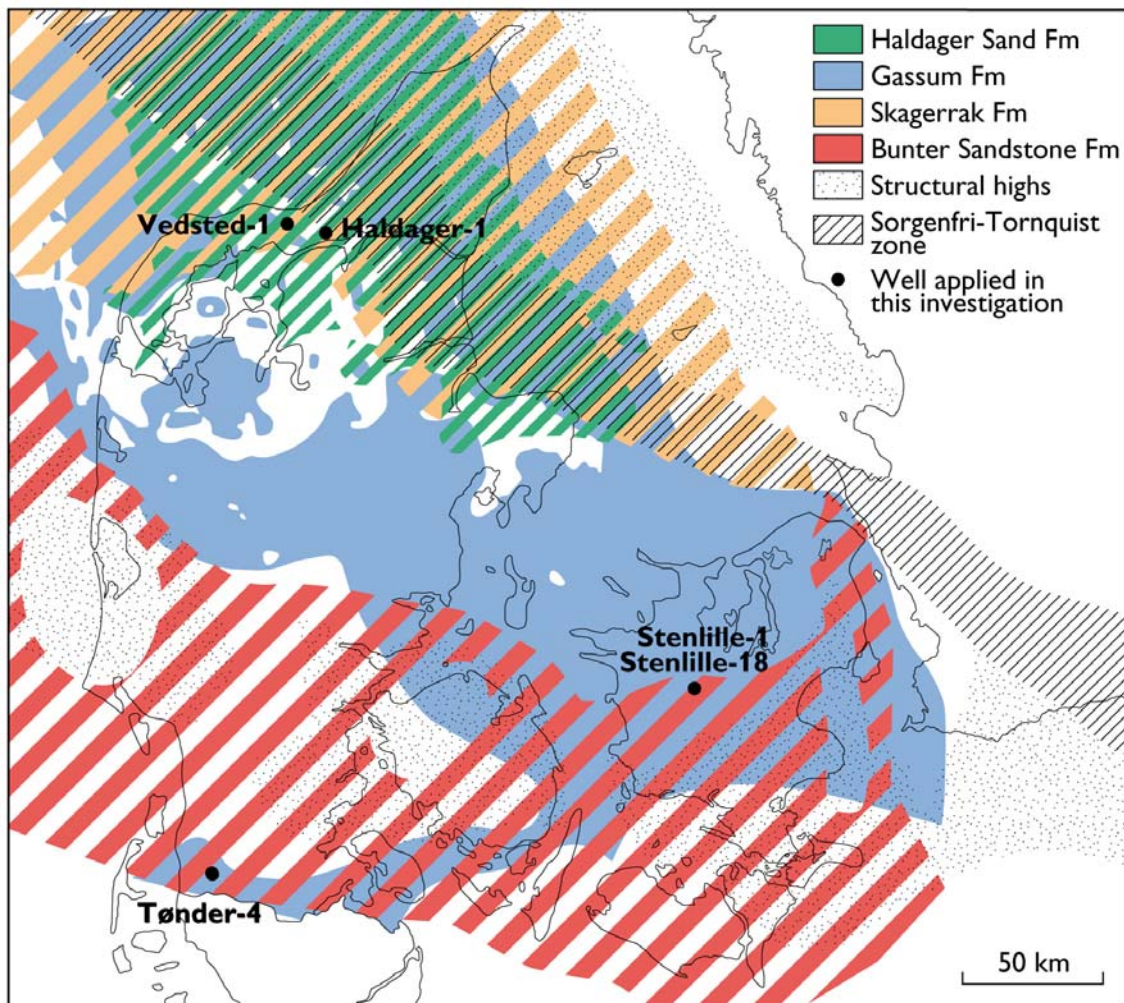
Fig. 2. 1. *Map of Denmark showing the regional extent of potential reservoir sandstones of Triassic-Jurassic age. The distribution of formations is shown for intervals thicker than 25 m and in the depth interval 800-3000 m. Modified after Anthonsen and Nielsen (2008).*

2.2 Stratigraphy and potential reservoirs

Reservoirs sandstones are found at several stratigraphic levels in the Mesozoic succession. Among these the Lower Triassic Bunter Sandstone Formation, the Triassic Skagerrak Formation, the Upper Triassic-lowermost Jurassic Gassum Formation and the Middle Jurassic Haldager Sand Formation (Fig. 2.2) constitute the principal reservoirs in the Danish part of the Norwegian-Danish Basin due to their distribution, burial depth and reservoir properties. Cores are available from the formations as they have been the target for previous hydrocarbon exploration activities. A number of samples were selected from the cores with the strategy of covering the variable petrographical composition shown by the formations. The variations cover primary differences related to source areas and depositional environments and secondary alterations caused by different diagenetic development re-

lated to different burial depths in the basin and also lithology of the embracing formations. This strategy was followed in order to obtain the best possible overview of the potential chemical reactions, which subsequently may be the target of further in-depths studies. The four formations are described below.
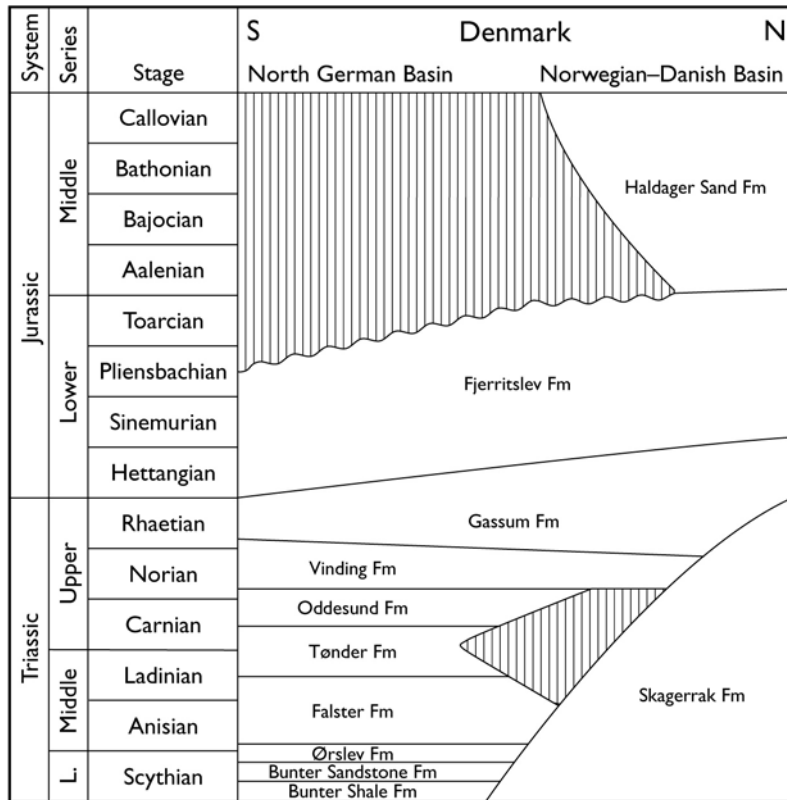

Fig. 2.2. *Stratigraphic scheme showing the Middle and Upper Jurassic formations in different sectors of the North Sea. B. Stratigraphic scheme of the Danish onshore Triassic and Jurassic sediments. Simplified after Clausen and Pedersen (1999), Michelsen and Clausen (2002) and Nielsen (2003).*

2.2.1 Bunter Sandstone Formation

The Bunter Sandstone Formation was defined by Rhys (1974) to include Lower Triassic (Scythian) sandy deposits in the Southern North Sea Basin. The formation is widely distributed in the North German Basin south of the Ringkøbing-Fyn High and on its flanks (Michelsen & Clausen 2002). Where fully developed it consists of up to 4 regional sandstone units mainly of fluvial and aeolian origin separated by thick mudstone units. The mudstone intervals are interpreted as having formed in sabkha, very shallow marine inland basin, playa-lake and lake depositional environments (Clemmensen 1979, 1985; Bertelsen 1980; Olsen 1987; Binot and Röhling 1988). The sandstone intervals have been interpreted as fluvial (Bertelsen 1980; Binot and Röhling 1988) or a mixture of ephemeral streams and

aeolian sand sheets (Clemmensen 1979, 1985; Olsen 1987). The clastic sand was primarily supplied to the basin from the Baltic Shield. The climate was arid to semi-arid with mega-monsoonal circulation, leading to strong seasonal rainfall (Clemmensen 1979). Closer toward the northern and eastern margin of the Danish part of the basin the Bunter Sandstone Formation passed into the poorly-moderately sorted, alluvial subarkosic-arkosic sandstones and mudstones of the Skagerrak Formation (Bertelsen 1980; Weibel & Friis 2004; Nielsen 2003).

2.2.2 Skagerrak Formation

The Skagerrak Formation was defined by Deegan & Scull (1977) to include the interbedded conglomerates, sandstones, siltstones and claystones that occur along the northern and north-eastern margin of the Norwegian-Danish Basin. These up to more than 2 km thick deposits are of Early–Late Triassic age and were mainly deposited as alluvial fans along the faulted basin margin. The alluvial fan deposits pass into braided river facies towards west (Pedersen & Andersen 1980; Priisholm 1983). The lower part of Skagerrak the formation is probably contemporaneous with the Bunter Sandstone Formation, while the middle part is contemporaneous with the Ørslev, Falster, Tønder and Oddesund Formations that mainly occur centrally in the basin. These formations consist primarily of marine–brackish claystones, marls, carbonates and evaporites without significant reservoir potential; only the Tønder Formation may contain sandstones with some potential. At the time of deposition of the Skagerrak Formation, the climate was arid to semi-arid (Bertelsen 1980), consistent with the occurrence of the contemporaneously evaporitic deposits.

2.2.3 Gassum Formation

The Gassum Formation was redefined by Bertelsen (1978) to include the well to moderately sorted, fine to medium-grained sandstones occurring between the restricted marine mudstones of the Upper Triassic Vinding Formation and the marine mudstones of the Lower Jurassic Fjerritslev Formation. The Gassum Formation becomes younger stepwise towards north and east, being mainly of Rhaetian age in the central parts of the basin, while it is of Rhaetian–Early Sinemurian age along the basin margin in North Jylland, Kattegat and eastern Sjælland. The Gassum Formation is widely distributed with thicknesses of 50–150 m in central and distal parts of the Danish part of the basin thickening at positions associated with salt-structures and major faults (up to 300 m in the Sorgenfrei-Tornquist Zone). On the Skagerrak-Kattegat Platform the thickness decreases (10–80 m) and is absent on most of the Ringkøbing-Fyn High due to later uplift and erosion (Nielsen & Japsen 1991).

The formation was deposited during a series of relative sea level falls and is dominated by shallow marine shoreface sandstones and fluvial-estuarine sandstones; offshore marine and lagoonal heteroliths and mudstones, and lacustrine claystones and thin coal seams constitute a significant but minor proportion of the formation (Nielsen 2003). The source area of the Gassum sand probably comprised reworked Bunter Sandstones in the southeastern part of the basin, whereas more heterogeneous bedrock to the north and east sup-

plied the sand to the northern and central parts of the basin causing a variable petrography of the formation. The formation records a general chance in climate from the dominantly arid to semi arid climate during the early–mid Triassic, which gradually became more humid during the Rhaetian as reflected in preservation of larger amounts of organic matter (Bertelsen 1978).

2.2.4 Haldager Sand Formation

The Haldager Sand Formation was redefined by Michelsen (1989) to include the Middle Jurassic sandstones occurring between marine mudstones of the Lower Jurassic Fjerritslev Formation and marine mudstones and sandstones of the Upper Jurassic Flyvbjerg and Børglum formations. The Haldager Sand Formation overlies the regional "Base Middle Jurassic Unconformity" (also termed the Mid Cimmerian Unconformity, MCU) and is thickest developed in the Sorgenfrei-Tornquist Zone, where slow subsidence prevailed during the Middle Jurassic uplift phase, that affected most of the Danish part of the basin including the Skagerrak-Kattegat Platform and parts of Skåne (Nielsen 2003). Generally, the formation consists of thick fluvial and shallow marine sandstones interbedded with thin mudstones. The sandstones are mostly medium to coarse-grained, slightly pebbly, well to moderately sorted sandstones and greywackes. The regional distribution of the formation is strongly controlled by faults and salt-structures. The formation is thin and patchy distributed in the southern and south-western part of the basin with thickness below 10 m. In the more central parts of the basin the thickness increases to 25–50 m; in the Sorgenfrei-Tornquist Zone the thickness further increases to ca. 175 m. On the Skagerrak-Kattegat Platform the formation thins to 15–30 m.

3. Samples

Mesozoic sediments onshore Denmark represent a wide spectrum of burial depths and are in this context obvious for investigations of the diagenetic evolution with burial depth. Cored intervals of the Skagerrak Formation have present day burial depth from 600 to 5100 m (Fig. 3.1). The corresponding estimated maximum burial depths are 1750 – 5900 m (with estimated errors of ± 200 m), which are corrected for Late Cretaceous to Early Palaeogene and Neogene uplift (Weibel 1999). Cored intervals of the Gassum Formation represent burial depths from 550 to 3360 m (Fig. 3.2), and 450 – 2500 m for the Haldager Sand Formation (Fig. 3.3).

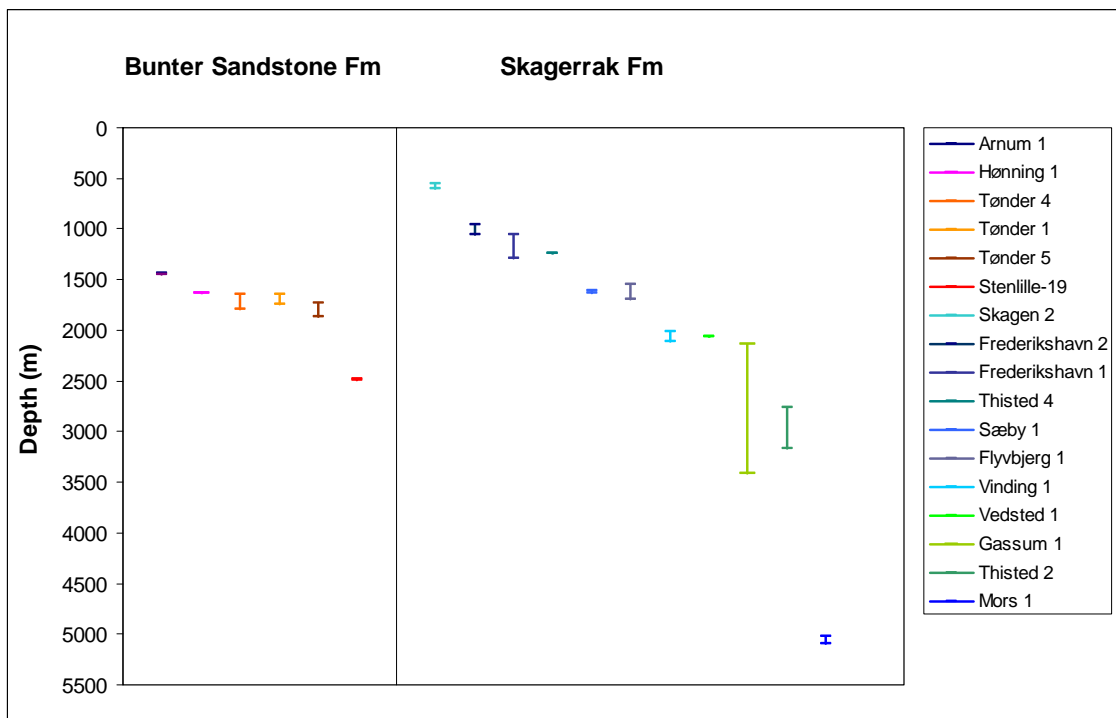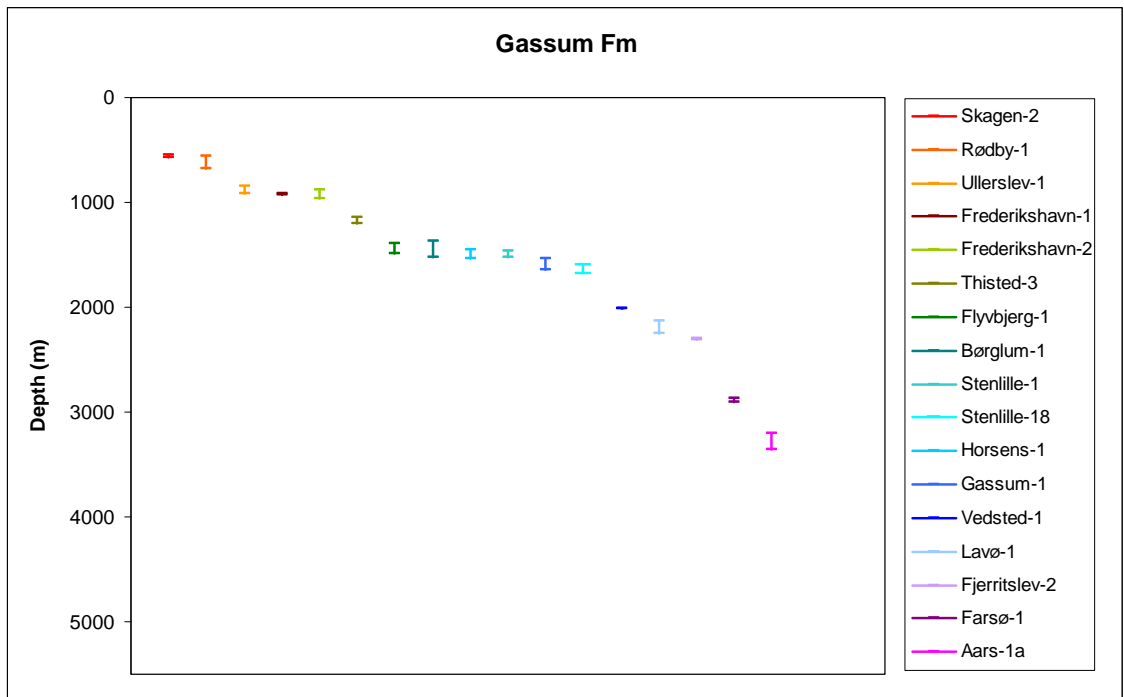**Fig. 3.1.** *Cored intervals of the Skagerrak and Bunter Sandstone formations onshore Denmark.*

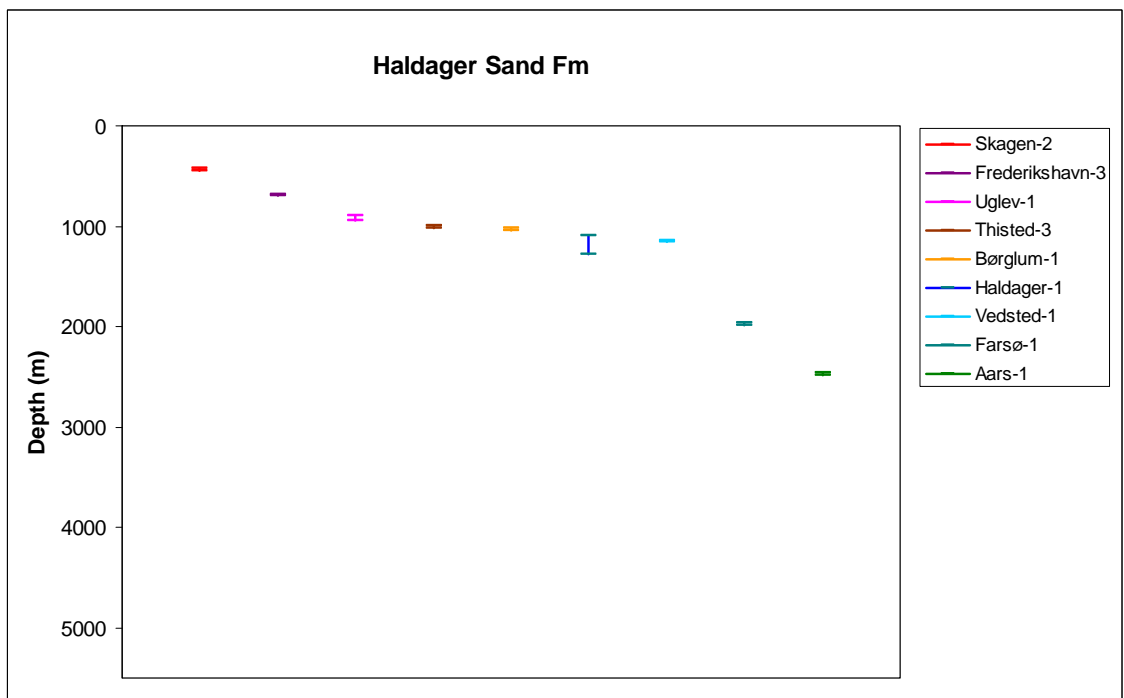**Fig. 3.2.** *Cored intervals of the Gassum Formation onshore Denmark.*

Fig. 3.3. *Cored intervals of the Haldager Sand Formation onshore Denmark.*

4. Laboratory methods

4.1 Petrography

Petrography was evaluated from transmitted light and reflected light microscopy of polished thin sections. The sedimentary rocks were impregnated with blue epoxy for easy identification of the porosity. Half of the polished thin section was stained for easy recognition of K-feldspar. Modal compositions of the sandstones were obtained by counting minimum 300-500 points in each thin section. Supplementary studies of crystal morphologies and paragenetic relationships were performed on gold coated rock chips mounted on stubs and on carbon coated thin sections using a Phillips XL 40 scanning electron microscope (SEM). The scanning electron microscope was equipped with secondary electron detector (SE), back-scatter detector (BSE), cathodoluminescence detector (CL); and with a Thermo Nanotrace 30 mm^2 detector surface window and a Pioneer Voyager 2.7 10 mm^2 window Si(Li) detector energy dispersive X-ray analysis (EDX) system. The electron beam was generated by a tungsten filament operating at 17 kV and 50-60 µA.

4.2 Microprobe analysis

Feldspar composition was analysed on carbon-coated polished thin sections on a JEOL© JXA-8200 microprobe at an acceleration voltage of 15 kV and a beam current of 15 nA.

4.3 X-ray diffraction (clay and bulk mineralogy)

The clay fraction samples were separated by sieving and gravitational settling and prepared as smear slides. Bulk samples were mounted with random orientation. Samples were scanned on an automated Philips© PW 3710 X-ray diffractometer with automatic divergence slit, using graphite monochromated CuKα radiation. The clay specimens were scanned air-dried; ethylene glycolated at 60°C; and after heating at 500°C for one hour. Criteria for identification of clay minerals can be found in Weibel (1999). Quantification of major mineral phases was done by Rietveld analysis of x-ray diffractograms of bulk-rock samples, whereas the clay minerals were evaluated semi-quantitatively.

4.4 Porosity and permeability

The porosity and permeability were measured according to the API RP-40 standard (API 1998). Gas permeability was measured at a confining P ~ 2.8 MPa (400 psi), and at a mean N_2 gas pressure of ~ 1.5 bar (bar absolute) = 0.15 MPa (permeabilities below 0.05 mD were measured using a bubble flowmeter). He-porosity was measured unconfined.

5. Petrography and diagenesis

The detrital composition and authigenic formed minerals will be presented for each formation: Bunter Sandstone Formation, Skagerrak Formation, Gassum Formation and Haldager Sand Formation. The detrital composition can be compared in several ways; in Figure 5.1 the amount of quartz, feldspar and rock fragments are compared according to the classification by McBride (1987). The mineralogical changes with burial depth will first be discussed for each formation prior to comparison of the diagenesis in the respective formations. The early diagnesis (eogenesis) is very different between the formations, as it is strongly tied to the depositional environment (Schmidt and McDonald 1979). The diagenesis during increased burial depth (mesogenesis) comprise the changes when interstitial water is no longer controlled by the surface environment (Schmidt and McDonald 1979) and is consequently strongly related to the stability and instablility of the detrital minerals (as well as their abundance). This can explain the remarkably degree of consistency in the diagenetic assemblages (illite, chlorite, ferroan carbonate, quartz cement and secondary porosity) formed at deep burial in sediment of a variety of environments and tectonic settings and it suggests that depth-related (mesogenetic) diagenetic processes conform to a pattern that may be predictable (Burley et al. 1985).
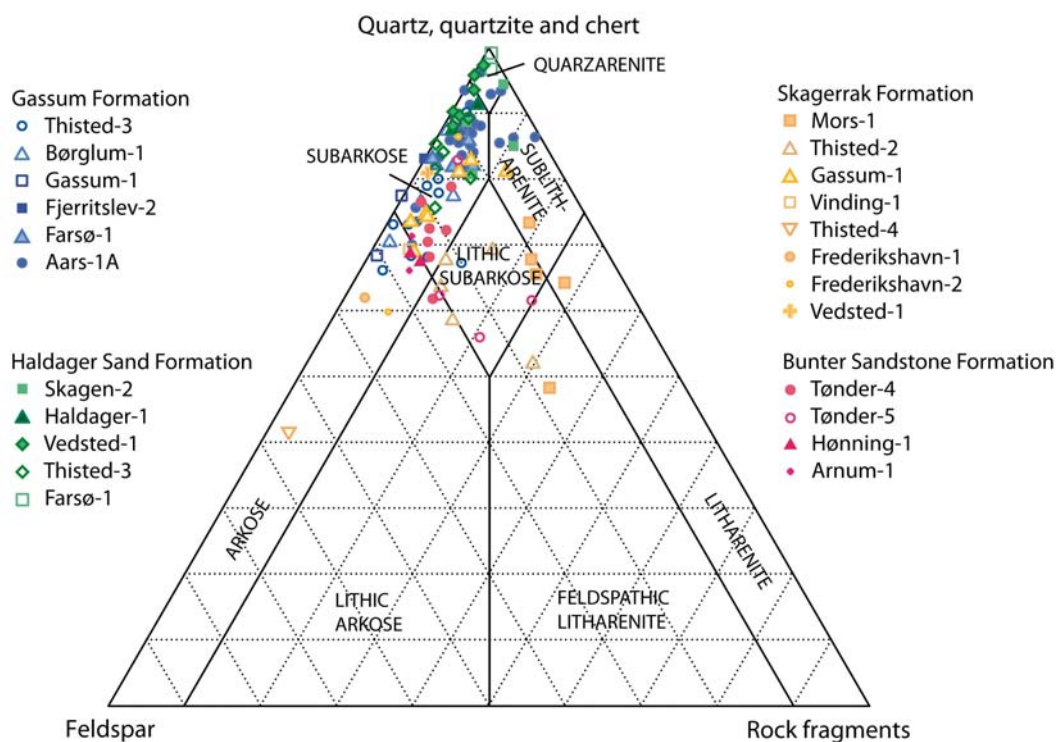

Fig. 5.1. *Ternary diagram showing the classification, according to McBride (1968), of the Danish Mesozoic onshore sandstones. Data for the Gassum Formation after Friis (1987).*

5.1 Bunter Sandstone Formation

The emphermal fluvial and aeolian deposits of the Lower Triassic Bunter Sandstone Formation occurs in the northern rim of the North German Basin (Bertelsen 1980) with thicknesses up to 300 m (Mathiesen et al. 2009) and burial depths varying from 1140–1800 m.

Detrital composition
The Bunter Sandstone Formation is dominated by well-sorted, fine-grained, homogeneous, laminated, or small-scale cross-bedded sandstone with occasional thin mudstone intervals. The framework grains are typically subrounded to rounded, whereas the "over-sized" clay clasts are more or less deformed.
The sandstones are mainly arkoses and subarkoses (Figs 5.1 & 5.2; Weibel and Friis 2004) according to the classification of McBride (1963). The feldspar grains are dominated by K-feldspar and minor Na-rich plagioclase. Sedimentary rock fragments are relatively more abundant than igneous and metamorphic rock fragments. Granitic rock fragments of a myrmekitic texture are common in some samples (especially ephemeral fluvial sandstones). Ephemeral stream deposits typically contain "rip-up" clasts from overbank strata. Ooids (Figs 5.4A & B) are numerous in aeolian sandstones, and may occur together with other detrital carbonate fragments in both fluvial and shoreline deposits. Recrystallised shell fragments are common only in shoreline deposits.

Authigenic phases
The most common porosity reducing authigenic phases are carbonates (calcite and dolomite), anhydrite and clay minerals (illite, chlorite, mixed-layer illite/smectite and mixed-layer smectite/chlorite) (Figs 5.3, 5.4 & 5.5). Accessory authigenic minerals of minor importance for the reservoir properties include analcime, red coatings, feldspar overgrowths, quartz overgrowths (Figs 5.6 & 5.7), barite, titanium-oxides and other opaque minerals (montroisite, chalcocite and covellite) (Weibel and Friis 2004).

Authigenic calcite occurs in several ways; as overgrowths (crystals in rhombohedral or scalenohedral forms) on ooids or other carbonate rock fragments (Figs 5.3A, B, C & D), as caliche and as poikilotopic cement. Dolomite occurs as pore filling cement and as rhombohedral-shaped crystals commonly inside clay clasts (Figs 5.3E & F).

Anhydrite may locally, especially in fluvial sandstones besides sabkha deposits, be an important porosity reducing cement where it occurs as poikilotopic cement. Anhydrite appears with displacive growth patterns in the fine-grained sabkha deposits (Figs 5.5C, D & E).

Infiltration clays (identified according to Wilson and Pittman 1977) consist of illite, chlorite and mixed-layer illite/smectite (Weibel and Friis 2004). This clay-mineral assemblage reflects the diagenetically changed composition, whereas the original might have contained more smectite, similar to the infiltration clay in the Triassic Skagerrak Formation (Weibel, 1999). Authigenic illite (and mixed-layer illite/smectite) as well as chlorite (and mixed-layer smectite/chlorite) are closely intergrown and too fine for chemical analysis of separate phases. Kaolin occurs preferentially in reduced samples but its associations are not nearly

as convincing as the observations from reduction spots in the Skagerrak Formation (Weibel 1999). Therefore the clay mineral identification is based on XRD (Weibel and Friis 2004). Furthermore, red coatings cover most detrital grains and obscure identification of the different clay minerals in thin sections.

Authigenic quartz occurs as thin syntaxial overgrowths (macroquartz) on detrital quartz grains (Fig. 5.6). Authigenic feldspar occurs as syntaxial overgrowths, but was also observed as non-epitaxial overgrowths. Analcime is almost ubiquitous and occurs as euhedral, eight-sided or six-sided crystals (commonly trapezohedra). The analcime crystals are characterised by internal dissolution voids, but with a preserved outer crystal-shape. A more Ca-rich zeolite in the centre has been identified in one case only. Halite is ubiquitous in samples from the Tønder wells, but it is difficult to determine whether halite was cement in the subsurface or whether it formed as the highly saline pore fluids in the cores dried out. Titanium-oxides occur as leucoxene replacing Ti-rich detrital minerals and as single crystals of anatase in pore spaces. Barite occurs as single crystals, and occasionally it is captured in anhydrite. Rare authigenic opaque minerals comprise pyrite and various copper, uranium and vanadium minerals (Weibel and Friis 2004).

Porosity and permeability
Low permeability and relatively high or medium porosity are typical of samples of abundant clay intraclasts, which have their highest abundance in the lowermost part of fluvial deposits and gradually decrease in abundance as the sediments fine upwards. The clay clasts are squeezed between other detrital grains during relatively shallow burial and may resemble allogenic clays. The lowest permeabilities and porosities are generally found in sabkha-related deposits because of the fine-grained nature of these sediments. Porosity (0-28%) is mainly registered as primary porosity except for a minor amount of secondary porosity (mouldic porosity or intragranular porosity. In the Tønder-5 samples, the sum of anhydrite cement and porosity is more or less constant at 26-28%. Since dissolution is generally not observed on the surface of anhydrite crystals, the porosity is therefore assumed to mainly represent uncemented primary porosity. Locally, however, porosity may be larger and appears to be partly secondary after dissolved cement.
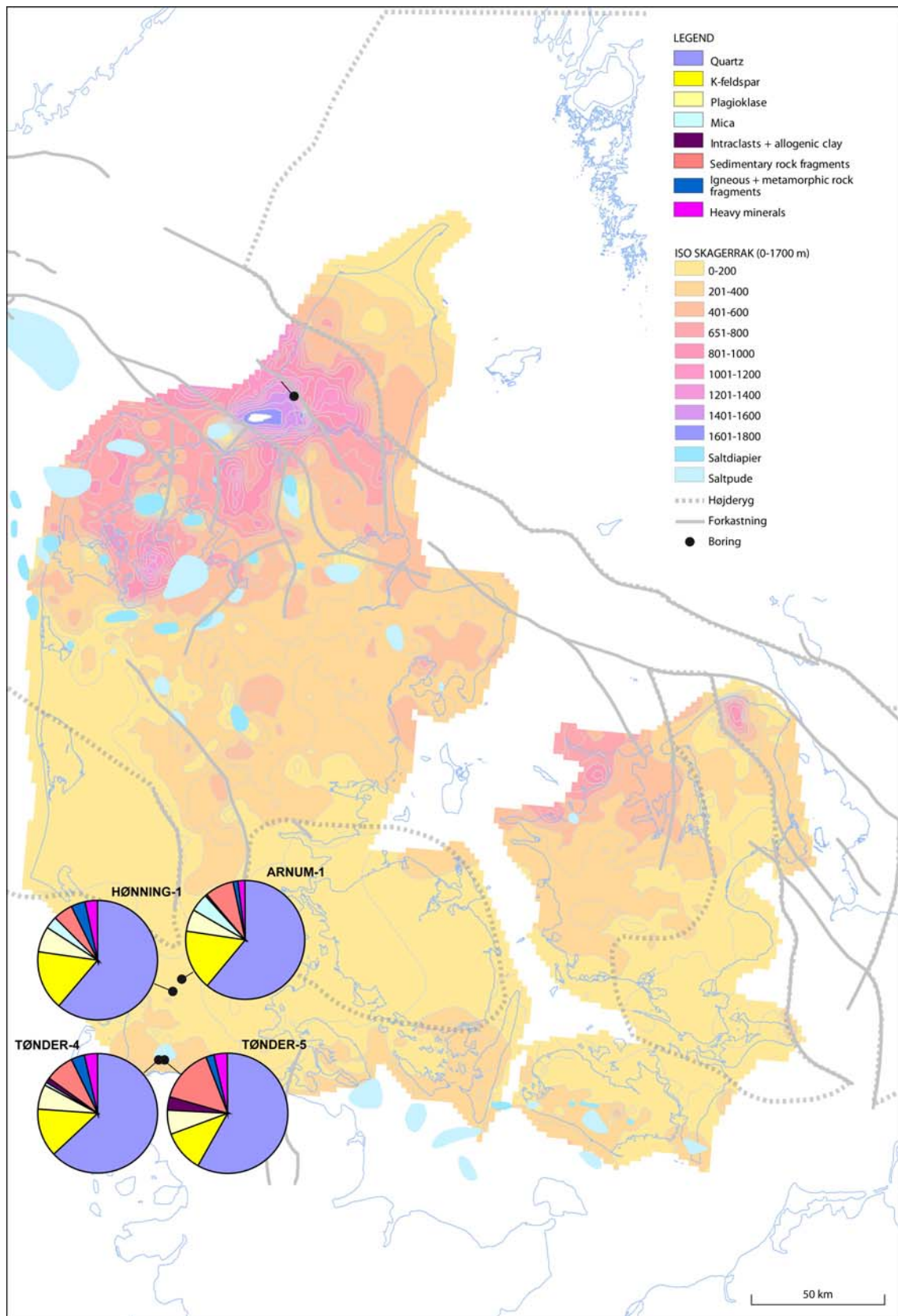
Fig. 5.2. *Average detrital composition of the Bunter Sandstone Formation shown as pie diagrams for each analysed well on isopach map of the Bunter Sandstone and Skagerrak formations (modified after Mathiesen et al. 2009).*

GEUS
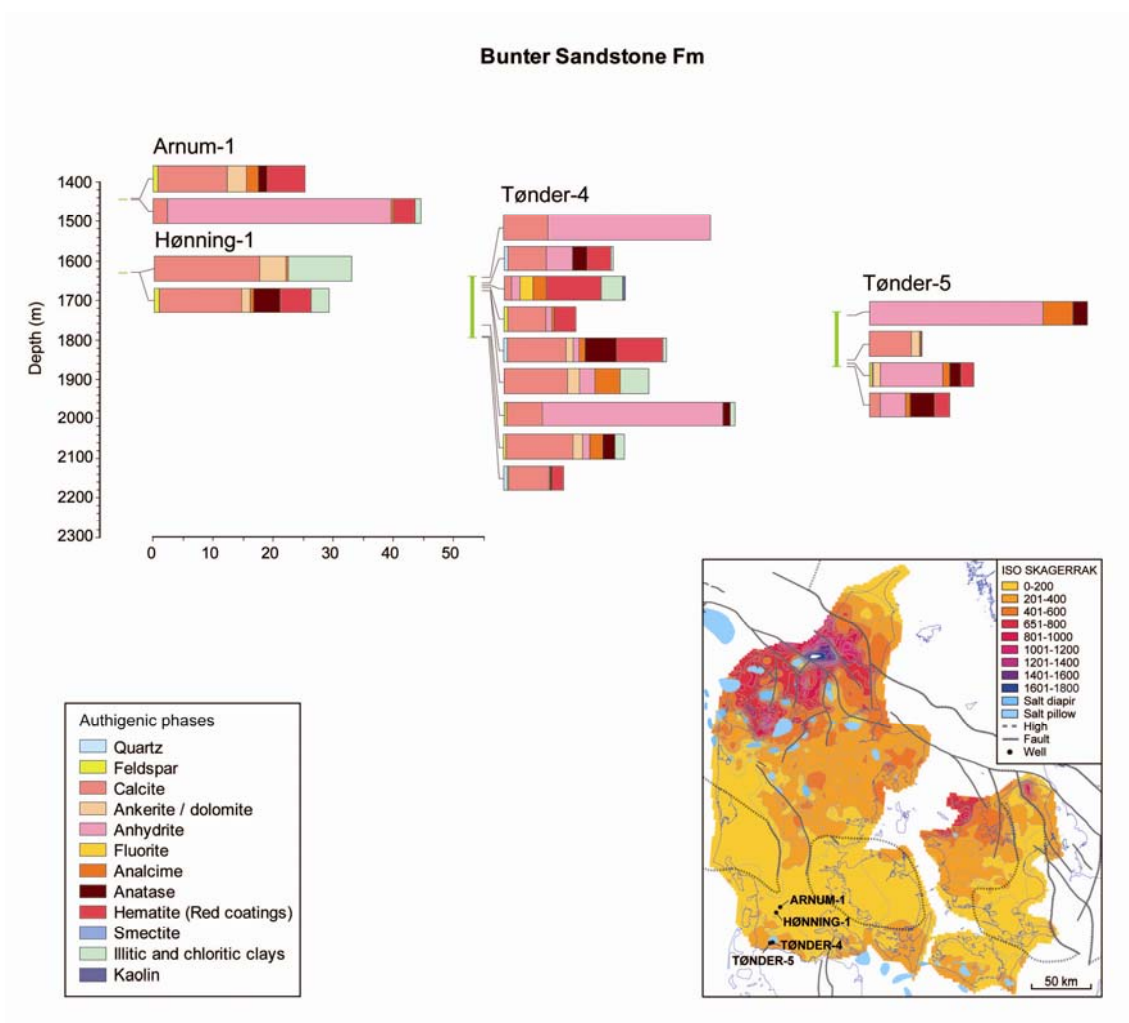
Fig. 5.3. *Authigenic phases, quantified by point counting, in the Bunter Sandstone Formation for different wells and consequently different burial depths.*
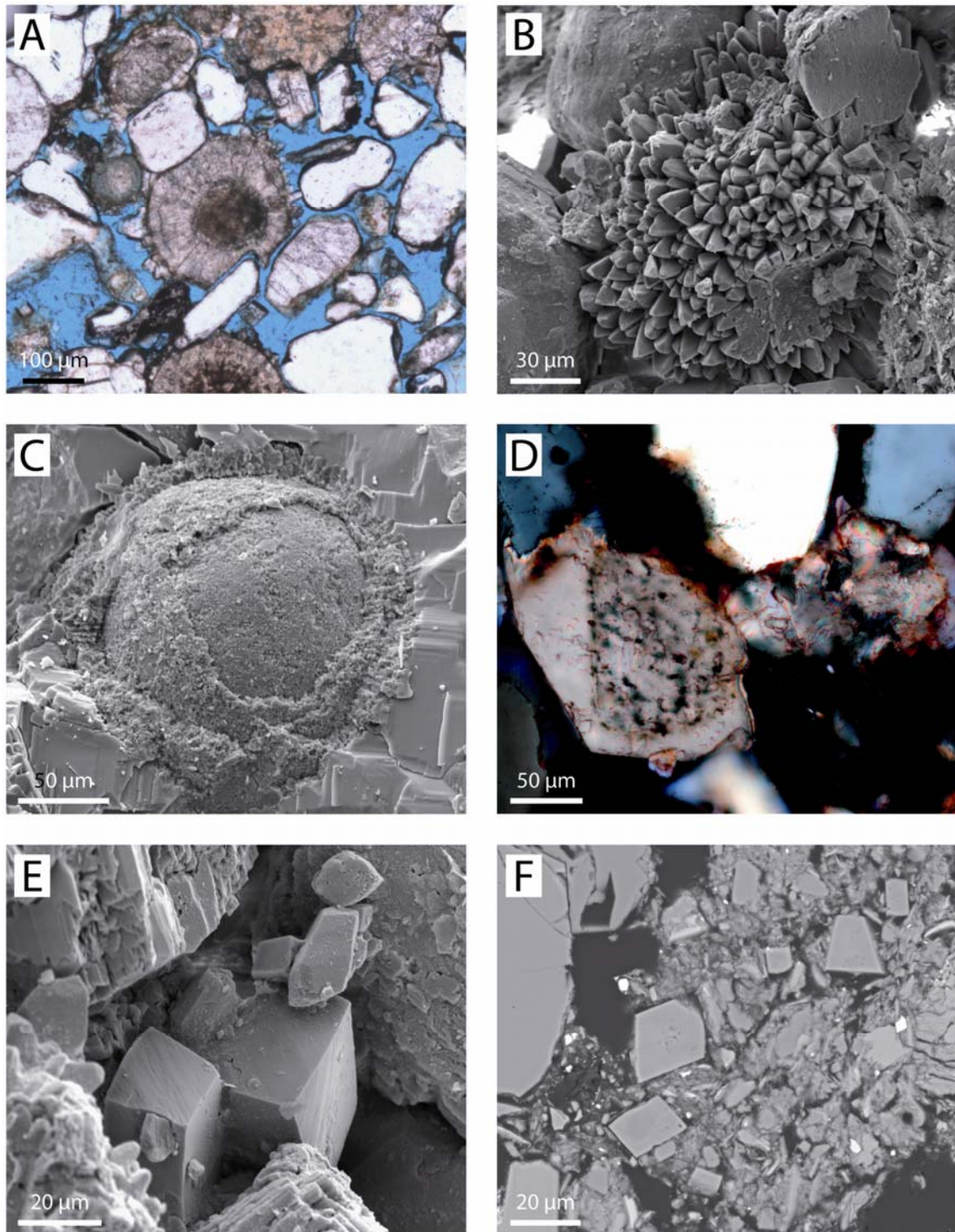
Fig. 5.4. *Carbonate diagenesis in the Bunter Sandstone Formation. A. Pressure dissolved ooid with calcite overgrowths, Tønder-4, 1796.33 m. B. Calcite crystals probably precipitated on an ooid, Tønder-4, 1678.16 m, scanning electron micrograph. C. Ooid completely enclosed in anhydrite, Tønder-4, 1683.66 m, scanning electron micrograph. D. Calcite overgrowth on detrital carbonate clast, Tønder-4, 1662.96 m. E. Dolomite rhombs, Tønder-4, 1663.27 m, scanning electron micrograph. F. Dolomite rhombs in mudclast, Tønder-4, 1663.24 m, backscatter electron micrograph.*
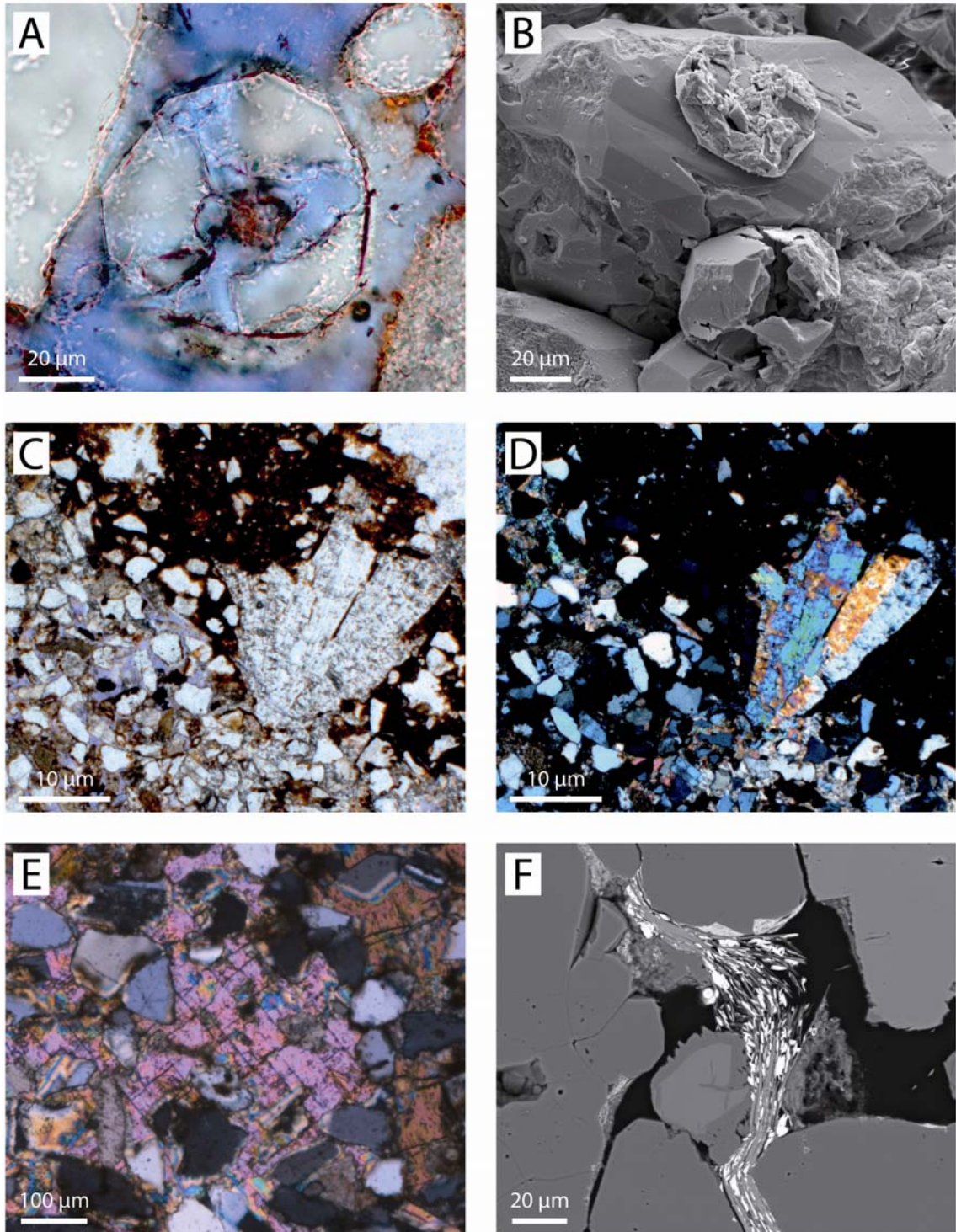
Fig. 5.5. *Characteristic authigenic phases in the Bunter Sandstone Formation. A. Analcime with internal dissolution voids, Tønder-4, 1662.96 m . B. Analcime crystal growing after quartz overgrowth, Tønder-4, 1663.27 m, scanning electron micrograph. C. Anhydrite with displasive growth texture, probably due to anhydrite replacment of the original gypsum, Tønder-4, 1662.96 m. D. Similar to C, crossed nicols. E. Pore filling anhydrite cement, Tønder-4, 1663.24 m, crossed nicols. F. Hematite crystals precipitated between the cleavage planes of mica, Tønder-4, 1649.47 m, backscatter electron micrograph.*
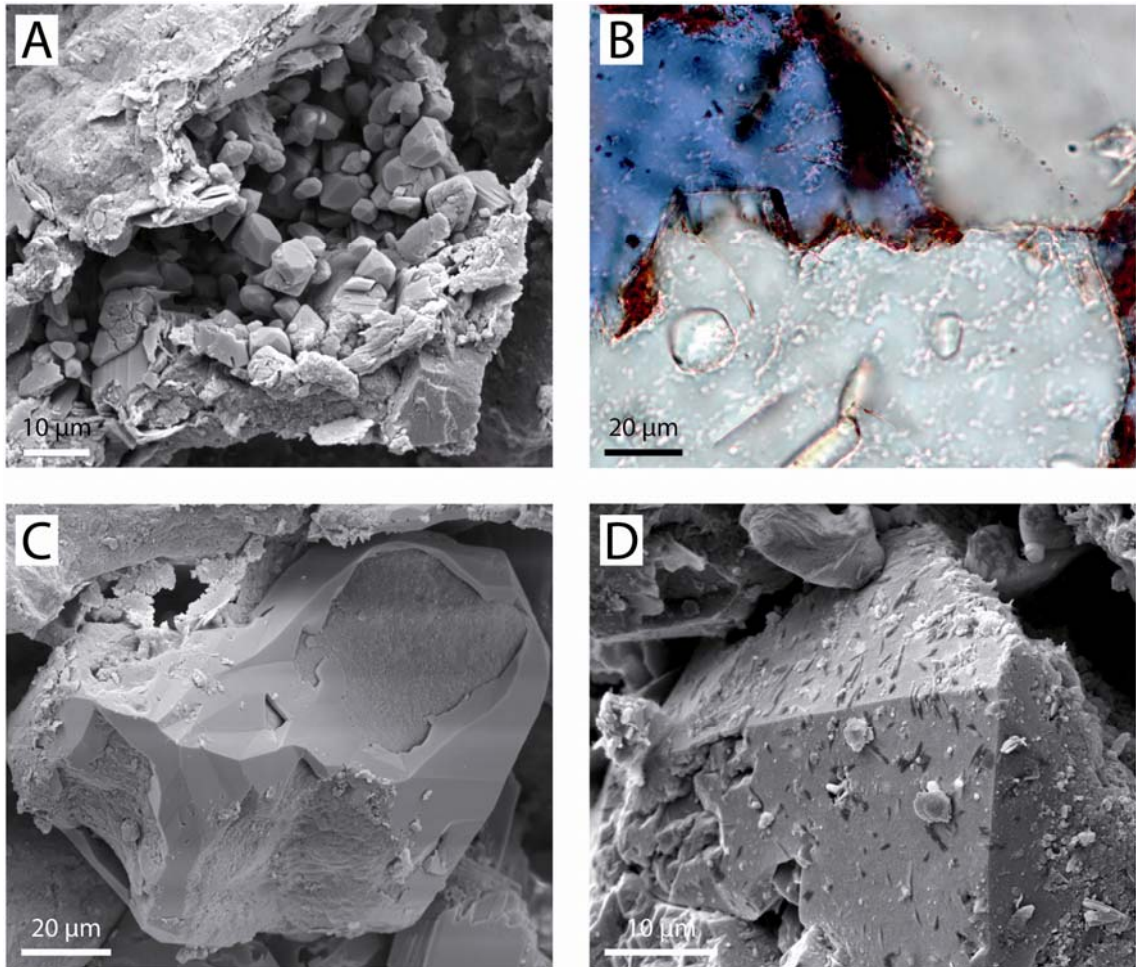
Fig. 5.6. *Quartz diagenesis in the Bunter Sandstone Formation. A. Numerous authigenic quartz crystals, Tønder-4, 1663.27 m, scanning electron micrograph. B. Small quartz overgrowth enclosing an iron-oxide/hydroxide coating, Tønder-4, 1662.96 m. C. Typical limited quartz overgrowth, Tønder-4, 1663.27 m, scanning electron micrograph. D. Large quartz overgrowth, Tønder-4, 1663.24 m, scanning electron micrograph.*
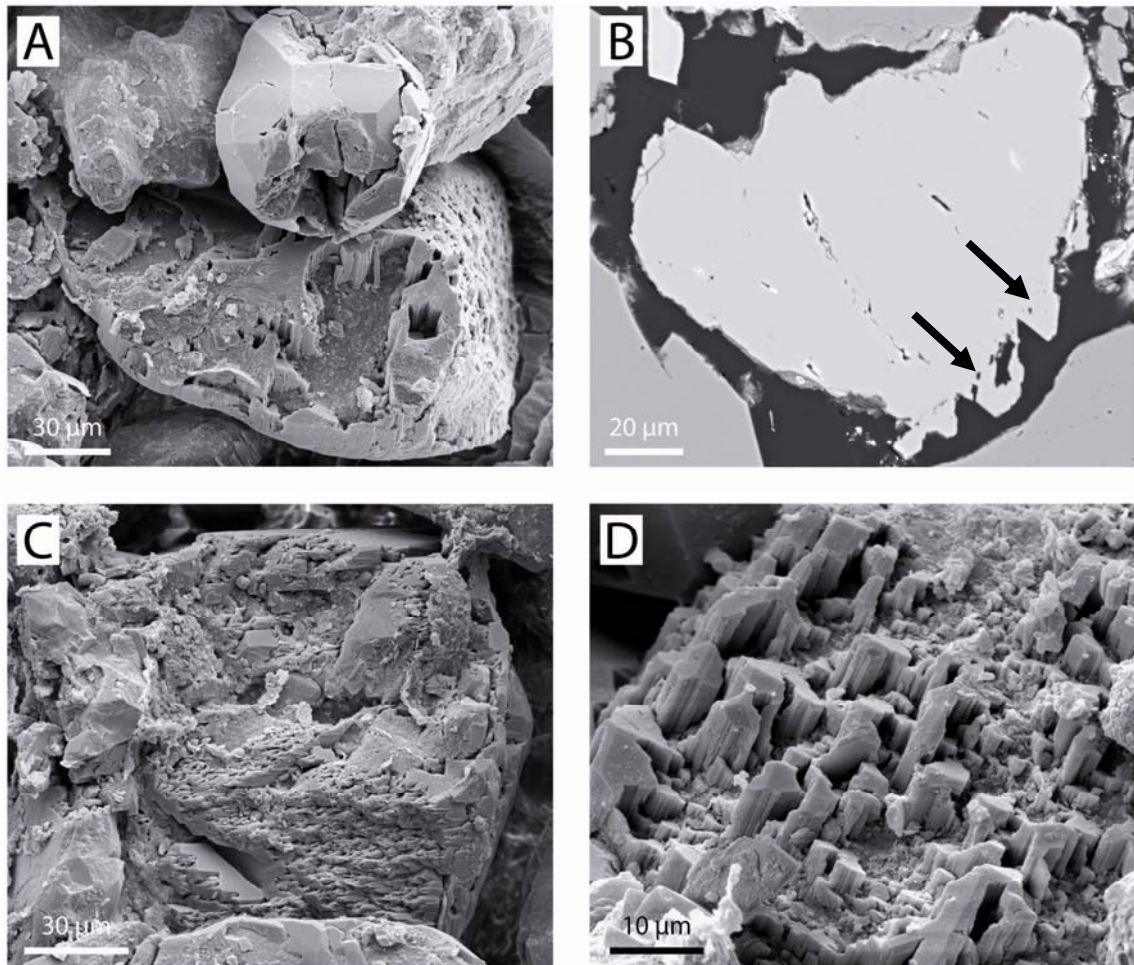
Fig. 5.7. *Feldspar alteration and authigenesis in the Bunter Sandstone Formation. A. K-feldspar overgrowths on detrital K-feldspar, Tønder-4, 1663.27 m, scanning electron micrograph. B. K-feldspar overgrowths (marked by arrows) on detrital K-feldspar, Tønder-4, 1663.24 m, backscatter electron micrograph. C. Partly dissolved detrital albite with local albite overgrowths, Tønder-4, 1663.27, scanning electron micrograph. D. Albite overgrowths, Tønder-4, 1663.24, scanning electron micrograph.*

Mineralogical changes with burial depth

The chronological order of these authigenic phases is shown in the paragenetic sequence of the Bunter Sandstone Formation (Fig. 5.8).

The eogenesis in the Bunter Sandstone Formation is strongly influenced by its deposition in an arid to semi-arid climate. Thick red coatings (of iron-oxide/hydroxide) begin their formation immediately after deposition in a similar way that desert varnish forms on grains in the present day deserts. An early gypsum precursor is both suggested by the displacive growth of anhydrite, especially seen in the fine-grained sabkha deposits, and by pore filling anhydrite occurring in amounts resembling filling of the original high porosity. Evaporation of ground water probably caused precipitation of gypsum cement and displacive gypsum

growth in the fine-grained sediments. Gypsum losses its crystal water during mesogenesis and is transformed to anhydrite. As there is no or extremely little bacterial sulphate reduction going on in these hostile environments more sulphate is available for anhydrite precipitation at increased burial. Other minerals, besides gypsum, that form due to the high evaporation in desert environments are calcite (calcrete) and dolomite. Calcrete, also known as caliche and hardpan, forms during soil development (calcisols) in arid or semi-arid regions (Bridges 1997).

In the arid or semi-arid climate the weathering is less intense resulting in relatively high contents of unstable grains in the deposits (Walker 1976). Dissolution and alteration of unstable grains during the following diagenesis promoted the formation of a variety of authigenic minerals. A smectitic composition is suggested for the first authigenic clay minerals, as wells as the infiltration clays. Later burial diagenesis leads to transformations into mixed-layer smectite/illite, illite, mixed-layer smectite/chlorite and chlorite, which represents the present day clay mineral assemblage (Weibel 1999). Silica is liberated during transformation of smectitic clays into more illitic clays. The limited occurrence of quartz and feldspar overgrowths is partly related to the shallow burial depth and partly to the thick red coatings which partly inhibited continued growth on the detrital grains. Alteration of Fe-Ti oxides results in formation of red coatings (iron-oxide/hydroxide coatings), leucoxene, anatase and occasionally pyrite in the reduction spots. Reduction spots form around rare organic matter, for example fragments of algal mats or large-scale reduced areas which may be caused by hydrocarbon migration (Weibel and Friis 2004).

Calcite and dolomite pore filling cement forms during increased burial, sometimes related to the early diagenetic calcrete (Burley et al. 1985) as well as detrital carbonate clasts and ooids. Weakly pressure solution of ooids and carbonate clasts liberates only limited amounts of calcium which precipitates as calcite overgrowths. Iron oxide/hydroxide rims of increased thickness along pressure solution contacts reflect the solubility of calcium and the relative immobility of iron in the oxidising environment (Fine 1986). Consequently, aeolian sediments, containing abundant ooids and carbonate clasts, are very loose due to the limited amounts of cement.

Highly saline pore fluids (115 g Na/l, 200 g Cl/l) are present in the Bunter Sandstone reservoirs of the Tønder wells (Laier 2008). Introduction of saline brines during burial is shown by an extraordinary authigenic mineralogy characterized by analcime, halite and copper minerals (Weibel and Friis 2004). Ubiquitous analcime in the Bunter Sandstone Formation (almost without volcanic rock fragments) also indicates migration of saline brines (see Van der Kamp and Leake 1996). These saline brines may originate from the underlying Zechstein evaporites, the overlying Ørslev Formation (Röt salt) or residual brines associated with the desert, sabkha or inland sea depositional environment. The relatively high bromide to chloride ratios of the pore fluids could indicate an origin as residual brines rather than dissolution of Zechstein evaporites, since halite has a lower bromide to chloride ratio compared to sea water (Laier 2008).

Mechanical compaction has been modest in the investigated Bunter Sandstone Formation, which has a maximum burial depth of 1880 m. Weak pressure solution of carbonate clasts and ooids occurs in several samples without resulting in a substantial porosity reduction.

	Eogenesis	Saline brines	Mesogenesis

Smectitic clays — infiltration clays
Gypsum
Calcite — caliche — poikilotopic — overgrowth
Dissolution of detrital minerals
Iron oxide/hydroxide — goethite hematite
Hematisation
Ilmenite alteration — leucoxene replacement — iron-oxide needle impregnation
Clay replacement
Illite — smectite → illite
Anatase
Chlorite
Quartz overgrowth
Feldspar overgrowth
Dolomite — rhombs — pore filling — dissolution
Analcime — dissolution
Halite
Chalcopyrite
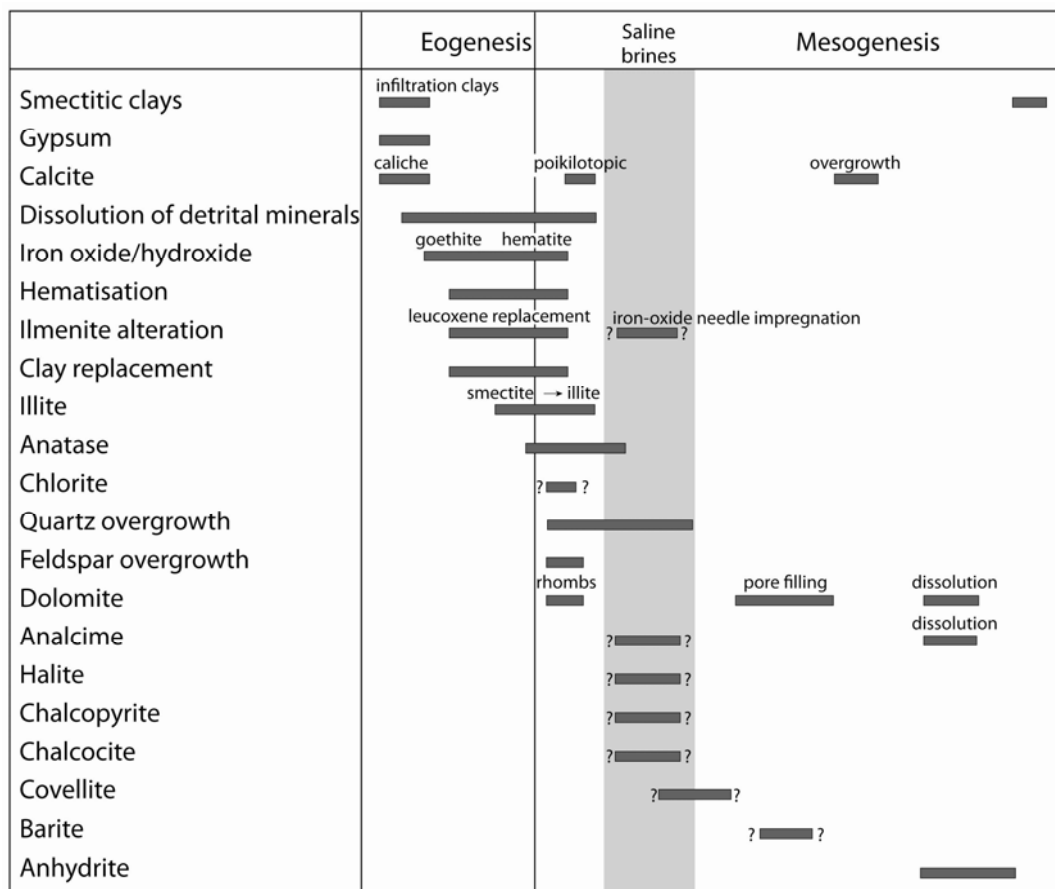Chalcocite
Covellite
Barite
Anhydrite

Fig. 5.8. *Diagenetic sequence for the Bunter Sandstone Formation, simplified after Weibel and Friis (2004).*

5.2 Skagerrak Formation

The alluvial fan and braided fluvial deposits of the Triassic Skagerrak Formation (Fig. 1) is found only in the Norwegian-Danish Basin (Fig. 1). The Skagerrak Formation has present day burial depths from 600–5000 m and total thicknesses up to 1700 meters (Mathiesen et al. 2009).

Detrital composition

The sediments are arkoses, lithic arkoses and subarkoses (Figs 5.1 & 5.9; Weibel 1998) according to the classification of McBride (1963). The sediments vary from fine-grained sandstones to conglomerates. The sorting is poor to moderate in the northeastern part of Denmark but the degree of sorting increases towards southwest. The grains are typically subangular to subrounded.

Monocrystalline quartz is the major framework grain, though polycrystalline quartz also occurs. The feldspar group is completely dominated by K-feldspar, though plagioclase grains have been identified. Alteration of feldspar grains includes dissolution, clay mineral or carbonate replacement, sericitisation and possible albitisation (only in the deeper reservoir sandstones, for example Thisted-2). Furthermore, a relatively high number of altered grains are probably altered feldspar grains.

The rock fragments are mainly igneous and rarely metamorphic, but volcanic rock fragments are common in a specific area (in the Mors-1, Thisted-2, Thisted-4 and Gassum-1 wells). Clay intraclasts that probably are rip-up clasts from overbank deposits occur in high abundance in few samples. Mica occurs in small amounts in most samples. Mica shows signs of oxidation, reduction (only in reduction spots), replacement by clay minerals or minor expansion due to precipitation of authigenic phases (hematite and anatase) between cleavage planes. Transparent (apatite, zircon, tourmaline, rutile, amphibole) and opaque heavy minerals are common accessory minerals, though they may be abundant in specific samples containing heavy mineral lamina. Opaque minerals may in specific samples be present in up to 20.3%. The alteration of opaque minerals includes among other leucoxene replacement of ilmenite and hematisation of magnetite (Weibel 1998; Weibel & Friis 2007).

Authigenic phases

The dominating porosity reducing cements in the Skagerrak Formation are carbonates and clays (Figs 5.10, 5.11 & 5.12). Clay minerals occur as pore-lining, pore filling cement as well as replacement of detrital grains, which, besides feldspar and mica, may include both volcanic rock fragments and heavy minerals. The clays are dominated by smectite in the shallow wells, whereas mixed-layer illite/smectite and illite become more abundant with increased burial depth (Weibel 1999). Infiltration clays (Fig. 5.11A), probably of smectitic composition, are volumetrically important in rare samples. Authigenic illite appears as radiating crystals either pore lining or intragranular on remnants of almost completely altered detrital minerals (Figs 5.12C & D). Chlorite occurs as a late diagenetic pore filling cement and is clearly separated from illite by red coatings (Figs 5.12E & F). Kaolin dominates the

clay mineral assemblage in the reduction spots and reduced areas, but is rare in the red host (Weibel 1998, 1999) (Figs 5.15 E & F).

Red coatings cover most detrital grains and are found in between some authigenic phases. The red colouration of the Skagerrak Formation origins from goethite in the shallow sandstones (< 2100 m), but from hematite in the deeper sandstones (>2700 m), where the goethite needles are pseudomorphous transformed into hematite (Weibel 1999; Weibel & Groberty 1999). Additionally hematite occurs as replacement of mica and amphiboles, syntaxial overgrowth on detrital hematite and as pore filling crystals arranged as rosettes which appear to be "doughnut" shaped in high resolution (SEM).

The carbonate cement is typically dolomite, which occurs either as rhombohedral-shaped crystals with distinct growth zones, or as pore filling poikilotopic and micritic cement, which may be replacive to other mineral phases (Figs 5.11E & F). The nucleation points for carbonate are altered plagioclase grains or clay intraclasts where they are present (Figs 5.11C & D). The micritic cement is common in between the cleavage planes of expanded mica, whereas the poikilotopic cement is pore filling and corrosive towards the other mineral phases. The pore filling carbonate often has a radiating extinction thereby resembling saddle dolomite. Occasionally the pore filling carbonate cement is calcite or ankerite. Calcite corrodes the rims of the detrital minerals which "float" in the calcite matrix. Calcite occurs as both micritic and poikilotopic cements. The micritic cement exhibits several of the Alpha calcrete fabric elements described by Wright (1990). For example the calcite crystals form a radiating rim on the detrital grains in some of the shallow wells (Frederikshavn-1, -2, Skagen-2 and Flyvbjerg-1) (Fig. 5.11A).

Of minor volumetrically importance are quartz overgrowths and feldspar overgrowths. Syntaxial quartz overgrowths occur as prismatic or pore filling crystals. Prismatic authigenic quartz (occasionally bi-pyramidal authigenic quartz) occurs where relatively thick clay rims or red coatings cover the detrital grains (Figs 5.13A & B). Pore filling quartz occurs only in rare very fine-grained (siltstone - fine-grained sandstone) cross-stratified samples. Authigenic macroquartz encloses other authigenic phases, such as red coatings (Fig. 5.13D), anatase, illite rims, fibrous illite, feldspar, early carbonate rhomb and occasionally prismatic quartz as observed in the deepest well (Mors-1). Pressure solution and fractural healing in detrital quartz grains (and abundant authigenic quartz) are common phenomena in the Gassum-1 well, which has a lower content of ductile rock fragments and authigenic clay minerals (Fig. 5.13F). Thick red coatings seem to have a prohibiting effect on the pressure solution.

Authigenic feldspars occur as syntaxial and rarely epitaxial overgrowths on detrital feldspar grains and as crystals precipitated on remnants of dissolved feldspars in the secondary porosity (Figs 5.14A, B & C). Authigenic feldspar encloses red coatings and illitic rims (Fig 5.14D). Feldspar overgrowths are more abundant than quartz overgrowths in the shallowest part of the cores from the Gassum-1 well, and in fine-medium grained samples in the Thisted-2 well.

Rare authigenic minerals include anatase, pyrite and anhydrite (Fig. 5.15). Titanium-oxides comprise leucoxene, which replaces detrital titanium-rich minerals, and single crystals of

anatase, which are precipitated in the pore space. Pyrite occurs as framboidal or euhedral cubic pore filling crystals or replacement of mica in the reduction spots (Figs 5.15C & D). Pyrite is commonly occurring together with kaolin. Crandallite group minerals occur as euhedral cubic pore filling crystals along the outer rim of reductions spots.

Anhydrite is the last authigenic phase and corrosive to all other mineral phases (Figs 5.15A & B). Anhydrite is very rare in the Skagerrak Formation.

Mechanical deformation of ductile grains such as mica, clay intraclasts and rock fragments is common in the deepest reservoir sandstones, whereas pressure solution of quartz occurs in sandstones with a low content of ductile grains.
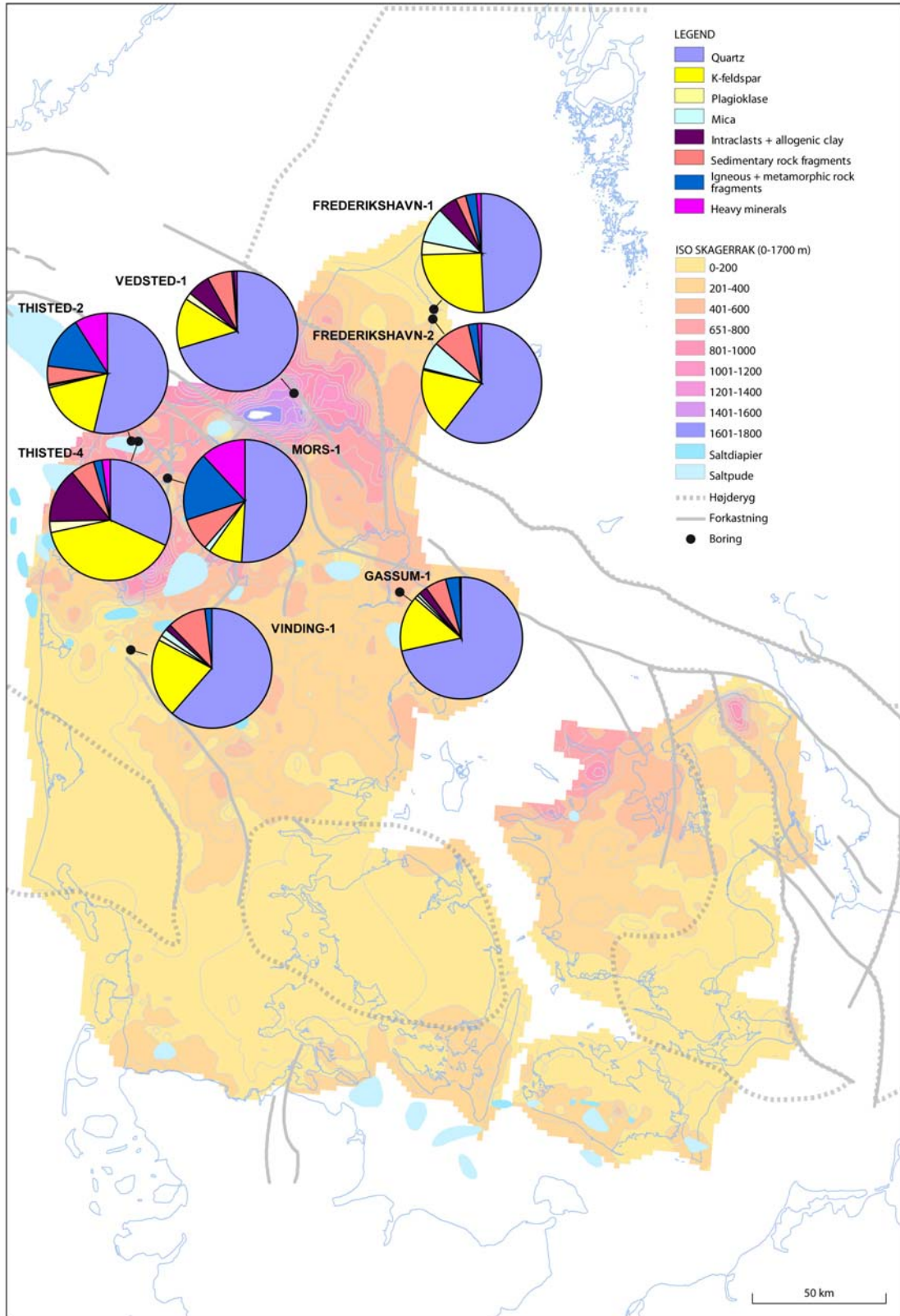
Fig. 5.9. *Average detrital composition of the Skagerrak Formation shown as pie diagrams for each analysed well on isopach map of the Bunter Sandstone and Skagerrak formations (modified after Mathiesen et al. 2009).*
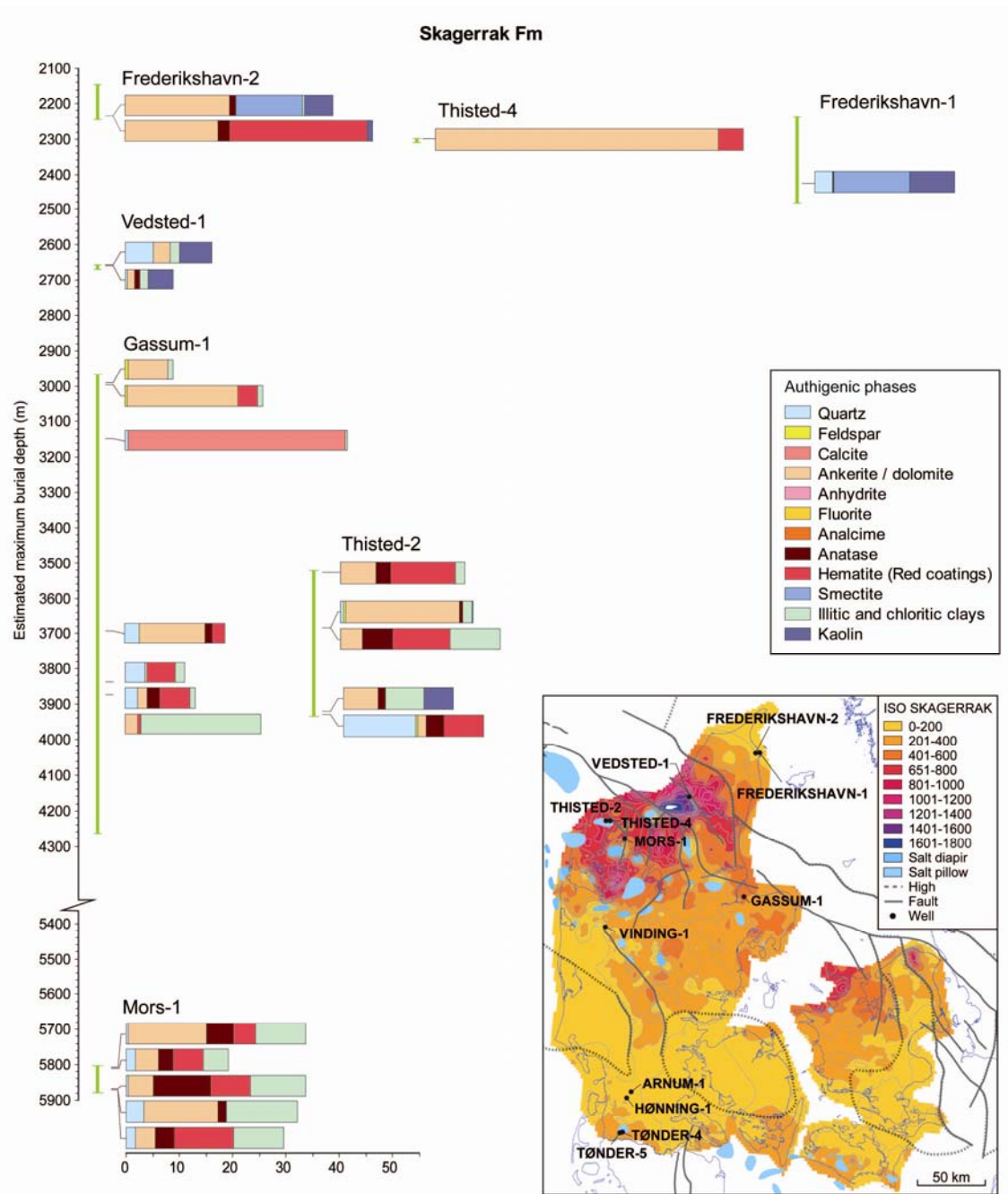
Fig. 5.10. *Authigenic phases, quantified by point counting, in the Skagerrak Formation for different wells and consequently different burial depths.*
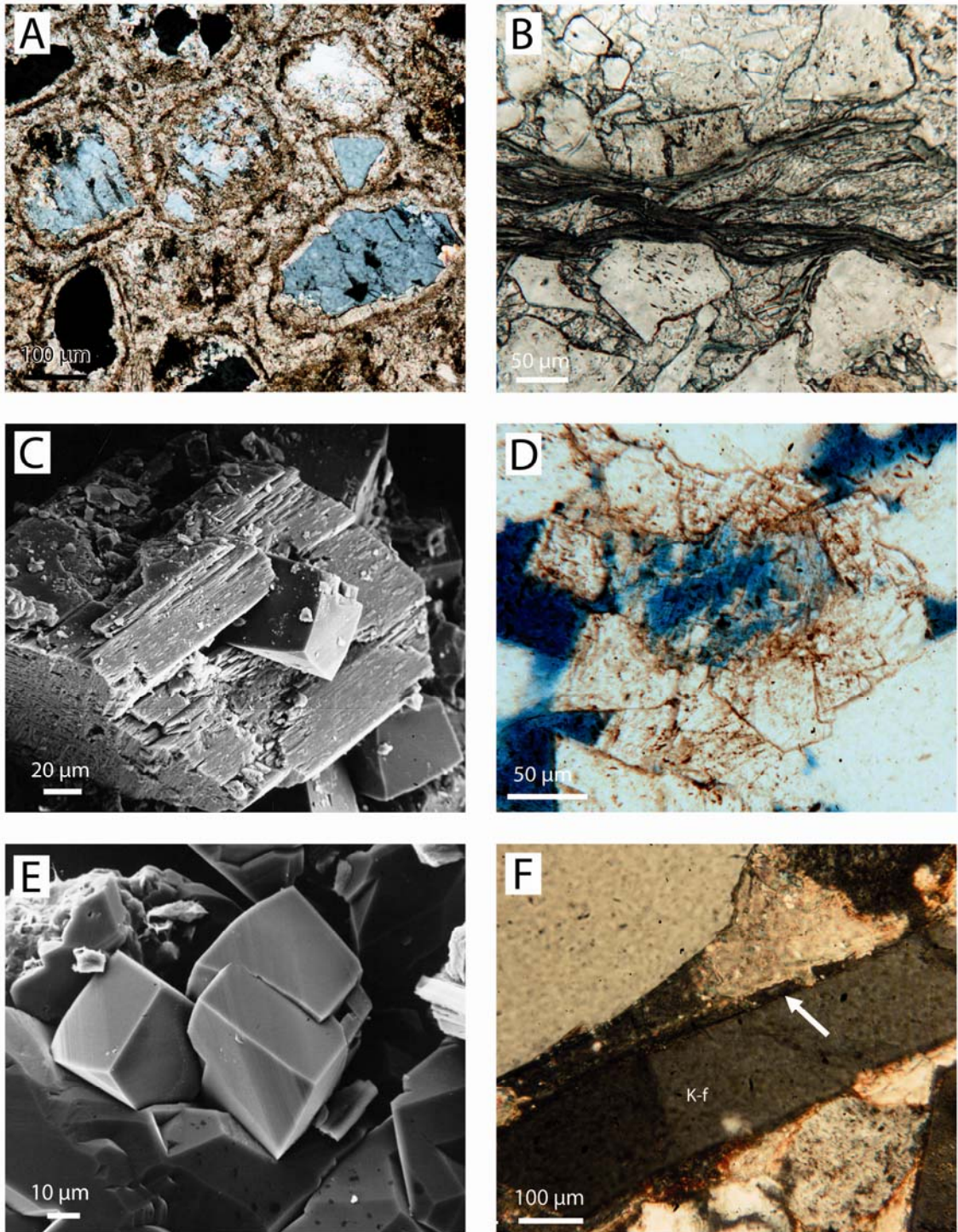
Fig. 5.11. *Carbonate diagenesis in the Skagerrak Formation. A. Calcrete showing radiating crystals on the detrital grains, Frederikshavn-2, 1050.95 m, crossed nicols. B. Early calcite cement precipitated between the cleavage planes of detrital chlorite, Gassum-1, 2153.73 m. C. Dolomite precipitation related to feldspar alteration. Gassum-1, 2153.71 m, scanning electron micrograph. D. Dolomite precipitation related to feldspar alteration, Gassum-1, 2153.40 m. E. Late dolomite precipitation after quartz overgrowth, Gassum-1, 2153.71 m, scanning electron micrograph. F. Late dolomite cement formed after feldspar overgrowth (marked by arrows) on detrital K-feldspar (K-f), Thisted-2, 2763.04 m.*
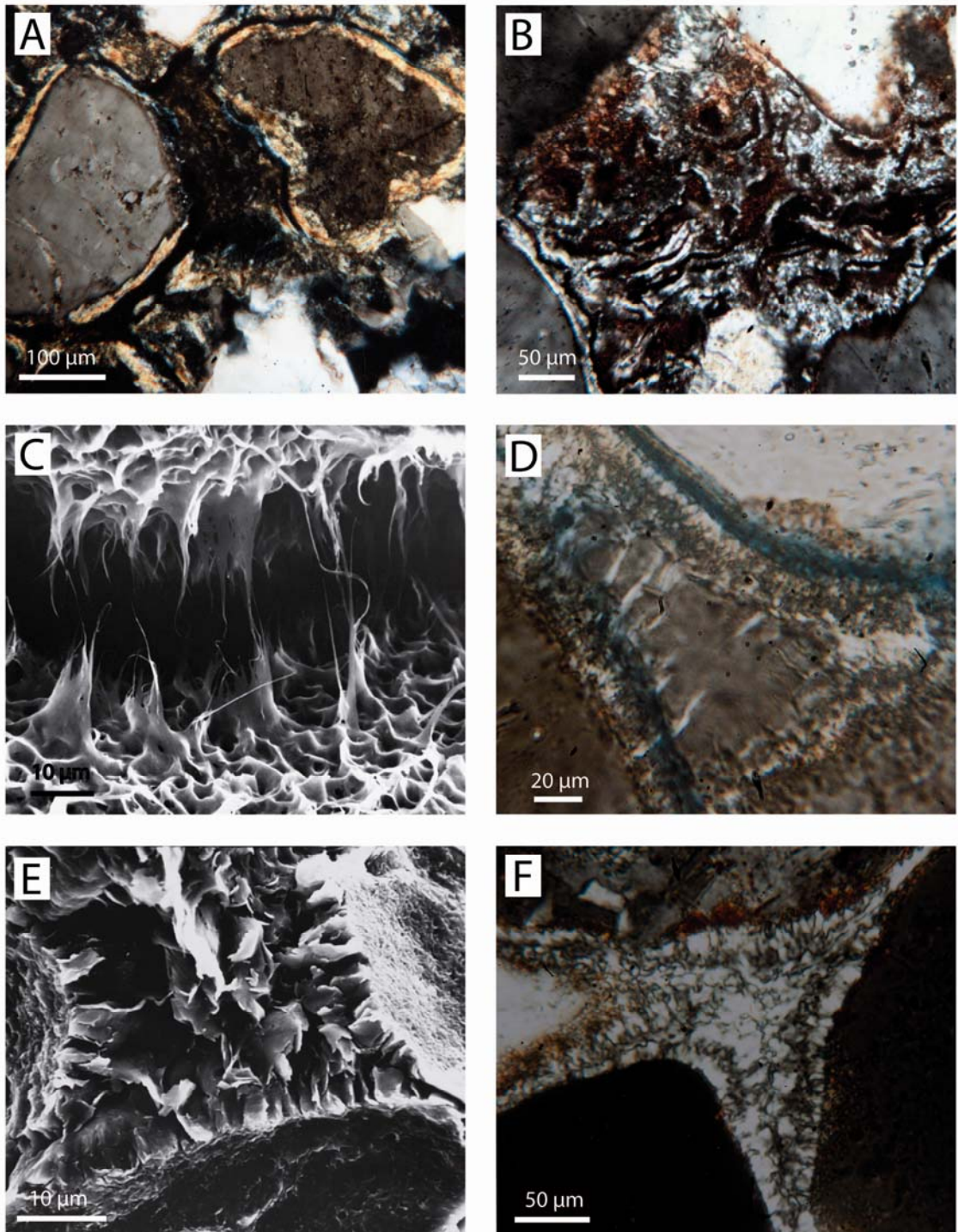
Fig. 5.12. *Clay minerals in the Skagerrak Formation. A. Smectitic infiltration clay orientated parallel to the detrital grain surface, Sæby-1, 1628.03 m, crossed nicols. B. Complete clay mineral and iron-oxide/hydroxide replacement of unstable silicate grain, Thisted-2, 2912.26 m, crossed nicols. C. Mixed-layer smectite/illte as indicated from their boxwork texture, from which illite whiskers grows, Thisted-2, 2761.40 m, scanning electron micrograph. D. Rim of illitic clay and illite whiskers prior to quartz cementation, Mors-1, 5081.93 m, crossed nicols. E. Rim of illitic clay preceding pore filling chloritic clays, Mors-1, 5032.22 m, scanning electron micrograph. F. Rim of illitic clay preceding pore filling chloritic clays, Mors-1, 5090.32 m, crossed nicols.*
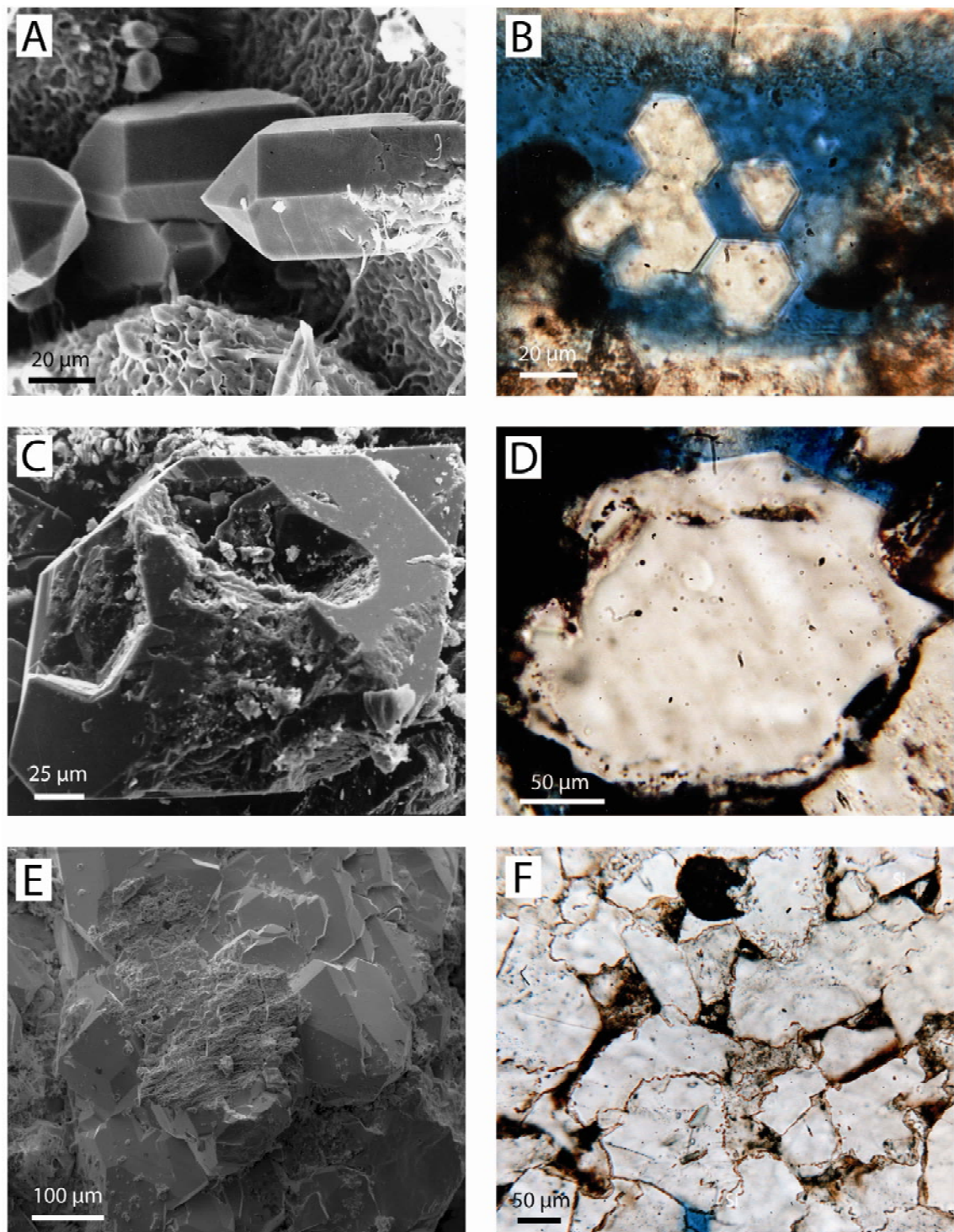
Fig. 5.13. *Quartz diagenesis in the Skagerrak Formation. A. Prismatic quartz outgrowths after thick clay coating, Thisted-2, 3162.29 m, scanning electron micrograph, B. Prismatic authigenic quartz in pore space, Thisted-2, 2919.33, C. Quartz overgrowths after iron-oxide/hydroxide coatings, Gassum-1, 2508.91 m, scanning electron micrograph, D. Quartz overgrowths after iron-oxide/hydroxide coatings Gassum-1, 2524.75 m, E. Quartz overgrowths enclosing partly dissolved feldspar, Vedsted-1, 2065.00 m, scanning electron micrograph, F. Pressure solution and sutured grain contacts between quartz grains, Gassum-1, 3122.48 m.*
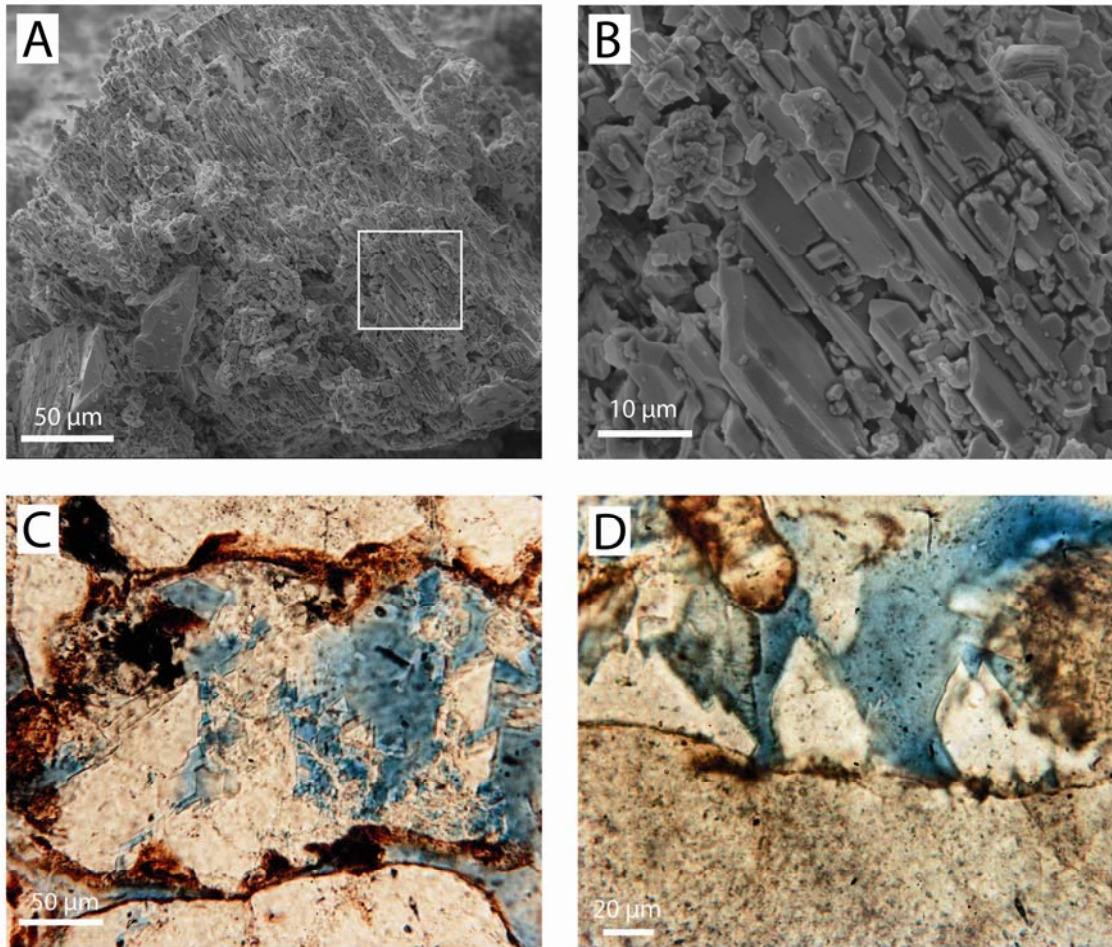
Fig. 5.14. *Feldspar alteration and authigenesis in the Skagerrak Formation. A. Partly dissolved detrital plagioclase with authigenic albite precipitations, Vedsted-1, 2064.94 m, scanning electron micrograph. B. Close up of A. C. Dissolution of feldspar (the iron-oxide/hydroxide coating marks to original size of the grain) and precipitation of feldspar (K-feldspar?), Thisted-2, 2764.62 m. D. Limited feldspar overgrowth formed after iron-oxide/hydroxide coating, Thisted-2, 2764.62 m.*
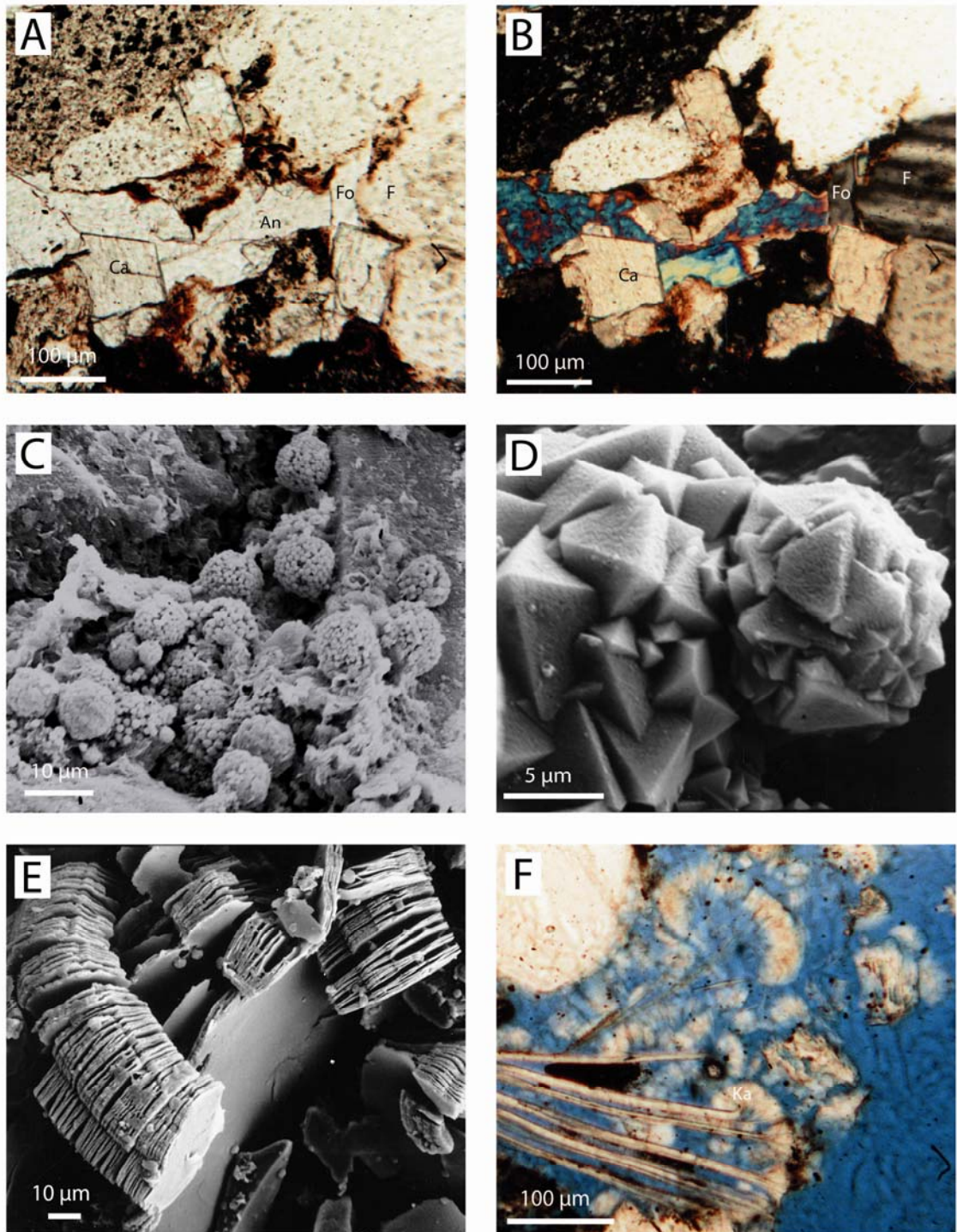
Fig. 5.15. *Minor authigenic phases in the Skagerrak Formation. A. Anhydrite (An) pore filling cement after carbonate cement (Ca) and feldspar overgrowth (Fo) on detrital feldspar (F), Thisted-2, 2763.04 m. B. As A, crossed nicols. C. Framboids of pyrite in reduction spot, Skagen-2, 562.00 m, scanning electron micrograph. D. Recrystallised framboids of pyrite in reduction spot, Gassum-1, 2153.73 m, scanning electron micrograph. E. Vermicular kaolinite, Frederikshavn-1, 1158.11 m, scanning electron micrograph. F. Kaolinite precipitated between the cleavage planes of muscovite, Sæby-1, 1613.25 m.*

Mineralogical changes with burial depth

The chronological order of these authigenic phases is shown in the paragenetic sequence of the Skagerrak Formation (Fig. 5.16).

Shortly after deposition of the Skagerrak Formation mineral alterations begin, such as dissolution of iron-magnesium silicates and leucoxene replacement of Fe-Ti oxides, which liberates iron. Due to the prevailing oxidising conditions in the interstitial water, a consequence of the arid to semi-arid climate during deposition of the Skagerrak Formation (Bertelsen 1980), direct precipitation of iron-oxides/hydroxides is promoted (Walker 1976; Durrance et al., 1978; Ixer et al., 1979, Weibel and Grobety, 1999). Direct precipitation of goethite occurs at shallow depths, whereas pseudomorphous transformation of goethite needles into hematite occurs in the deeper parts of the Skagerrak Formation (Weibel 1999; Weibel and Grobety 1999). Red coatings continued to precipitate into the early mesogenetic regime, as they can be observed between authigenic phases, such as mesogenetic quartz, dolomite and clays (Weibel 1998). Authigenic hematite is also recognised as overgrowths and replacement of other minerals.

The fact that the red pigments in most Mesozoic red sediments consist of hematite, whereas ferrihydrite and goethite are more common in younger sediments, has lead several authors (Van Houten 1961, Walker 1967, Schluger and Roberson 1975, Turner 1980) to the assumption that ferrihydrite and goethite ages into hematite. Though the Skagerrak Formation spans over approximately 30 Ma, it is all of Triassic age. Thus the transformation of goethite into hematite seems mainly to be temperature dependent (Weibel 1999, Weibel and Grobety, 1999).

Smectite is the dominant clay mineral of infiltration clays and 'rip-up' clasts from the shallow-buried part of the Skagerrak Formation. The honeycomb texture of illitic phases indicates transformation of smectite into mixed-layer illite/smectite and finally illite (Figs 5.12C & D; Weibel 1999). Transformation of smectite into random mixed-layer smectite-illite has occurred in the part of Skagerrak Formation exposed to estimated burial temperatures of 47-68°C (Weibel 1999). This is consistent with the findings of Sŕodoń (1984), who describes the transformation of smectite layers into illite layers in mixed-layer smectite-illite to begin at temperatures ~ 50°C, though the reaction rate may also depend on smectite chemistry and K-activity in the pore fluids (Chang et al. 1986; Ramseyer and Boles 1986). Ordered mixed-layer illite/smectite occurs in deep wells with an estimated burial temperature of > 74°C (Weibel 1999). Other investigations (Perry and Hower, 1970; Chang et al. 1986; Pearson and Small 1988; Pollastro 1993) suggest higher temperatures in the range of 90-125°C before ordering of mixed-layer illite/smectite takes place. This variation in temperatures may be a result of relatively high K-activity in the pore fluids possibly caused by K-rich brines from the underlying Zechstein evaporates. Authigenic illite, recognised by its fibrous appearance (Fig. 5.12C), occurs in samples exposed to maximum burial temperatures > 105°C (Weibel 1999).

Smectite transformation into random mixed-layer smectite/chlorite occurs at 58°C estimated minimum burial temperature, and into ordered mixed-layer chlorite/smectite (corrensite) at > 105°C in the Skagerrak Formation. Ordering of mixed-layer smectite/chlorite has been observed to take place at 60°C in sandstones and 70°C in shales (Chang et al. 1986)

whereas corrensite forms at temperatures > 100°C in mudrocks (Hillier 1993). Direct precipitation of chlorite may have been favoured by the liberated elements from the transformation of smectite into illite (see Burley 1984).

Kaolin is abundant in shallow wells where it is associated with alteration of muscovite and feldspars, but decreases in abundance with increased burial depth (Weibel 1999). A vermicular morphology is common in samples from shallow wells, whereas blocky crystal growth between the vermicular flakes occurs at increased burial depth; and at maximum burial depth kaolin has a blocky morphology. Formation of kaolin due to meteoric water flushing (Bjørlykke and Aagaard, 1992) can only be considered a possibility under the humid condition during deposition of the following Gassum Formation and in case of very slow burial. Recycling of the Skagerrak Formation during deposition of the Gassum Formation is another possible explanation. Replacement of vermicular kaolin with a more blocky morphology (probably dickite) begins at estimated burial temperatures < 75°C (Weibel 1999). Investigations by Ehrenberg et al. (1993) show that transformation of vermicular kaolinite to blocky dickite occurs at ~ 120°C, however this may reflect the completion temperature, whereas the 75°C reflects the onset of the transformation, which seems to be a gradual process, as described Beaufort et al. (1998).

Two or more episodes of quartz precipitation occur. The first formation of prismatic authigenic quartz outgrowths, rather than quartz overgrowths, probably reflects a limited silica concentration in the pore fluid as well as limited access to detrital quartz surfaces due to thick clay rims or red coatings. Thus authigenic clay rims and iron-oxide/hydroxide coatings inhibit quartz diagenesis, as previously described for chlorite (Ehrenberg, 1993) and illite (Storvold et al. 2002). Macroquartz is more abundant in the deeper wells (Mors-1, Thisted-2 and Gassum-1) probably reflecting increased liberation of silica from feldspar alteration, and from pressure solution in the samples with the lowest content of ductile fragments (mica, rock fragments) and authigenic clays. The sandstones in the Gassum-1 well generally have lower contents of ductile fragments and thinner red coatings, consequently fractural healing, pressure solution and thick quartz coatings are more abundant here. The quartz diagenesis is thus depending on the detrital composition and the previous diagenetic evolution as well as the burial depth.

The micritic carbonate cement is formed early diagenetic, as it exhibit displacive growth textures (between cleavage planes of expanded mica) and it forms rims of radiating crystals on detrital grains and is frame-work supporting. The carbonate thus exhibits several of the Alpha calcrete fabric elements described by Wright (1990). Calcrete is only found in relatively shallow parts of the Skagerrak Formation from the northeasternmost wells (Frederikshavn-1, -2, Skagen-2 and Flyvbjerg-1). Calcrete and dolocrete are common in the arid to semi-arid Triassic non-marine sediments (i.e. Mader 1983; Burley 1984). Calcrete was either not formed in the deeper part of the Skagerrak Formation or recrystallisation and growth of larger crystals at the expense of smaller may have taken place at deeper burial depths. Formation of calcrete can only take place if there is discontinued sedimentation and time enough for pedogenetic processes to be active. In marginal areas, dominated by ephemeral streams, mature calcretes developed, whereas in the distal, sandy braided stream environments with more continuous sedimentation poikilotopic and nodular cements

formed instead (Burley 1984). Alluvial fan deposits characterise the Skagerrak Formation in the proximal northeasternmost part of the Norwegian-Danish Basin, whereas braided stream deposits are more dominating towards the distal southwesternmost part of the basin. Lack of pedogenetic developments in the southwesternmost part may therefore best explain the observed lateral differences in the Skagerrak Formation.

Poikilotopic carbonate cement probably forms later. The pore filling carbonate often has a radiating extinction thereby resembling saddle dolomite. Saddle dolomite forms at temperatures higher than 60-80°C and lower than 90-160°C under the influence of pore fluids of higher salinity than seawater (Spötl and Pitman 2009). Occasionally the poikilotopic carbonate cement is calcite or ankerite cement. Ankerite can form at temperatures similar to dolomite, i.e. 110-165°C in the Triassic Sherwood Sandstone Group, U.K. (Schmid et al. 2004).
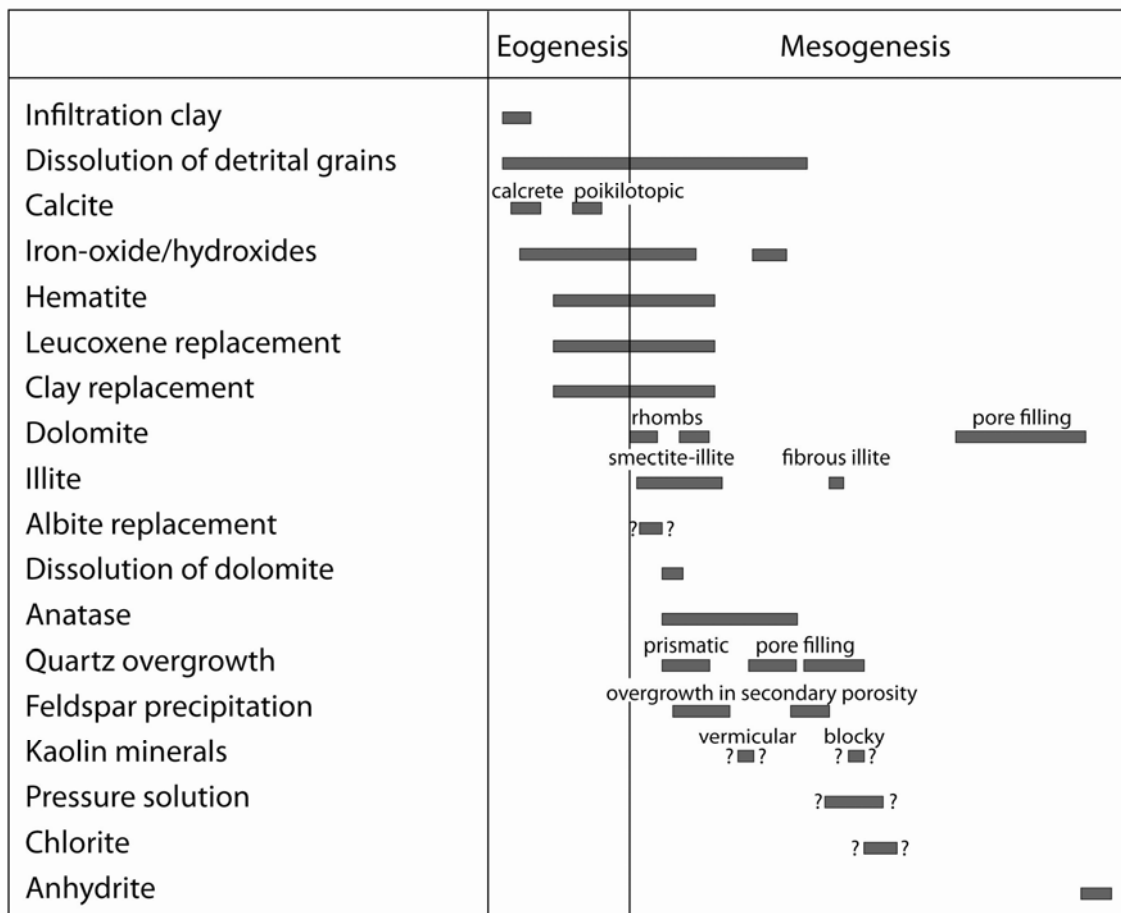

Fig. 5.16. *Diagenetic sequence for the Skagerrak Formation, simplified after Weibel (1998).*

5.3 Gassum Formation

The Upper Triassic – Lower Jurassic shallow marine and paralic sandstones of the Gassum Formation) are present in most of Denmark (Fig. 1; Nielsen 2003). It occurs with thicknesses up to 400 m (Mathiesen et al. 2009) and present day burial depths varying from 550–3350 m.

Detrital composition

The Gassum Formation comprises fine to medium-grained, well-sorted sand with occasional oversize clay clasts between otherwise subangular to subrounded detrital grains. Rare bimodal sorting of the sand can be found in samples from the Vedsted-1 well. The sandstones of the Gassum Formation are mainly subarkoses and arkoses (Figs 5.1 & 5.17; Friis 1987) according to the classification by McBride (1963). Monocrystalline quartz, with subordinate polycrystalline quartz, dominates the framework grains. The feldspar abundance varies across the Danish Subbasin and feldspar is relatively more abundant in the northwestern part than in the eastern part. K-feldspar is generally the dominating feldspar in the northern part of Denmark, whereas albite is characteristic in the eastern part of Denmark, i.e. in the Stenlille wells (Fig. 5.17; Appendix 2). Ca-rich plagioclase has not been identified. Alteration of feldspar grains includes partly dissolution, seritization, replacement by kaolin or carbonate and incipient albitisation in the deepest buried sandstones. Some oversize pores with clay-lining mould ("ghost rim") are inferred to originate from completely dissolved feldspar grains. Rock fragments are generally rare; the only exception being the very coarse-grained sandstones. Plutonic, micaceous metamorphic and sedimentary rock fragments are equally abundant. Mica is present in all samples and is commonly abundant in the fine-grained samples. Mica is dominated by muscovite with subordinate biotite and chlorite. Mica shows varying degree of alteration from expansion along cleavage planes caused by precipitation of authigenic minerals (e.g. siderite) to compaction along stylolites in the deepest wells. Organic matter occurs in most samples. Accessory minerals include tourmaline, rutile, zircon and opaque heavy minerals, the latter being dominated by ilmenite intensively altered to leucoxene.

Authigenic phases

The porosity reduction is mainly due to compaction in sandstones of burial depths down to 1500 m (Friis, 1987). The exception is occasionally extensive siderite precipitation in mica rich samples. At increasing burial depth quartz diagenesis, carbonate precipitation and feldspar alteration becomes important porosity influencing processes, whereas pyrite only locally may be important as pore filling cement (Figs 5.18, 5.19, 5.20, 5.21, 5.22, 5.23 & 5.24).

Siderite is the first authigenic phase and appears as occasional displacive spherulites and numerous rhombs (up to 15 µm large) in the open pore space or between cleavage planes of mica (preferentially biotite or chlorite) resulting in expansion of the micas original size (Fig. 5.19A, B & D). The last type of siderite has only been identified in shallow buried sandstones, where it may be a porosity reducing factor.

Pyrite is ubiquitous in all samples and may occur in three phases, first framboids, followed by euhedral crystals and presumably a tertiary pore filling cement (Fig. 5.20). Pyrite is commonly associated with organic matter or altered Fe-bearing minerals e.g. ilmenite replaced by leucoxene. Pyrite framboids precipitate early diagenetic more or less simultaneously with the siderite rhombs, as pyrite framboids may occur enclosed in the siderite rhombs (Fig. 5.20C) or nucleated on them. Euhedral pyrite crystals enclose pyrite framboids and kaolin booklets (Figs 5.21D & E). Pore filling pyrite commonly encloses partly dissolved K-feldspar grains. Marcasite has been observed in a few samples, where it occurs as clusters of crystals and, locally, as pore filling cement and, occasionally, partly inside pyrite concretions.

Kaolin booklets typically fill the primary pores commonly adjacent to partly dissolved feldspar grains and more rarely within the intragranular porosity, i.e. the secondary porosity of feldspar and mica. Kaolin in oversize pores is inferred to represent replacement of detrital feldspar grains (Figs 5.21A, E & F). Extremely fine kaolin crystals form between the cleavage planes of mica, in particular muscovite, leading to expansion of its original size. Fine kaolin crystals may also occur in secondary porosity possibly as replacement of mica. Kaolin booklets may be enclosed in euhedral pyrite crystals, authigenic quartz and ankerite.

Authigenic quartz, as syntaxial overgrowths, is common in most samples (Figs 5.22 & 5.23). The amount of authigenic quartz may be underestimated, where there are no distinct boundary between the overgrowths and the detrital grain, i.e. poorly developed dust lines. However, the size of individual quartz overgrowths may be up to 100 µm on monocrystalline quartz grains (Friis 1987). Authigenic quartz encloses authigenic anatase, pyrite and clay minerals as chlorite, illite, kaolin (Figs 5.21, 5.23A, 5.22F & 5.24F),whereas barite and ankerite enclose authigenic quartz.

The carbonates (mainly ankerite) can be pervasive in intensely cemented samples or appearing as rhombohedrons (typically calcite and siderite) in sporadic cemented parts (Figs 5.19C, D, E & F). Pore filling carbonate can be corrosive or replasive towards all other minerals. Siderite rhombehedrons, on the other hand, tend to have displasive growth and may occasionally in shallow buried sandstones form intensely cemented parts of the sediments. Calcite and siderite dominate in the Stenlille-18 well, whereas ankerite dominates some samples in the Vedsted-1 well (Appendix 1). XRD analysis showed that dolomite is the dominating carbonate cement in the Aars-1 well (Krabbe & Nielsen 1984; Larsen 1986). However, microprobe analysis showed that the actual composition of the carbonate resembles ankerite more than dolomite (Friis 1987). Ankerite cement commonly encloses remnants of detrital albite. Siderite is abundant in the fine-grained facies (mudstones and the heterolithic sandy/silty-mudstones), whereas ankerite dominates the more coarse-grained facies with coarse to fine-grained sandstones (Friis 1987).

Volumetrically minor authigenic phases in the deep wells include illite, chlorite, pyrite, albite and K-feldspar. Chlorite is important, in specific samples, as pore lining and pore filling cement. Chlorite abundance is related to depositional environment in such a way that chlorite forms very thick coatings in offshore sandstones, but thinner coatings in shoreface and estuarine environments, and chloritic clay coatings have even been observed in fluvial de-

posits (Fig. 5.21F). Chlorite typically constitutes less than 2 % of the clay minerals (Schmidt 1985; Friis 1987).

Authigenic albite occurs as overgrowths and as crystals growing on remnants of partly dissolved detrital feldspar grains. Though authigenic albite is common in samples of intermediate or deep burial (i.e. from the Gassum-1 and deeper wells) it is of minor volumetric importance. Authigenic K-feldspar besides authigenic albite on detrital feldspar grains were described in samples with burial depths of more than 1500 m by Friis (1987).

Rare pore filling barite encloses authigenic quartz (Fig. 5.25A) and is enclosed in ankerite. Anatase occurs as replacement of detrital Fe-Ti oxides and as single crystals formed in the open pore space (Figs 5.25A, E & F). Rare apatite overgrowths occur on detrital apatite and rare monazite encloses kaolin and possibly authigenic albite (Fig 5.25C). Authigenic anatase, pyrite and crandallite group minerals occur in association with stylolites (Figs 5.25D & F).

Meniscus forming clays containing tiny barite and fluorite crystals, found in the Stenlille-18 and Stenlille-12 wells, are considered to be infiltrated drilling mud. The smectitic clays identified by XRD are probably drilling mud and consequently not part of the Gassum Formation.

Porosity and permeability
Primary porosities (from point counting) up to 34 % have been registered in the shallowest sandstones (in the Thisted-3 well, 1180 m). With increasing burial the average porosity decreases and the contribution from secondary porosity increases (up to 5 % in the Aars-1 well out of a total porosity of 10 %).
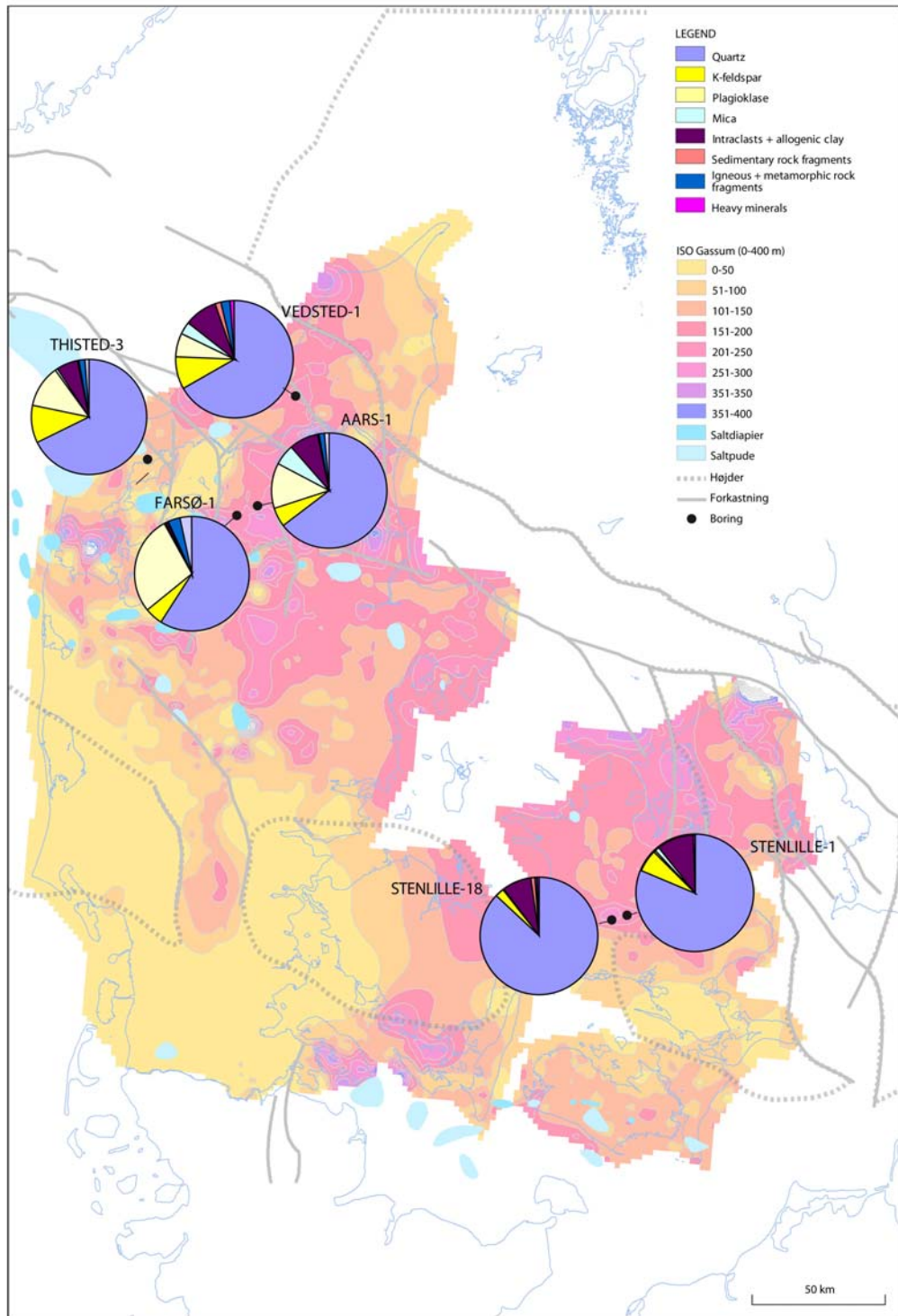
Fig. 5.17. *Average detrital composition of the Gassum Formation shown as pie diagrams for each analysed well on isopach map of the Gassum Formation (modified after Mathiesen et al. 2009).*
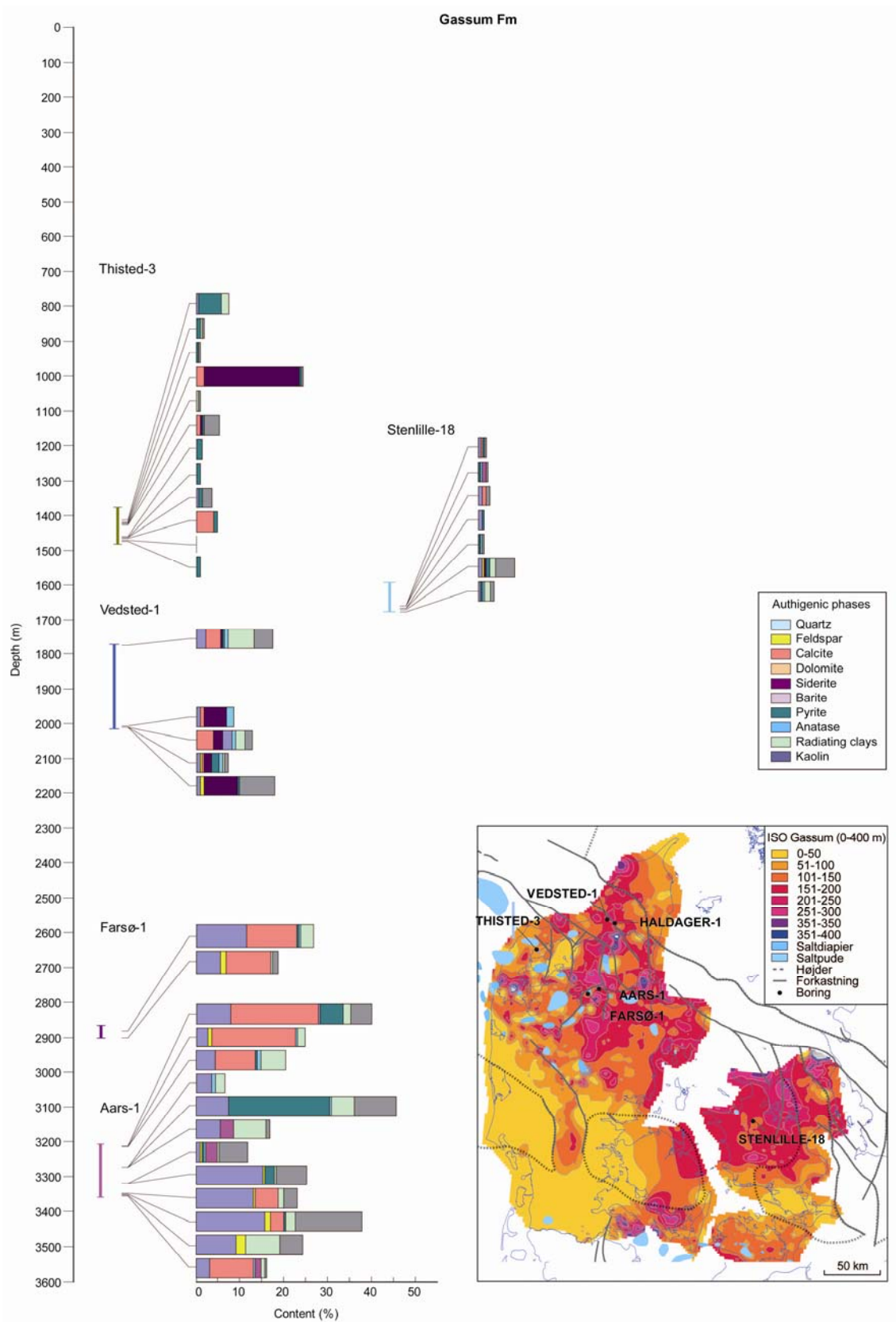
Fig. 5.18. *Authigenic phases, quantified by point counting, in the Gassum Formation for different wells and consequently different burial depths.*
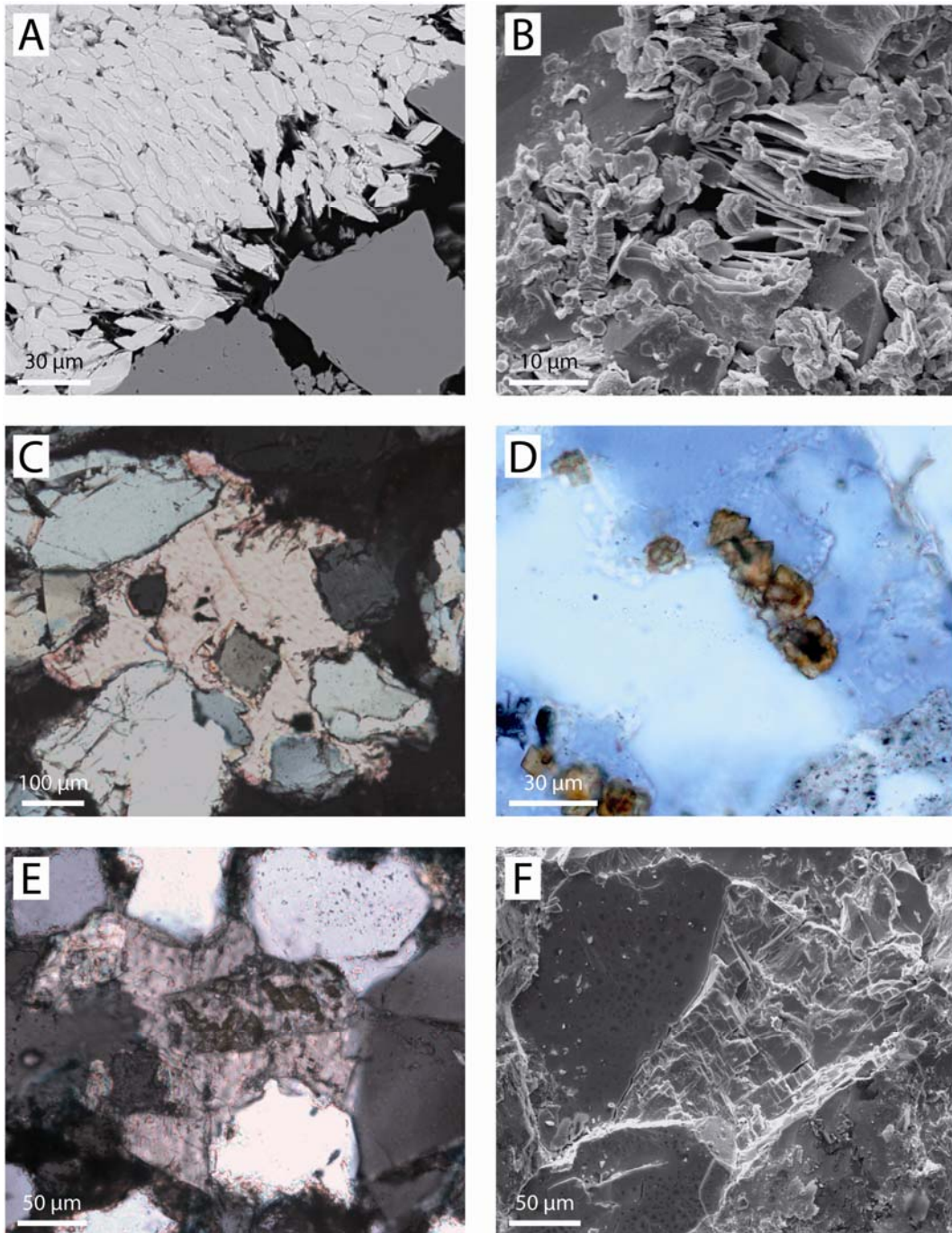
Fig. 5.19. *Carbonate diagenesis in the Gassum Formation. A. Siderite rhombs growing between the cleavage planes in mica, thereby expanding its size several times, Gassum-1, 1540.16 m, backscatter electron micrograph. B. Siderite growing between the cleavage planes in mica, Vedsted-1, 2010.12 m, scanning electron micrograph. C. Pore filling carbonate (calcite?) cement, Thisted-3, 1225.62 m, crossed nicols. D. Siderite cores with ankerite rims, Vedsted-1, 2009.69 m. E. Pore filling ankerite cement growing around partly dissolved K-feldspar (stained), Aars-1, 3215.70 m, crossed nicols. F. Pore filling ankerite cement around quartz grains, Aars-1, 3208.75 m, scanning electron micrograph.*
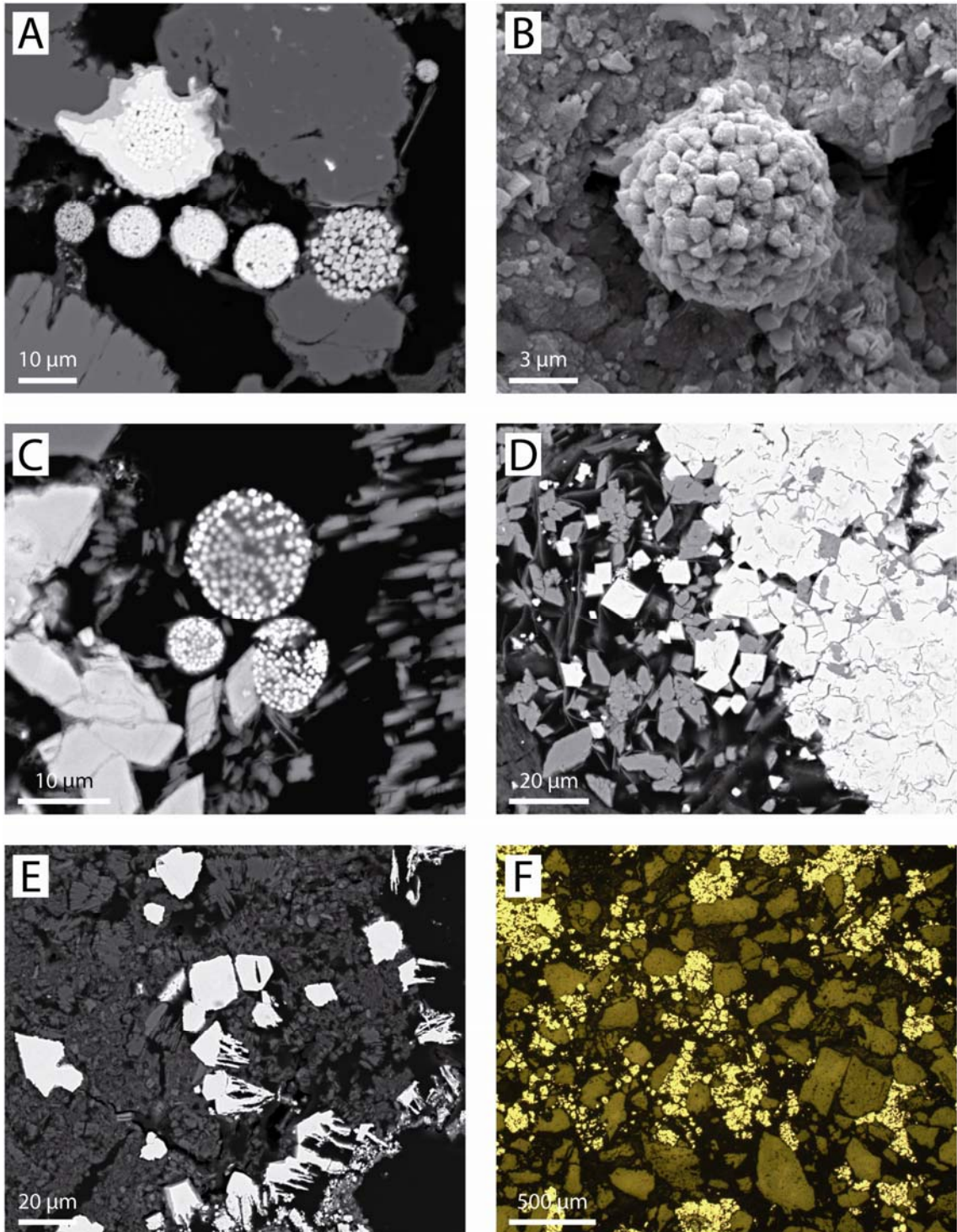
Fig. 5.20. *Pyrite diagenesis in the Gassum Formation. A. Pyrite framboids in a row and one pyrite framboid enclosed in euhedral pyrite, Frederikshavn-2, 925.61 m, backscatter electron micrograph. B. Pyrite framboid, Stenlille-18, 1662.47 m, scanning electron micrograph. C. Pyrite framboids, some enclosed in siderite rhombs, Gassum-1, 1540.16 m, backscatter electron micrograph. D. Euhedral and concretionary pyrite enclosing siderite rhombs, Frederikshavn-2, 885.85 m, backscatter electron micrograph. E. Euhedral pyrite enclosing kaolin crystals, Stenlille-18, 1662.07, backscatter electron micrograph. F. Pore filling pyrite, Thisted-3, 1211.25 m, reflected light.*
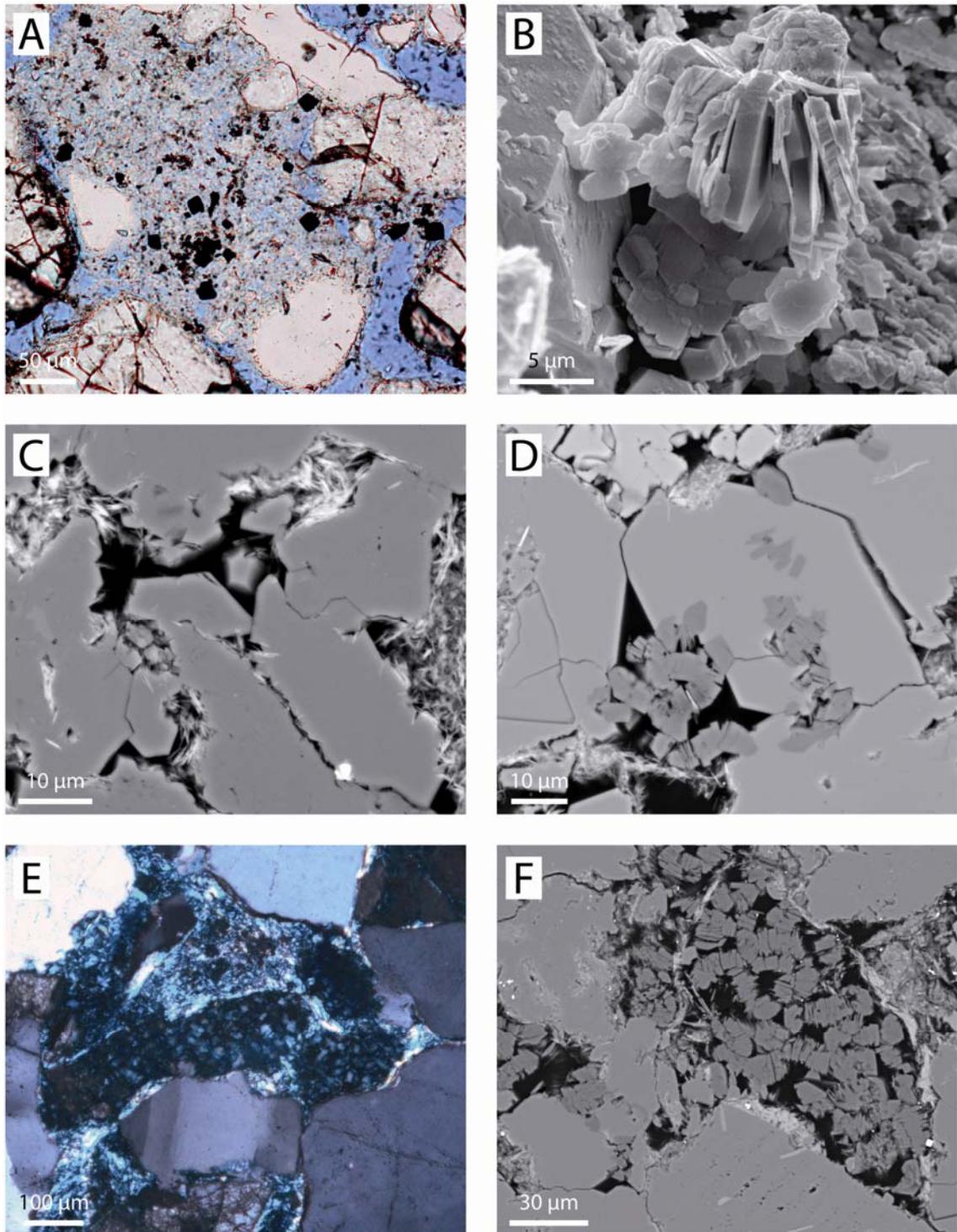
Fig. 5.21. *Clay minerals in the Gassum Formation. A. Kaolin and pyrite filling an oversized pore, Stenlille-18, 1662.45 m. B. Blocky dickite growing between vermicular kaolinite, Vedsted-1, 2010.12 m, scanning electron micrograph. C. Illite rims partly captured in authigenic quartz, Farsø-1, 2880.11, backscatter electron micrograph. D. Kaolin enclosed in authigenic quartz, Aars-1, 3208.72 m, backscatter electron micrograph. E. Moldic pores marked by illite rims and partly filled by kaolin minerals, Aars-1, 3321.52 m, crossed nicols. F. Chlorite rim around completely kaolin replaced grain, Aars-1, 3208.72 m, backscatter electron micrograph.*
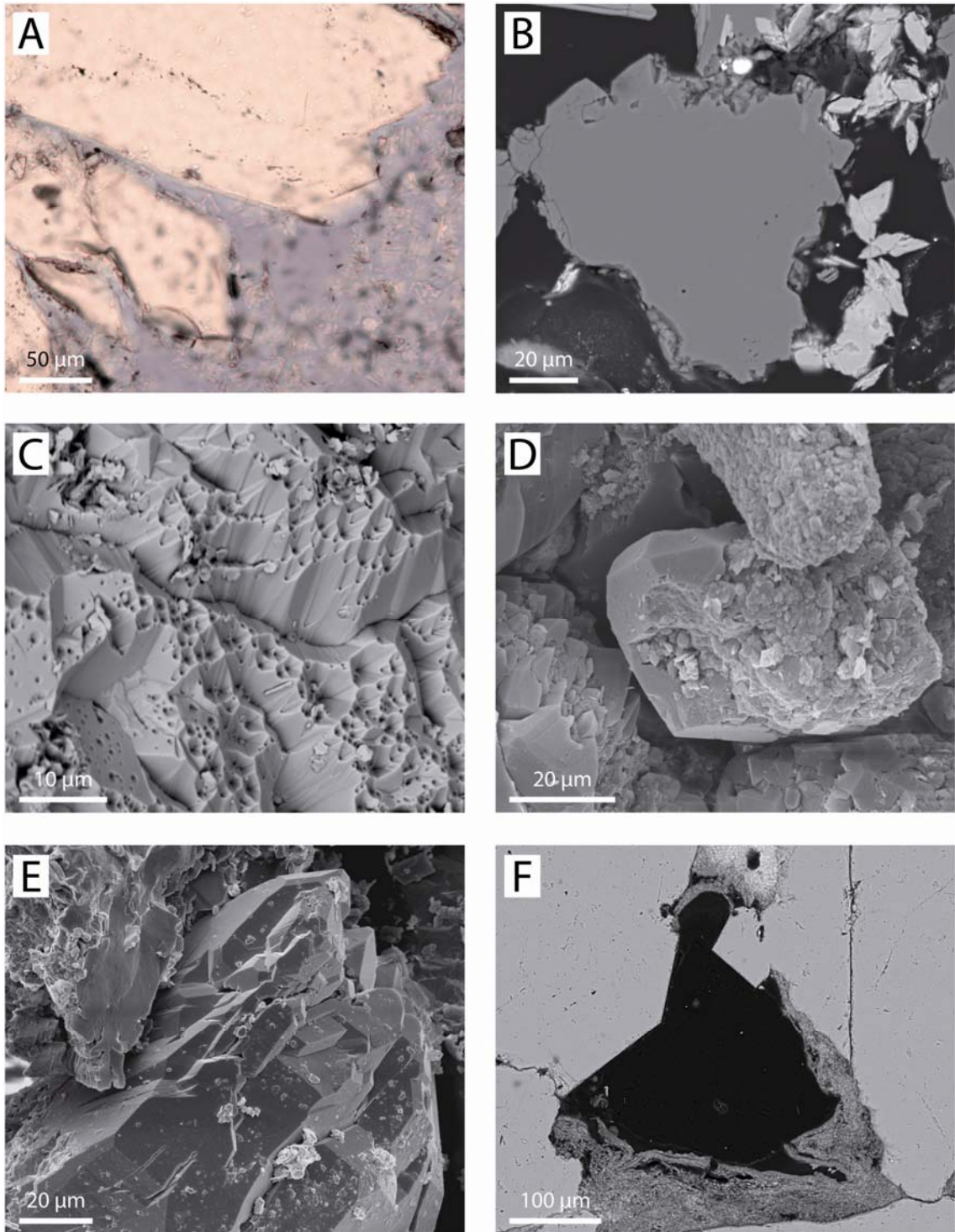
Fig. 5.22. *Quartz diagenesis in the Gassum Formation. A. Small quartz overgrowth, Thisted-3, 1211.03 m. B. Small quartz overgrowths, Gassum-1, 1540.16 m, backscatter electron micrograph. C. Authigenic quartz in shape of 'quartz mountains', Thisted-3, 1225.62 m, scanning electron micrograph. D. Limited quartz overgrowths on detrital quartz, Thisted-3, 1173.68 m, scanning electron micrograph. E. Macroquartz completely covering the detrital quartz grain, Vedsted-1, 2010.12 m, scanning electron micrograph. F. Quartz overgrowths inhibited where thick chlorite coatings are present, Farsø-1, 2869.85 m, back-scatter electron micrograph.*
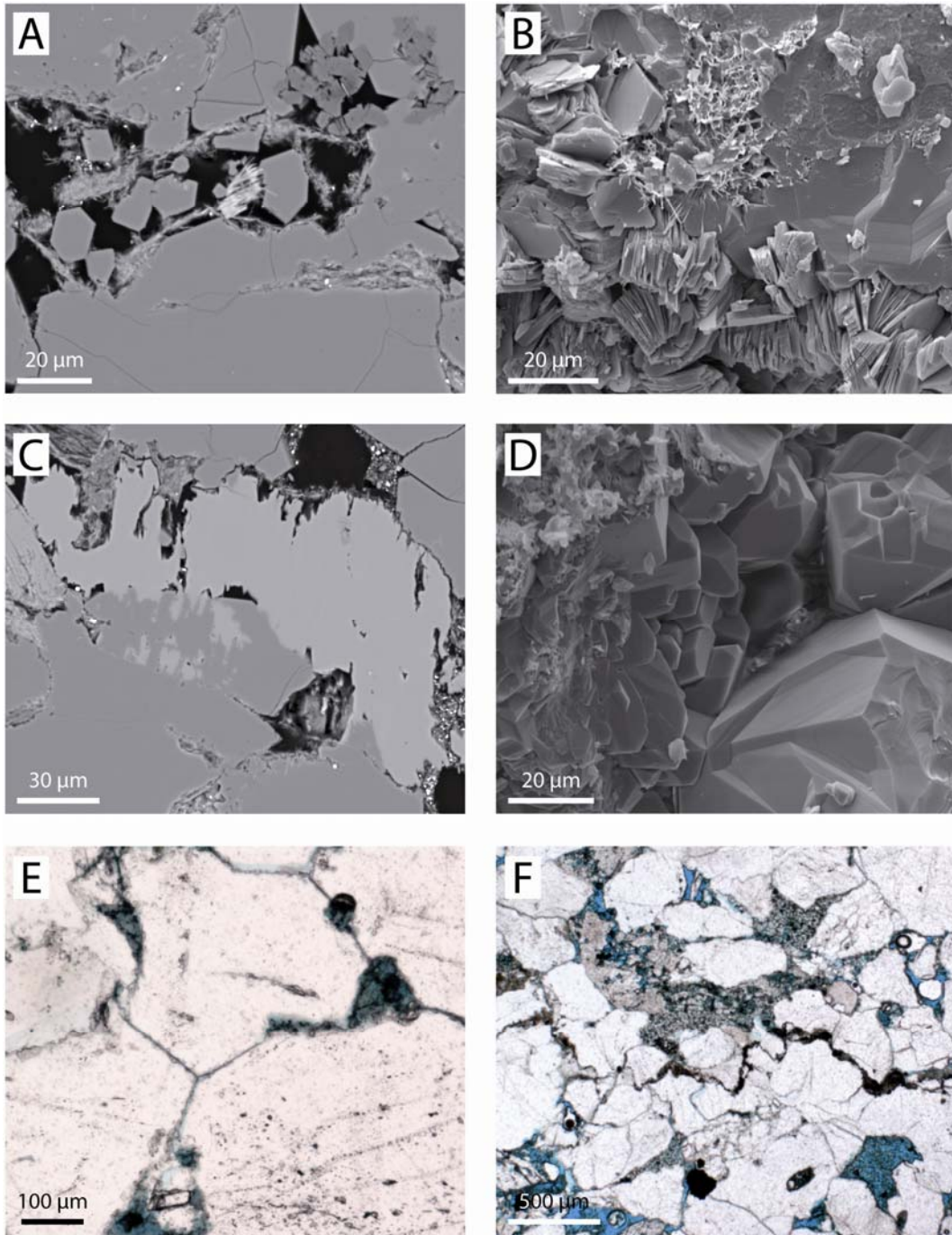
Fig. 5.23. *Quartz diagenesis in the Gassum Formation. A. Authigenic quartz enclosing kaolin minerals and chlorite, which locally seem to inhibit the authigenic quartz growth, Aars-1, 3208.72 m, backscatter electron micrograph. B. Authigenic quartz enclosing illite and kaolin minerals, Aars-1, 3275.35 m, scanning electron micrograph. C. Authigenic quartz growing into secondary porosity after K-feldspar dissolution, Aars-1, 3208.72 m, backscatter electron micrograph. D. Macroquartz on all detrital quartz grains, Aars-1, 3208.40 m, scanning electron micrograph. E. Macroquartz completely closing the primary porosity, Aars-1, 3319.65 m. F. Stylolite marked by concentration of bending mica, Aars-1, 3277.45 m.*
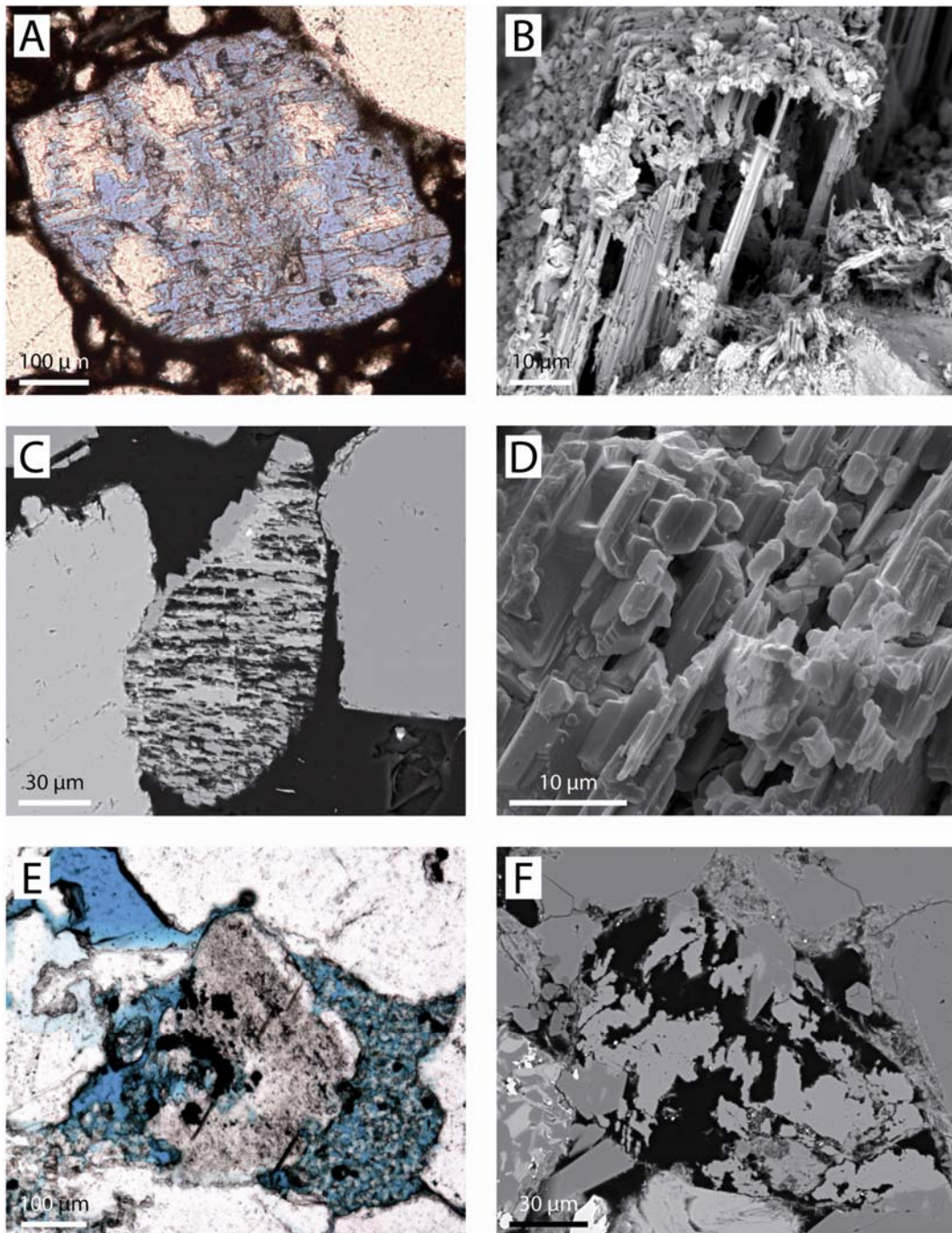
Fig. 5.24. *Feldspar alteration and authigenesis in the Gassum Formation. A. Feldspar dissolution after pore filling siderite formation, Thisted-3, 1183.95 m. B. Intense feldspar dissolution, Thisted-3, 1233.38 m, scanning electron micrograph. C. Albite overgrowths on perthite remnants, where the intergrown K-feldspar is partly dissolved, Gassum-1, 1640.03 m, backscatter electron micrograph. D. Authigenic albite precipitated on partly dissolved feldspar, Vedsted-1, 2010.03 m, scanning electron micrograph. E. Feldspar overgrowth on partly altered feldspar grain, Aars-1, 3277.45 m. F. Secondary porosity after partly dissolved K-feldspar which original outline is marked by a chloritic rim. Authigenic quartz grows partly into the secondary porosity, Aars-1, 3208.72 m, backscatter electron micrograph.*
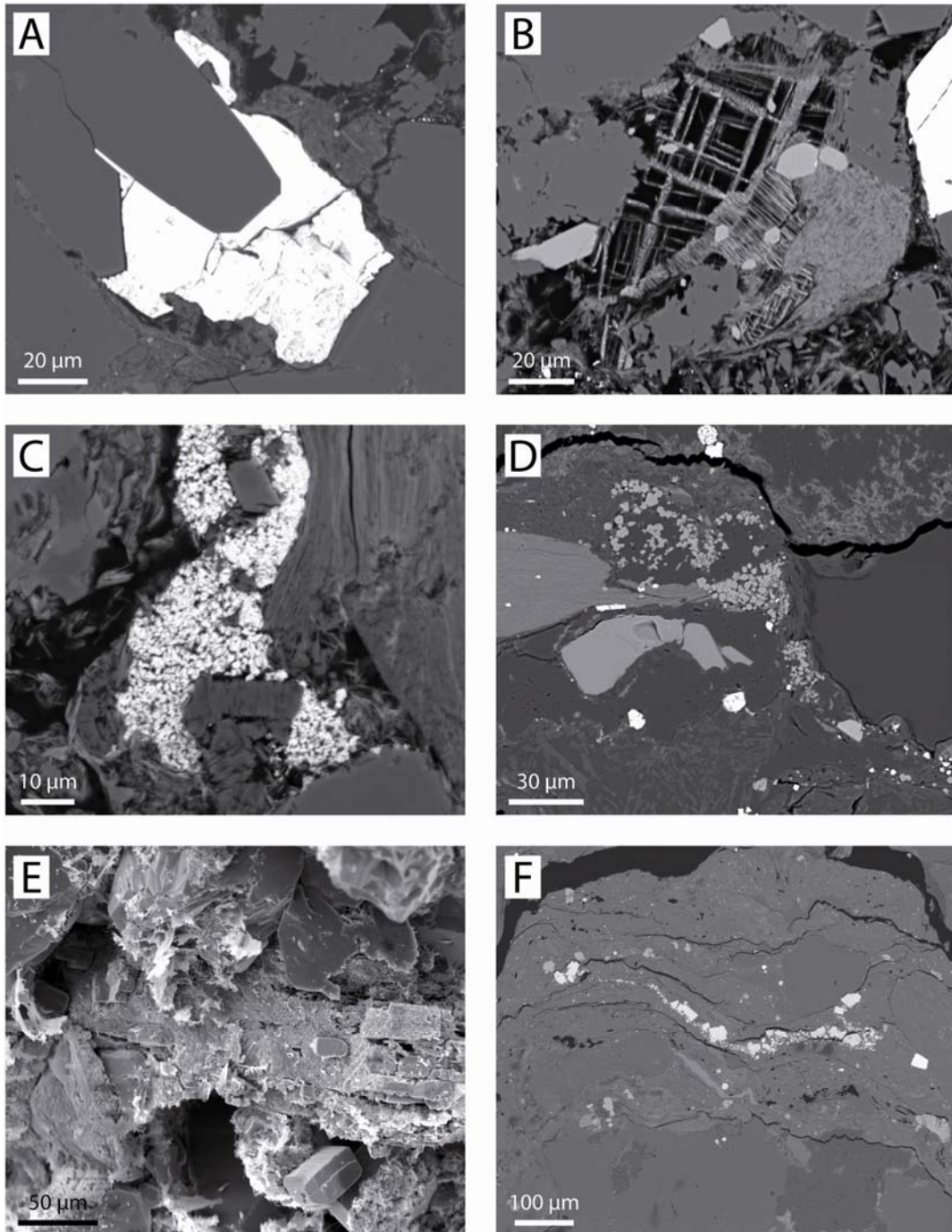
Fig. 5.25. *Accessory authigenic phases in the Gassum Formation. A. Pore filling barite formed after authigenic quartz, illitic and chloritic rims, Aars-1, 3208.72 m, backscatter electron micrograph. B. Apatite precipitating after leucoxene replacement of Fe-Ti oxide, Aars-1, 3208.72 m, backscatter electron micrograph. C. Authigenic monazite enclosing kaolin and authigenic? albite, Vedsted-1, 2007.77 m, backscatter electron micrograph. D. Crandalite group minerals precipitated along stylolite zone, Aars-1, 3352.54 m, backscatter electron micrograph. E. Anatase on partly dissolved leucoxene, Aars-1, 3353.05 m, scanning electron micrograph. F. Pyrite and anatase precipitated in the stylolite zone, Aars-1, 3352.54 m, backscatter electron micrograph.*

Mineralogical changes with burial depth

The chronological order of the authigenic phases is shown in the paragenetic sequence of the Gassum Formation (Fig. 5.26).

In a vegetated humid environment, as during deposition of the Gassum Formation, the organic matter plays an important role in the eogenesis. Organic matter creates reducing conditions, under which iron is highly solvable, and it serves as an energy sources for microbes. Sulphate reducing bacteria promote the precipitation of pyrite framboids, which therefore commonly form near organic matter. Iron-oxides and -hydroxides (ferrihydrite, lepidocrosite, goethite and hematite) are unstable under the reducing conditions and are considered possible sources for pyrite framboids (Canfield et al. 1992). Textural evidence suggests that altered Fe-Ti oxides acts as an iron source for euhedral pyrite in the Gassum Formation during increased burial and probably only where iron sources are limited (possibly in deltaic or fluvial deposits). The pyrite formation slows down during burial, as less reactive organic matter is available and due to more slowly liberation of iron from detrital iron-rich minerals (Canfield et al. 1992). Concretionary pyrite precipitation in the Aars-1 well seems to have formed beneath a marine (transgressive) erosional boundary. The level containing pyrite concretions have probably been situated in the sulphate reducing regime for a longer period than comparative sediments. Ferric iron, which is highly solvable, is likely to migrate to such places of sulphate reduction (Berner 1969).

The displasive growth of siderite (spherulite and precipitation in between cleavage planes of mica; Fig. 5.19A) and its interaction with pyrite framboids emphasise its early diagenetic formation. Alternating pyrite and siderite precipitation occurs early diagenetic in the Gassum Formation and can be related to small changes in pH and Eh conditions or variations in CO_3^{2-} or H_2S saturation (Coleman & Raiswell 1981). Sulphate reducing bacteria can under specific conditions (in a consortium with microbial fermenters) reduce Fe^{3+} using hydrogen, formed during fermentation, instead of sulphate (Coleman 1993). During bacterial sulphate reduction, simple organic molecules (CH_2O) are oxidised to HCO^{3-}, which can precipitate as carbonates and siderite if the Fe-content is not limited. In this way, the same sulphate reducing bacteria may promote formation of pyrite or siderite depending on the associated microbial activity. Siderite is therefore not necessarily an indicator of methanogenic environments where little or no sulphate is present (as suggested by e.g. Thyne and Gwinn, 1994; Bailey et al., 1998) nor does alternating pyrite and siderite precipitation have to be explained by moving freshwater/seawater interface as a response to sea level changes (as suggested by Machemer and Hutcheon, 1988). Mica may have liberated iron during its alteration, or served as a protective site for the bacteria colony, which could explain the numerous siderite crystals that precipitate between the mica cleavage planes and result in expansion of mica to several times its original size.

The ankerite rims on the siderite cores in the Gassum Formation are clear evidence that with increased burial the Fe content of the pore fluids decreases and the carbonate cement becomes more Mg (and Ca) rich. This phenomenon is also known from fluvio-deltaic sedi-

ments from the Norwegian North Sea (Hammer et al. 2010) and from the Salam field (Egypt's Western Desert) (Rossi et al. 2001). A change from a brackish influenced pore water to more marine influenced pore water (for example by marine transgression of lagoonal sediments) could also lead to relatively increase of Mg, Mn and Ca in the siderite as observed in spherulitic siderite in Holocene coastal deposits (Choi et al. 2003) and in siderite from fluvial-deltaic sediments under influence from marine waters (Rossi et al. 2001). The estimated temperatures (140-170°C) of ankerite formed at deep burial (c. 3500-4500 m) in Jurassic sandstone from Central North Sea (Hendry et al. 2000) seem to be rather high compared to the burial depth of sandstones containing ankerite cement in the Gassum Formation. The differences may come from a relatively longer period of ankerite precipitation in the Gassum Formation, though ankerite, similar to the Jurassic sandstone in the Central North Sea, is one of the last forming authigenic cements.

Preferential occurrence of chlorite in marine influenced sediments (thickest chlorite coating is observed in the offshore sandstones) suggests that chlorite formed early diagenetic by direct precipitation in the anoxic pore waters in an estuarine and marine environment (see Burley et al. 1985). Transformation of smectitic infiltration clays into chlorite, as the fluids evolve to become more Fe and Mg rich with increased burial (which could be related to elements liberated by smectite to illite transformations) is another possibility, which can explain chlorite in fluvial sandstones.

Variation in the feldspar composition between the northern and the eastern part of the Danish Subbasin (eastern part of the Norwegian-Danish Basin) is indicative of sediment source area differences. The sediment supply to the eastern part may have been dominated by high quartz contents from kaolinised basement for example in southern Sweden (Ahlberg et al. 2003), whereas the northern part may be characterised by a continued more northerly sediment source. Feldspar dissolution preferentially affects the plagioclase grains at shallow burial depth but also the K-feldspar grains at deeper burial depth. Variations in the degree of feldspar alteration within each sandstone sample are common in the Gassum Formation probably reflecting inherited chemical variations, crystallographic weaknesses etc. Secondary porosity, mainly the result of feldspar dissolution, may constitute up to 5 % of the total porosity of 11 % in the deepest buried sandstones from the Aars-1 well. However, in the deepest sandstones the intragranular porosity in feldspar grains is partly filled by authigenic phases (quartz or kaolin), including albite, which grows on the remnants of detrital feldspar (Figs 5.24D & F). This incipient albitisation process, where albite crystals grow along the cleavage planes in the parent K-feldspar grains with high intragranular porosity, occurs at 65-90°C in Jurassic-Lower Cretaceous sediments offshore Norway (Saigal et al. 1988). Whereas albitisation represented by blocky albite crystals and lack of any dissolution porosity in K-feldspar occurs at higher temperatures > 90°C (Saigal et al. 1988). Other investigations also point towards albitisations of both plagioclase and K-feldspar taking place at higher temperatures (120-160°C, Boles and Ramseyer 1988; 120-150°C, Baccar et al. 1993; 100-130°C, Mansurbeg et al. 2008). Different reactivity of feldspar grains to albitization can be caused by variation in amounts of grain surface areas in contact with

pore fluid, degree of fracturing, chemical composition and structural state (Ramseyer et al. 1991). Carbonate probably formed as by-product of albitisation (Morad et al. 1990), which explains why ankerite cement is commonly associated with feldspar.

Kaolin typically precipitates close to altered feldspar grains, and over-size pores filled completely by kaolin probably represent completely altered feldspar grains. Flushing of meteoric water shortly after deposition is responsible for dissolution of feldspar grains and precipitation of kaolin (see Bjørlykke 1998). The fresh water is diluted on most ionic species and therefore causes dissolution of the feldspar grains and other unstable grains, which leads to formation of kaolin. This process is likely to occur in the fluvial, lacustrine and deltaic environment, however not in the marine sediments.

The intensity of quartz diagenesis increases with burial depth, from being characterised by quartz mountains (see Weibel et al. 2010 for a detailed description) in shallow sandstones (for example in the Thisted-3 well, 1180 m; Fig. 5.22C), to large quartz overgrowths (macroquartz) in the deeper buried samples (for example the Farsø-1 well, 2900 m and the Aars-1 well, 3300 m; Figs 5.23 D & E) and follows the typical diagenetic trend of increasing authigenic quartz abundance with burial for marine influenced sandstones (Bjørlykke et al. 1986, Land & Fisher 1987, Ehrenberg 1990, Weibel et al. 2010). Pressure solution of quartz and sutured grain contacts are limited to deeper buried sediments (in the Gassum-1 and Aars-1 wells). Sutured quartz grain contacts (microstylolites) occur in the Jurassic Brent Group at depths greater than 2700 m and temperatures higher than c. 100°C (Harris 1992). Stylolites only occur in the fluvial deposits in the Aars-1 well at large burial depths of 3280 m (Fig. 5.23F). These sediments are characterised by only small amounts of ductile grains and limited amounts of authigenic clay coatings.

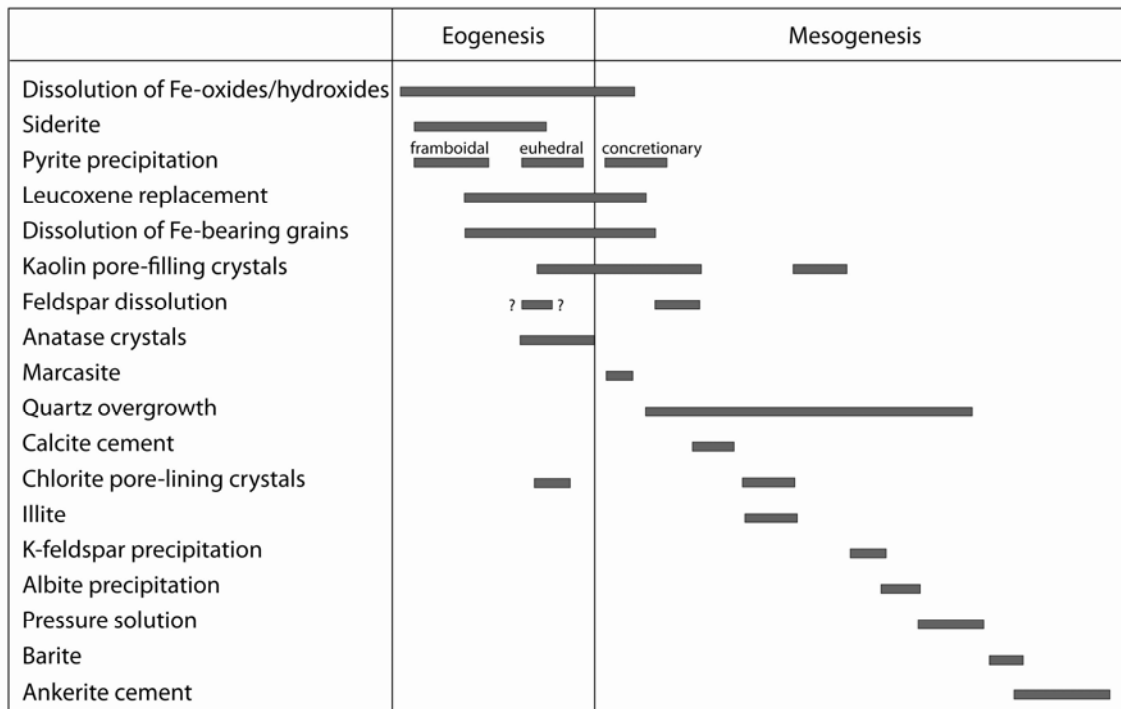|	Eogenesis	Mesogenesis
Dissolution of Fe-oxides/hydroxides		
Siderite		
Pyrite precipitation	framboidal · euhedral	concretionary
Leucoxene replacement		
Dissolution of Fe-bearing grains		
Kaolin pore-filling crystals		
Feldspar dissolution	? · ?	
Anatase crystals		
Marcasite		
Quartz overgrowth		
Calcite cement		
Chlorite pore-lining crystals		
Illite		
K-feldspar precipitation		
Albite precipitation		
Pressure solution		
Barite		
Ankerite cement		

Fig. 5.26. *Diagenetic sequence for the Gassum Formation, modified after Friis (1987).*

5.4 Haldager Sand Formation

The Middle Jurassic fluvial, estuarine and shallow marine sandstones of the Haldager Sand Formation) occur in restricted areas in the northern part of Denmark (Fig. 1; Nielsen 2003). It has thicknesses up to 200 m (Mathiesen et al. 2009) and present day burial depth of 400–2500 m.

Detrital composition

The Haldager Sand Formation is characterized by quartz arenites and subordinate subarkoses (Fig 5.1 & 5.27). Quartz dominates the framework grains. K-feldspar is more common than plagioclase, which is extremely rare in the deepest buried sediments. Sparse rock fragments are of plutonic, metamorphic or sedimentary origin. Organic matter is abundant in some samples and commonly concentrated together with mica. Mica is dominated by muscovite. A characteristic kaolinitised muscovite is found in most samples of the Haldager Sand Formation, but not in the Gassum Formation. Heavy minerals are dominated by a very stable assemblage (zircon, tourmaline, rutile). Occasionally samples have abundant intraclasts and allogenic clays, some of which may be infiltration of drilling mud.

Authigenic phases

The porosity reduction is low in the shallow buried Haldager Sand Formation and mainly due to compaction, as the amount of authigenic phases is very low compared to the other formations (compare Fig. 5.28 with 5.18). Kaolin is the most abundant authigenic phase (Fig. 5.29). Quartz, siderite, pyrite, iron-oxide/hydroxides and anatase are minor but common authigenic phases (Figs 5.30 & 5.31).

Kaolin is strongly related to alteration of K-feldspar, and it forms intragranular in cracks and along cleavages planes, as well as in the adjacent pore spaces (Figs 5.29A, B, C & D). Intense kaolin alteration of muscovite is also common (Figs 5.29E & F). Kaolin precipitates between the cleavage planes of mica thereby expanding its original size. Pore filling kaolin occurs in spotted areas of the deepest samples, but most of the pore space remains open. Kaolin forms after framboidal pyrite (Fig. 5.30C) and prior to quartz overgrowths (Fig. 5.31D).

Framboidal pyrite is the first authigenic phase to form and is occasionally associated with organic matter. Framboidal pyrite commonly occurs with an outer oxidation rim (5.30C). Euhedral pyrite encloses framboidal pyrite and occasionally occurs with internal round dissolution voids (Figs 5.30B &E). Euhedral pyrite commonly forms around altered Fe-Ti oxides (Fig. 5.30F).

Authigenic quartz (quartz mountains) occurs on detrital quartz grains and locally they may merge together to thin quartz overgrowths (Fig. 5.31).

Porosity and permeability

Changes in the reservoir properties with increasing burial depth are mainly the result of mechanical compaction, as only limited amounts of authigenic phases such as siderite, pyrite and calcite occur. Generation of secondary porosity by feldspar dissolution has only minor influence.
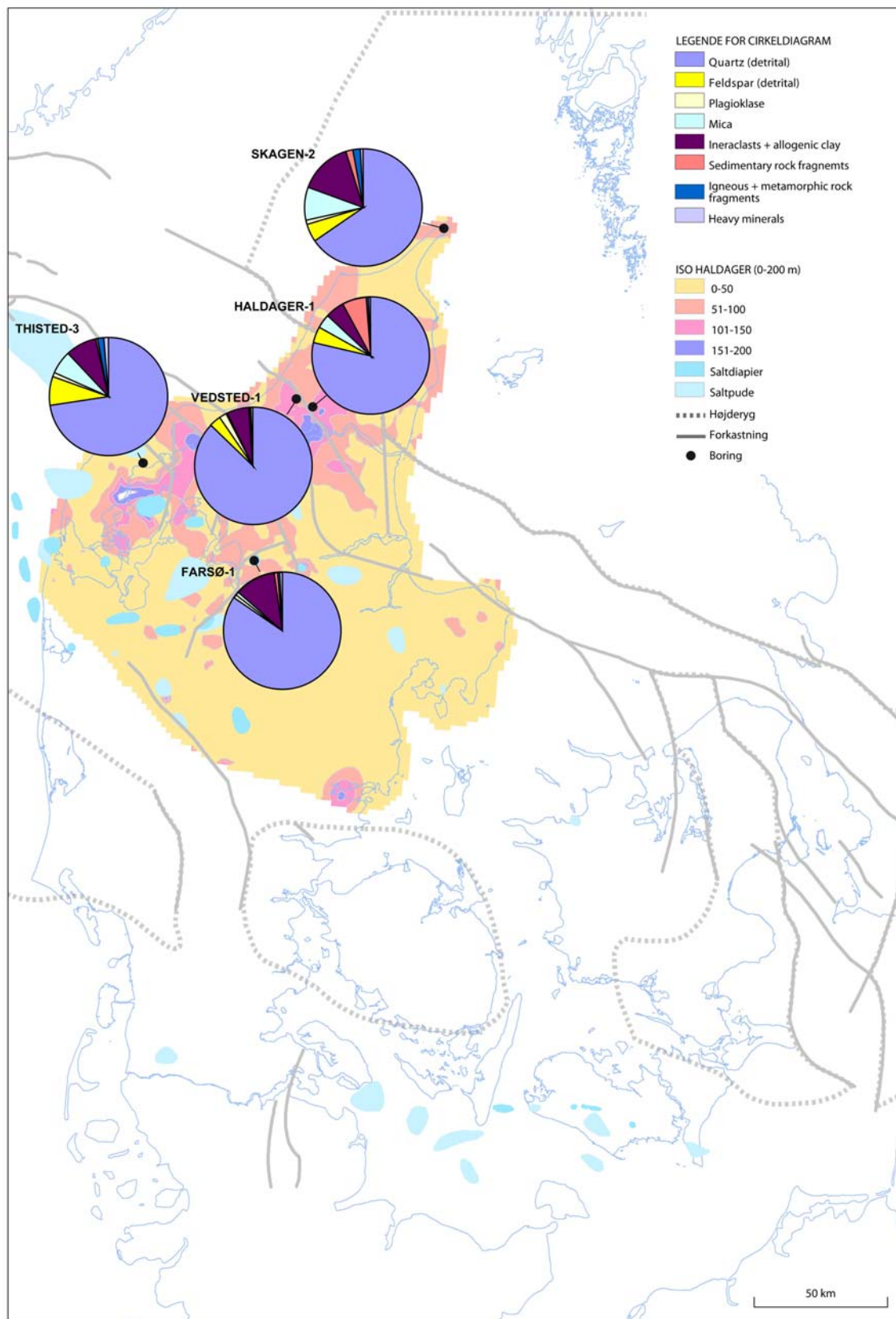
Fig. 5.27. *Average detrital composition of the Haldager Sand Formation shown as pie diagrams for each analysed well on isopach map of the Haldager Sand Formation (modified after Mathiesen et al. 2009).*
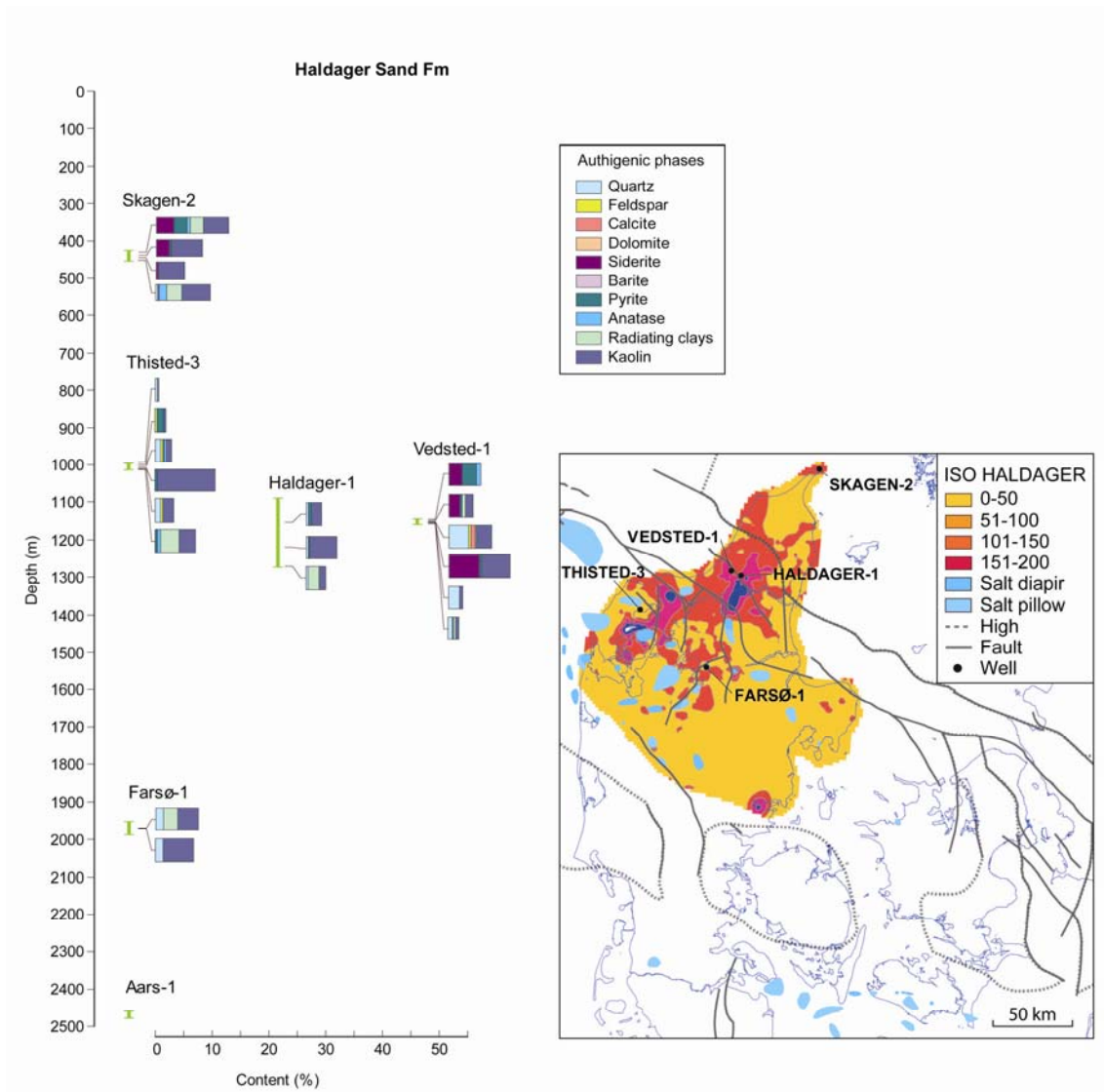
Fig. 5.28. *Authigenic phases, quantified by point counting, in the Haldager Sand Formation for different wells and consequently different burial depths.*
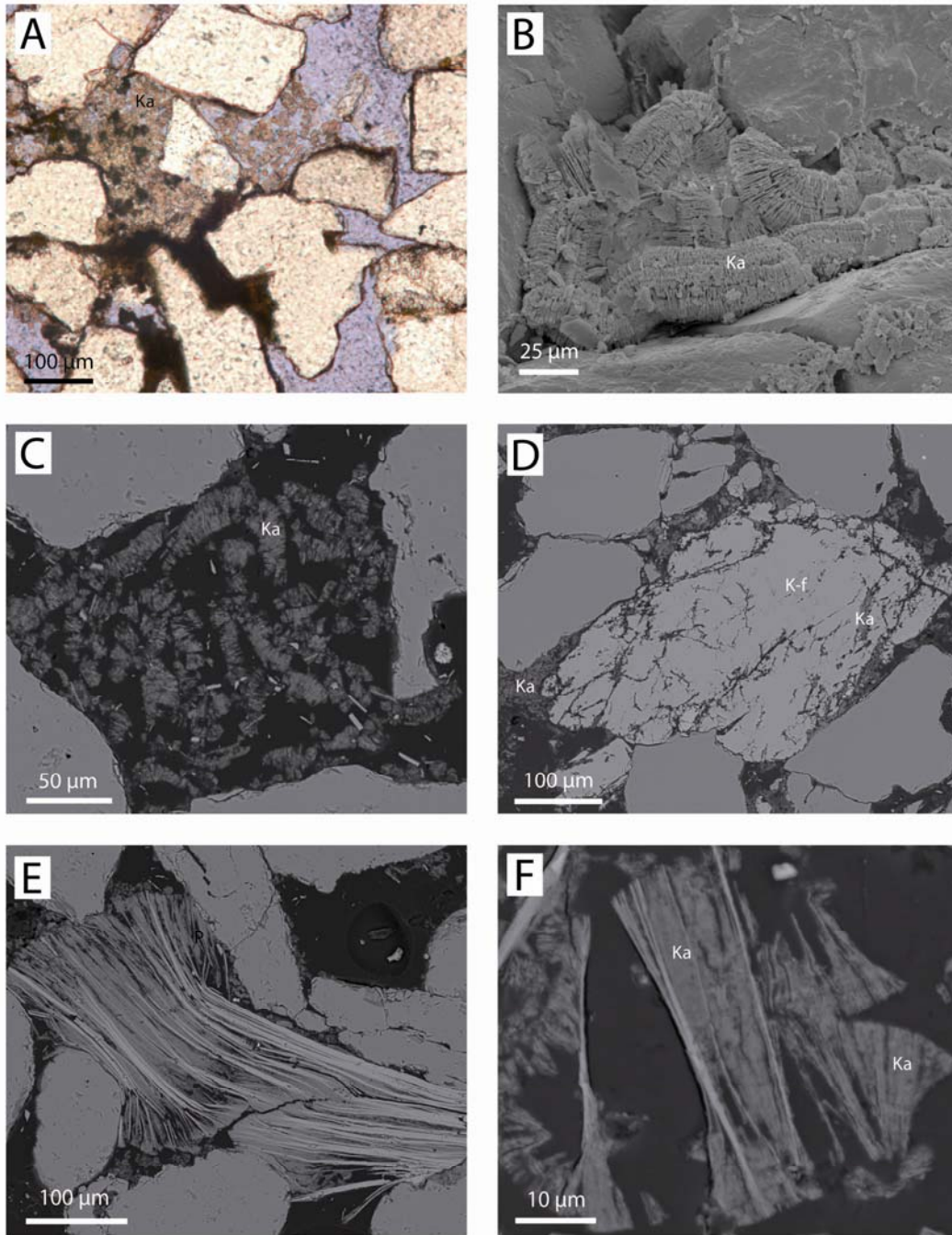
Fig. 5.29. *Kaolin precipitation in the Haldager Sand Formation. A. Local area with pore filling kaolin, Vedsted-1, 1151.35 m. B. Pore filling vermicular kaolin, Vedsted-1, 1155.50 m, scanning electron micrograph. C. Pore filling kaolin in over-size pore, Vedsted-1, 1155.50 m, backscatter electron micrograph. D. Vermicular kaolin growing within cleavage planes of K-feldspar and in the adjacent pore space, Vedsted-1, 1155.44 m, backscatter electron micrograph. E. Kaolin precipitating between the cleavage planes of muscovite and in the adjacent pore space, Vedsted-1, 1155.50 m, backscatter electron micrograph. F. Kaolin precipitating between the cleavage planes of muscovite, Vedsted-1, 1155.50 m, backscatter electron micrograph.*
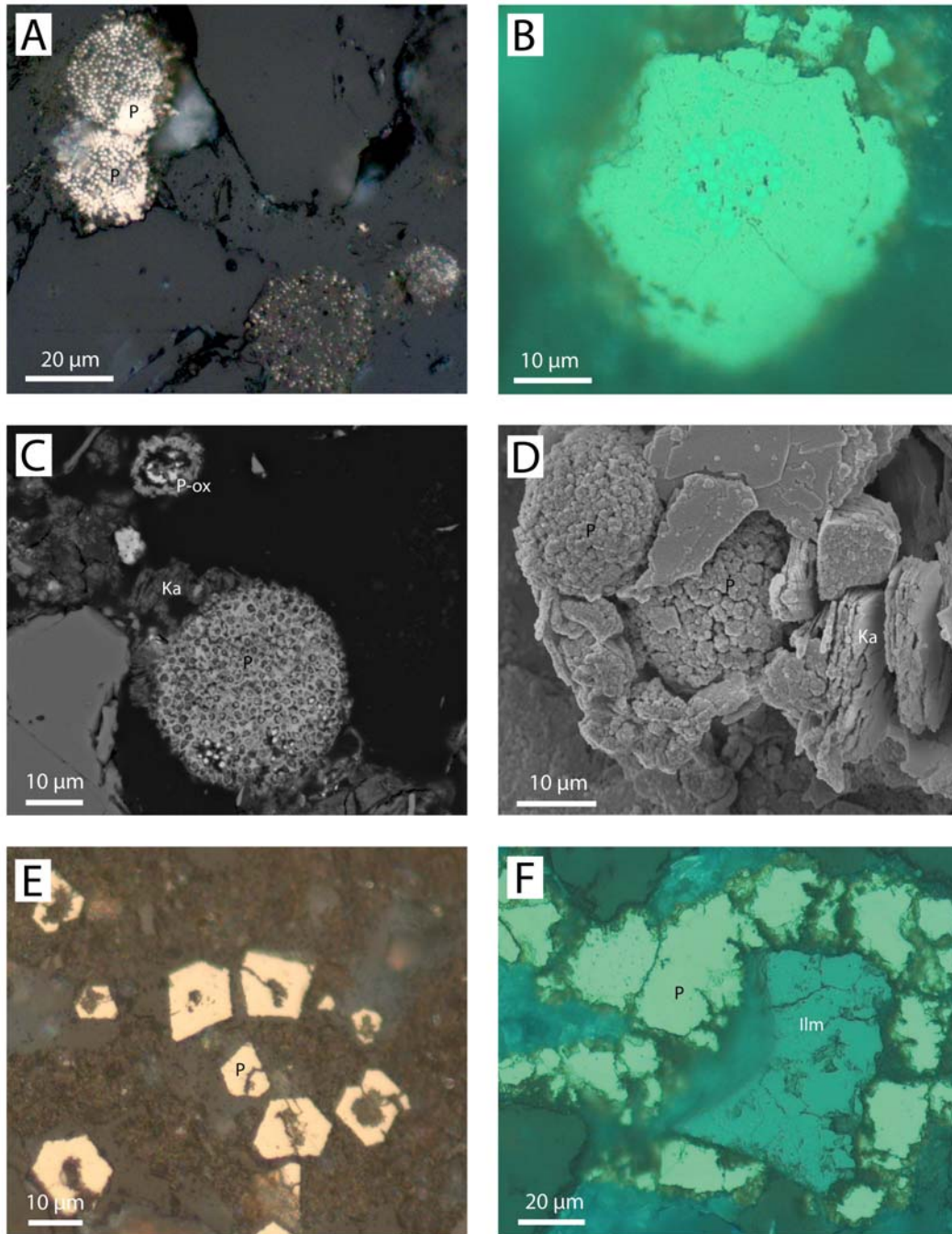
Fig. 5.30. *Pyrite in the Haldager Sand Formation. A. Framboidal pyrite in pore space, Vedsted-1, 1151.12 m, reflected light. B. Framboidal pyrite enclosed in euhedral pyrite, Vedsted-1, 1147.95 m, reflected light. C. Framboidal pyrite with an oxidation rim partly enclosed by kaolin minerals, Vedsted-1, 1155.50 m, backscatter electron micrograph. D. Framboidal pyrite with an outer oxidation rim surrounded by kaolin minerals, Vedsted-1, 1155.50 m, scanning electron micrograph. E. Euhedral pyrite with round internal dissolution voids, possibly after framboidal pyrite, Vedsted-1, 1148.90 m, reflected light. F. Euhedral pyrite formed around leucoxene altered ilmenite grain, Vedsted-1, 1147.95 m, reflected light.*
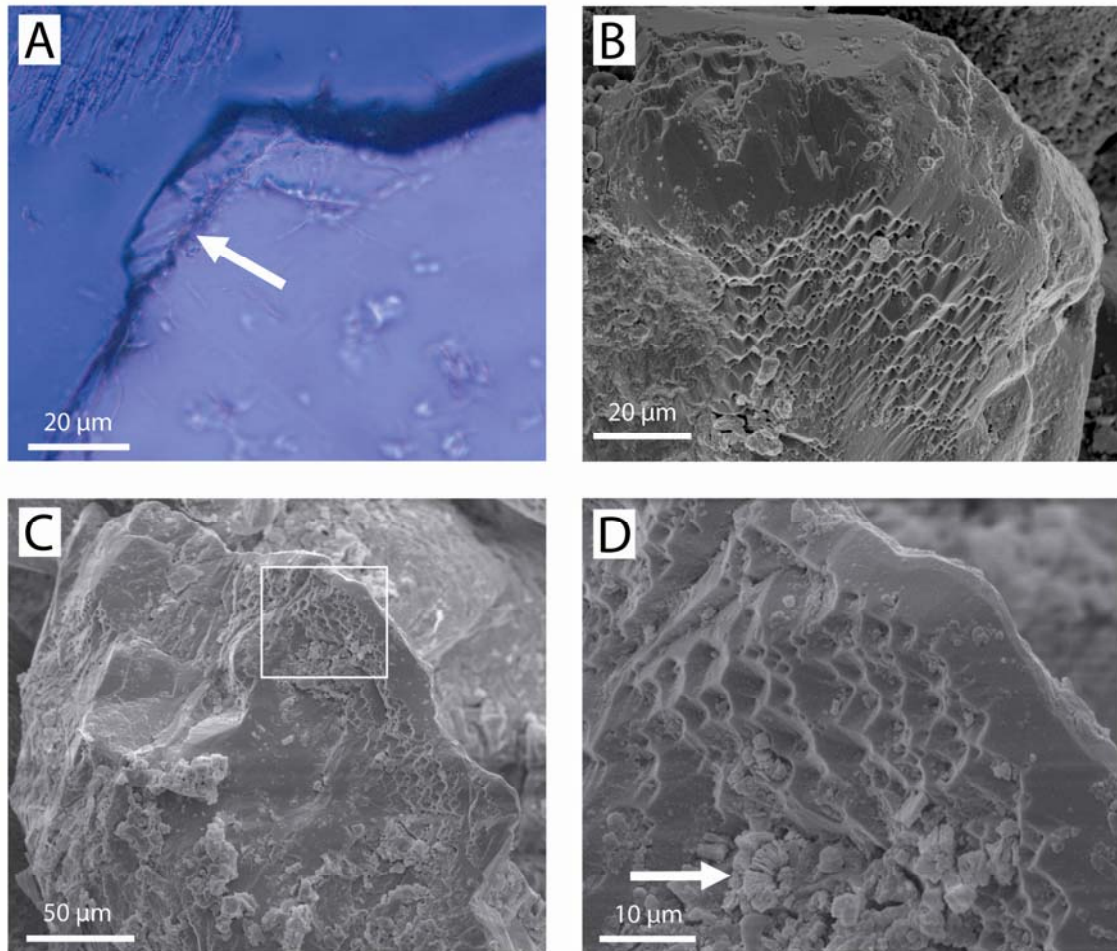
Fig. 5.31. *Quartz diagenesis in the Haldager Sand Formation. A. Small quartz overgrowth, Vedsted-1, 1147.95 m. B. Quartz mountains merging into small overgrowth, Vedsted-1, 1155.50 m, scanning electron micrograph. C. Quartz mountains, Vedsted-1, 1155.47 m, scanning electron micrograph. D. Close up of C. Note that the vermicular kaolin (arrow) seem to have inhibited the authigenic quartz growth, scanning electron micrograph.*

Mineralogical changes with burial depth

An approximately diagentic sequence for the Haldager Sand Formation is presented in Fig. 5.32.

Immediately after deposition begins the first, volumetric insignifican diagenetic changes. Abundant organic matter creates reducing and weakly acid conditions. Pyrite forms due to the activity of sulphate reducing bacteria, and is therefore commonly associated with organic matter. The common oxidation rim on pyrite is likely to have formed in the cores, and consequently not necessarily a diagenentic event related to burial.

Flushing by meteoric water, undersaturated by most ionic species, promotes the dissolution of feldspar and mica and the formation of kaolin minerals (see Bjørlykke 1993). Mica is intensely altered and replaced by kaolin probably due to the mature detrital composition of the sediments.

Other authigenic phases is not identified in the Haldager Sand Formation, though calcite cement has been described as important in the marine deposits (Nielsen and Friis 1984), whereas this investigation has focused on the fluvio-deltaic sediments.

The general shallow burial and the mature detrital composition of the Haldager Sand Formation result in a less significant diagenetic imprint compared to the other reservoir sandstones. The mature detrital composition, with dominance of quartz, few feldspar grains and rock fragments and very stable heavy mineral assemblage, also means that fewer unstable grains could enter into the diagenetic reactions.

	Eogenesis	Mesogenesis
Dissolution of Fe-oxides/hydroxides	▬▬▬▬	
Siderite	▬▬	
Pyrite precipitation	framboidal euhedral	
Leucoxene replacement	▬▬▬	
Kaolin	▬▬▬	
Feldspar dissolution	▬▬	
Anatase crystals	? ▬ ?	
Quartz overgrowts	▬▬	

Fig. 5.32. *Diagenetic sequence for the Haldager Sand Formation.*

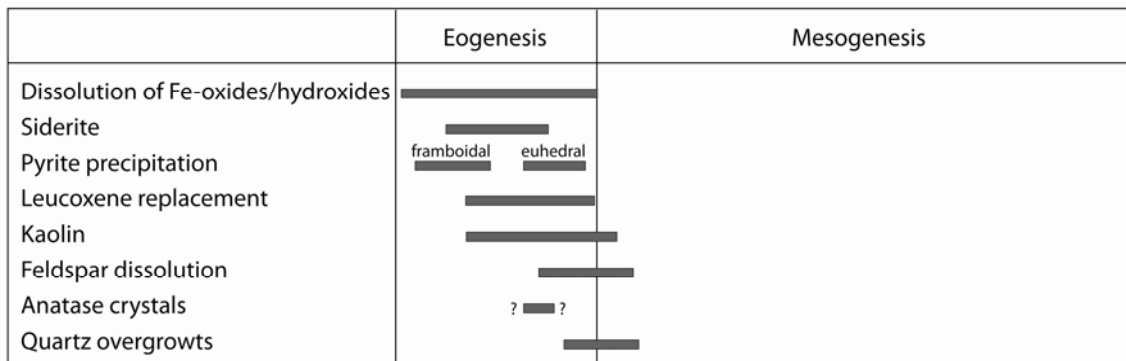# 6. Mineralogical similarities and differences

The detrital mineralogy and the diagenetic alterations of the Bunter Sandstone, Skagerrak, Gassum and Haldager Sand formations are compared in the following. First the small variations between the two arid to semi-arid deposits (Bunter Sandstone and Skagerrak formations) and between the humid deposits (Gassum and Haldager Sand formations) are compared. Finally the variations between the humid and the arid deposits are discussed.

Comparison of the Bunter Sandstone Formation with the Skagerrak Formation

The proximal deposits (Skagerrak Formation) are more immature than the more distal deposition of the Bunter Sandstone Formation resulting in a higher abundance of feldspar, heavy minerals and igneous rock fragments in the Skagerrak Formation than in the Bunter Sandstone Formation. A possible Norwegian volcanic source may have supplied material to the western part of the Norwegian-Danish Basin during deposition of the Skagerrak Formation. K-feldspar is the dominating feldspar in both the Bunter Sandstone and the Skagerrak formations. The aeolian contribution is more dominant in the Bunter Sandstone Formation, which, compared to the alluvial fan deposition of the Skagerrak Formation, has a dessert resembling depositional environment dominated by sabkhas, sandsheets, ephemeral rivers with occasional terminal fans. Wind blown ooids and carbonate clasts can contribute substantially to the detrital composition especially in the aeolian and some fluvial deposits. The location or locations of the sediment sources that supplied the ooids and detrital carbonate clasts are not known, and reworked contemporaneous and Permian carbonate sediments are both possibilities.

The diagenetic sequences of the Bunter Sandstone and Skagerrak formations represent several similar diagenetic events tied to the arid depositional environment. The similarities include mineral reactions related to the eogenesis in an arid to semi-arid climate, such as iron-oxide/hydroxide coatings, hematisation, calcrete, authigenic clay minerals dominated by illite and mixed-layer illite/smectite, carbonates and anhydrite. The differences in the authigenic composition between the Skagerrak and Bunter Sandstone formations are mainly on the amount of authigenic clay minerals, the type of carbonate (calcite in the Bunter Sandstone Formation, dolomite and ankerite in the Skagerrak Formation) and the abundance of authigenic phases related to high saline pore fluids (analcime, anhydrite, halite and copper minerals are common in the Bunter Sandstone Formation, whereas only rare anhydrite has been recognized in the Skagerrak Formation).

The high clay mineral abundance in the Skagerrak Formation is partly related to its deeper burial (higher burial temperatures) in connection with more immature detrital composition (more rock fragments, including volcanic rock fragments, and unstable heavy minerals) compared to the Bunter Sandstone Formation. The morphology of the authigenic quartz varies between the two formations. Prismatic quartz outgrowths are common in the Skagerrak Formation due to the thick clay coatings, whereas macroquartz is more typical in the Bunter Sandstone Formation. Ooids and carbonate clasts dominate the rock fragments in

the Bunter Sandstone Formation, and consequently do not promote clay mineral formation but rather carbonate cement. Carbonate cement is typically calcite in the Bunter Sandstone Formation, probably due to a combination of preferential calcite precipitation in the arid environment and some degree of carbonate pressure solution from the ooids, carbonate clasts and the sparse carbonate fossils.

As the sabkha environment does not exist in the proximal parts (i.e. for the Skagerrak Fm) early gypsum is not as likely to form in the Skagerrak Formation as in the Bunter Sandstone Formation. Sulphate, besides intensive evaporation, is necessary for early gypsum to precipitate and is more abundant in sabkha and inland sea environments than in alluvial fan and braided fluvial environments of the Skagerrak Formation. During burial gypsum is transformed into anhydrite. The pore fluids in the Skagerrak Formation are also likely to have been less saline than the pore fluids in the Bunter Sandstone Formation. The differences in some of the authigenic mineral assemblages may be caused by introduction of highly saline fluids during burial in the Bunter Sandstone Formation that promoted formation of analcime, halite and copper minerals (Weibel & Friis 2004).

Comparison of the Gassum Formation with the Haldager Sand Formation

The detrital mineralogy of the Gassum Formation in the eastern part of the Norwegian-Danish Basin (Stenlille wells) resembles that of the Haldager Sand Formation with dominance by quartz and low abundances of feldspar and rock fragments. Towards west feldspar grains seem to be a more common part of the detrital mineralogy of the Gassum Formation. Mineral difference (different heavy mineral composition and K-feldspar content) could indicate contribution from different sediment sources of the eastern and western parts of the Gassum Formation, where high quartz amounts in the eastern part could be sourced by a kaolinised basement for example in southern Sweden (Ahlberg et al. 2003).

The Gassum and Haldager Sand formations have almost similar diagenetic sequences and mainly differ with the amount of authigenic phases. Dominance of quartz and stable grains in the Haldager Sand Formation means less reactive minerals which can enter the diagenetic reactions and lead to new authigenic minerals. Similar climate and depositional environment results in eogenetic pyrite, siderite and kaolin formation.

Comparison of the hot dry deposits with the vegetated (humid) deposits

The eogenesis reflects the depositional environment to such a degree that the Gassum and Haldager Sand formations have almost similar diagenetic sequences, though the abundance differs. Both formations were deposited in a vegetated warm wet climate in fluvial,

deltaic, estuarine and shallow marine environments. In a similar way, the Skagerrak and Bunter Sandstone formations, deposited in ephemeral fluvial, aeolian, or lacustrine environments in an arid to semi-arid climate, have resembling diagenetic sequences. However, the diagenetic alterations are markedly different between the deposits from arid and humid climates.

The iron-rich minerals formed in the eogenetic regime vary according to the depositional environments, as iron-oxide/hydroxide coatings form in the arid Triassic alluvial fan, ephemeral fluvial, lacustrine and aeolian environment, whereas siderite and pyrite are characteristic for the humid fluvial, parallic and shallow marine deposits. Abundant organic matter in the humid vegetated sediments leads to reducing conditions, whereas the arid to semi-arid conditions typically have oxidising conditions. Oxidised iron precipitates as iron-oxide/hydroxides close to its source (altered iron silicates or Fe-Ti oxides), whereas reduced iron can be transported longer and results in dispersed or concretionary pyrite and siderite formation. Concretionary pyrite and siderite growth can be associated with microbial populations. Sulphate reducing bacteria will promote pyrite formation, but some normal sulphate-reducing bacteria can in a consortium with fermenters reduce Fe^{3+} directly to Fe^{2+} by using hydrogen, formed during fermentation, as the electron donor (Coleman 1993). In this way the microbes may also promote siderite precipitation. Concretions in the arid deposits are gypsum/anhydrite or calcite (calcrete), which probably formed by evaporation of groundwater.

The dominating clay minerals vary between the arid deposits and the humid deposits. Kaolin is the dominating clay mineral in both the Gassum and the Haldager Sand formations, whereas it occurs only in the reduced parts of the Skagerrak and Bunter Sandstone formations. Illite and mixed-layer illite/smectite are the typical clays in the Skagerrak and Bunter Sandstone formations, though the abundance of chlorite seems to increase with burial depth. In sediments rich in rock fragments and heavy minerals (Skagerrak Formation), the pore fluid will easily become enriched by several ions. The dissolution of feldspar grains will therefore not be as intensive as in sediments dominated by quartz and feldspar (arkoses), where the pore fluids will be diluted in respect to most ions and consequently will be very corrosive towards the feldspar grains (Gassum Formation). The dominating clay mineral, associated with feldspar dissolution, is therefore kaolin.

Authigenic albite precipitation and albitisation is generally considered a process occurring at high temperatures (Saigal et al. 1988; Morad et al. 1990; Baccar et al. 1993), though few authors has suggested that albite may precipitate at low temperatures in pore fluids of high sodium concentration (Parcerissa et al. 2010). Albitisation is clearly a temperature dependent (deep burial) process, as even in the Bunter Sandstone Formation it does not occur under influence of highly saline pore fluids with abundant sodium present. Authigenic albite precipitation and albitisation are more pronounced in the Gassum Formation than in the Skagerrak Formation at corresponding burial depth. Consequently, the abundance of plagioclase may also be important, as its skeletal remnants form excellent precipitation sites for albite. Organic matter leads to liberation of CO_2 and formation of carboxylic acid in the pore fluids and thus promotes dissolution of feldspar grains (Surdam et al. 1984). Therefore

a more intensive dissolution of feldspar grains occurs in the Gassum Formation compared to the Bunter Sandstone and Skagerrak formations.

Prismatic quartz overgrowths occur in the Skagerrak Formation (and the Bunter Sandstone Formation) whereas authigenic quartz occurs with the morphology named 'quartz mountains' by Weibel et al. (2010) in shallow samples of the Haldager Sand and Gassum formations. The pore lining clay coatings on all detrital grains in the Skagerrak and Bunter Sandstone formations inhibit authigenic quartz growth, which therefore becomes prismatic or wider but with few contact points. The pore filling kaolin in the Gassum and Haldager Sand formations has less influence on the growth of authigenic quartz on the detrital quartz grains. Authigenic quartz therefore begins on most detrital quartz grains, though only forming limited thin quartz overgrowths (as quartz mountains), which eventually during deeper burial evolve into full macroquartz overgrowths (see Weibel et al. 2010).

Abundance authigenic quartz is controlled by several factors:
- Burial depth.
- Thickness and continuity of the pore lining chlorite, which may inhibit authigenic quartz formation.
- Stylolite formation and pressure solution, which sources silica for authigenic quartz formation. Pressure solution will only occur in samples with few ductile grains and only thin clay coatings on the detrital quartz grains. Stylolite formation seems to be associated with detrital mica.
- Silica sources. Dissolution of feldspar liberating silica for authigenic quartz formation. Feldspar occurs with highest abundance in fluvial sediments.
- Monocrystalline or polycrystalline detrital quartz grains' relative abundance, as the crystal size of authigenic quartz is related to the 'type' of detrital quartz grains, as larger overgrowths tend to form on monocrystalline quartz grains contrary to polycrystalline quartz grains (Lander et al. 2008). On the other hand pressure solution is much more common in coarse-grained sandstones with limited amounts of ductile detrital grains and detrital and authigenic clays.

7. Conclusion

The sandstone formations selected diagenetic investigations comprise the Bunter Sandstone Formation, Skagerrak Formation, Gassum Formation and Haldager Sand Formation. The mineralogical composition and the diagenetic influence play a major role in the evaluation of the optimum reservoir therefore detailed petrographical investigations have been performed on the formations of interest.

The Fennoscandian Shield constitutes the major sediment source area for the sediments in the eastern part of the Norwegian-Danish Basin. Different climate, depositional environments, transport distances and alterations lead to differences in the detrital composition. The proximal Skagerrak Formation, which was deposited in the alluvial fans and braided streams, has the highest content of unstable minerals, such as heavy minerals, rock fragments and feldspar grains. The Bunter Sandstone Formation is deposited farther away from the sediments source, though under similar climatic conditions, and has a somewhat lower content of heavy minerals and rock fragments, but still a fairly high proportion of feldspar grains. Only minor alteration of feldspar grains occurred in the arid climate. Windblown ooids and carbonate clasts play an important role in parts of the distale Bunter Sandstone Formation. The Gassum and Haldager Sand formations were deposited in fluvial, parallic and shallow marine environments under a humid, wet climate. Under these conditions detrital mineral alteration probably took place in the hinterland as well as in situ the sediment. The Gassum and the Haldager Sand formations therefore contain more stable minerals than the Bunter Sandstone and the Skagerrak formations.

During burial the porosity is reduced due to mechanical compaction and precipitation of authigenic minerals. Dissolution of unstable minerals (formation of secondary porosity) may counteract some of the porosity reduction. The porosity reduction in the Skagerrak Formation is mainly due to carbonate cement and clay minerals. The deep burial of the Skagerrak Formation in combination with a high proportion of unstable minerals have lead to abundant clay precipitation. Carbonate and clay minerals are also, together with anhydrite important porosity reducing minerals in the Bunter Sandstone Formation. The porosity changes in the Gassum Formation are influenced by carbonate cement, precipitation of clay minerals, quartz diagenesis and feldspar dissolution. Porosity gain from feldspar dissolution is partly destroyed by authigenic phases growing into the secondary porosity. Quartz diagenesis becomes more intensive with burial, as pressure solution of detrital quartz leads to abundant precipitation of authigenic quartz. The porosity reduction of the Haldager Sand Formation is due to its shallow burial mainly related to mechanical compaction. Precipitation of clay minerals (kaolin) played an insignificant role in the porosity reduction. The Haldager Sand Formation can approximately be considered as a shallow equivalent to the Gassum Formation.

8. Acknowledgement

9. References

Ahlberg, A., Olsson, I., Simkevicius, P. 2003. Triassic-Jurassic weathering and clay minerals dispersal in basement areas and sedimentary basins of southern Sweden. Sedimentary Geology 161, 15-29.

Anthonsen, K. L. and Nielsen, L. H. 2008: COC-02 Assessment of the potential for CO_2 storage in the Norwegian-Danish Basin, International Geological Conference, Olso, 2008 (Abstract).

Audigane, P., Gaus, I., Czernichowski-Lauriol, I., Pruess, K. & Xu, T. 2007: Two-dimensional reactive transport modelling of CO_2 injection in a saline aquifer at the Sleipner site, North Sea. American Journal of Science **307**, 974–1008.

Baccar, M.B., Fritz, B. & Madé, B., 1993. Diagenetic albitization of K-feldspar and plagioclase in sandstone reservoirs: thermodynamic and kinetic modelling. Journal of Sedimentary Petrology 63, 6, 1100-1109.

Bailey, A. M., Roberts, H. H. & Blackson, J. H. 1998. Early diagenetic minerals and varables influencing their distribution in two long cores (> 40 m), Mississippi River delta plain. Journal of Sedimentary Research 68, 185-197.

Baines, S. J. and Worden, R. H. 2004. The long-term fate of CO_2 in the subsurface: natural analogues for CO_2 storage. In: Baines, S. J. and Worden, R. H. (eds.), Geological storage of carbon dioxide. Geological Society of London, Special Publication 233, 59-85.

Bertelsen, F. 1978: The Upper Triassic–Lower Jurassic Vinding and Gassum Formations of the Norwegian-Danish Basin. Geological Survey of Denmark **B 3**, 25pp.

Bertelsen, F. 1980: Lithostratigraphy and depositional history of the Danish Triassic. Geological Survey of Denmark **B 4**, 59 pp.

Binot, F. Röhling, H. G. 1988: Lithostratigraphie und natürliche Gammastrahlung des Mittleren Buntsandsteins von Helgoland – Ein Vergleich mit der Nordseebohrung J/18-1. Zeitschrift der Deutschen Geologischen Gesellschaft 139, 33-49.

Bjørlykke, K., Aagaard, P., Dypvik, H., Hastings, D.S., Harper, A.S., 1986. Diagenesis and reservoir properties of Jurassic sandstones from the Haltenbanken area, offshore mid-Norway. In: Spencer, A.M., Holter, E., Campell, C.J., Hanslien, S.H., Nelson, P.H.H., Nysaether, E., Ormaasen, E.G. (Eds.), Habitat of Hydrocarbons on the Norwegian Continental Shelf. Graham and Trotman, London, pp. 275– 286.

Bjørlykke, K., 1998, Clay mineral diagenesis in sedimentary basins; a key to the prediction of rock properties, examples from the North Sea Basin. Clay Minerals 33, 15-34.

Boles, J. R. and Ramseyer, K. 1988: Albitization of plagioclase and vitrinite reflectance as paleothermal indicators, Sand Joaquin Basin. SEPM Pacific Section, 219-139.

Bridges, E. M. 1997: World soils, 3rd edition, University Press, Cambridge, United Kingdom, 170p.

Britze, P. & Japsen, P. 1991. Geological map of Denmark 1: 400,000. The Danish Basin. "Top Zechstein" of the Triassic (two-way traveltime and depth, thickness and interval velocity). Geological Survey of Denmark Map Series 31. 4 maps and 4 pp.

Burley, S. 1984: Patterns of diagenesis in the Sherwood Sandstone Group (Triassic), United Kingdom. Clay Minerals 19, 403-440.

Burley, S., Kantorowicz, J. D. and Waugh, B. (1985). "Clastic diagenesis." Journal of Sedimentary Petrology 49, 53-70.

Choi, K. S., Khim, B. K. & Woo, K. S. 2003: Spherulitic siderites in the Holocene coastal deposits of Korea (eastern Yellow Sea). Elemental and isotopic composition and depositional environment. Marine Geology 202, 17-31.

Clausen, O. R. & Pedersen, P. K. 1999: Late Triassic structural evolution of the southern margin of the Ringkøbing-Fyn High, Denmark. Marine and Petroleum Geology 16, 653-665.

Clemmensen, L. B. 1979. Triassic lacustrine red-beds and palaeoclimate: The "Buntsandstein" of Helgoland, Geologische Rundschau 74, 519-536.

Clemmensen, L.B., 1985. Desert sand plain and sabkha de- posits from the Bunter Sandstone Formation (L. Triassic) at the northern margin of the German Basin. Geologische Rundshau 74, 519-536.

Coleman, M. L. and Raiswell., R. 1981: "Carbon, oxygen and sulphur isotope variations in concretions from the Upper Lias of N. E. England." Geochimical et Cosmochimical Acta 45, 329-340.

Coleman, M. L. 1993: Microbial processes: Controls on the shape and composition of carbonate concretions. Marine Geology 113, 127-140.

Chadwick, A., Arts, R., Bernstone, C., May, F., Thibeau, S. & Zweigel, P. 2009: Best practice for the storage of CO_2 in saline aquifers. British Geological Survey Occasional Publication **14**, 267p.

Clausen, O. R. and Pedersen, P. K. 1999: Late Triassic structural evolution of the southern margin of the Ringkøbing-Fyn High, Denmark. Marine and Petroleum Geology **16**, 653-665.

Ehrenberg, S.N., 1990. Relationship between diagenesis and reservoir quality in sandstones of the Garn Formation, Haltenbanken, mid-Norwegian continental shelf. AAPG Bull. 74, 1538– 1558

Ehrenberg, S. N. 1993. Preservation of anomalously high porosity in deeply buried sandstones by grain-coating chlorite; examples from the Norwegian continental shelf. AAPG Bulletin 77, 1260-1286.

Fine, S. 1986: The diagenesis of the Lower Triassic Bunter Sandstone Formation, Onshore Denmark: Geological Survey of Denmark, A 15.

Friis, H. 1987: Diagenesis of the Gassum Formation Rhaetian-Lower Jurassic, Danish Subbasin. Geological Survey of Denmark **A 18**, 41pp.

Gaus, I., Azaroual, M. & Czernichowski-Lauriol, I. 2002: Preliminary modelling of the geochemical impact of CO_2 injection on the caprock at Sleipner. Confidential report, BRGM/RP-52081, 44pp.

Harris, N. B. 1992. Burial diagenesis of the Brent sandstones: a study of the Statfjord, Hutton and Lyell fields. In Moron, A. C., Haszeldine, R. S., Giles, M. R., Brown, S. Geology of the Brent Group. Special Publications of the Geological Society of London 61, 351-375.

Hendry, J. P., Wilkinson, M., Fallick, A. E. and Haszeldine, R. S. 2000: Ankerite cementation in deeply buried Jurassic sandstone reservoirs of the Central North Sea. Journal of Sedimentary Research 70, 227–239.

Japsen, P., Green, P. F., Nielsen, L. H., Rasmussen, E. S. and Bidstrup, T. (2007): Mesozoic–Cenozoic exhumation events in the eastern North Sea Basin. A multidisciplinary study based on palaeothermal, palaeoburial, stratigraphic and seismic data. Basin Research 19, 451–490.

Kastner, M. and Siever., R. 1979: "Low temperature feldspars in sedimentary rocks." American Journal of Science 279, 435-479.

Krabbe, H. & Nielsen, S. 1984: Rapport om bulk- og lermineralogien i de danske landboringer Års-1 og Farsø-1. Geologisk Institut, Aarhus Universitet, 66pp.

Land, L.S., Fisher, R.S., 1987. Wilcox sandstone diagenesis, Texas Gulf coast: a regional isotopic comparison with the Frio Formation. In: Marshall, J.D. (Ed.), Diagenesis of Sedimentary Sequences. Spec. Publ.-Geol. Soc. London, vol. 36, pp. 219–235.

Lander, R.H., Larese, R.E. and Bonell, L.M., 2008. Toward more accurate quartz cement models: The importance of euhedral versus noneuhedral growth rates. AAPG Bulletin, 92: 1537-1563

Larsen, F. 1986: En sedimentologisk og diagenetisk undersøgelse af Gassum Formationen – II. Kvartscementering af sandsten i Gassum Formationen. Upubliceret Speciale ved Københavns Universitet, 100pp.

Liboriussen, J., AAshton, P. & Thygesen, T. 1987: The tectonic evolution of the Fennoscandian Border Zone in Denmark. In: Ziegler, P. A. (ed.), Compressional intraplate deformations in the Alpine Foreland. Tectonophysics 137, 21-29.

Nielsen, L. H. 1995: Genetic stratigraphy of Upper Triassic- Middle Jurassic deposits of the Danish Basin and Fennoscandian Border Zone 1, 2, 3, 162pp. Unpublished PhD, University of Copenhagen, Denmark.

Nielsen, L. H. 2003: Late Triassic-Jurassic development of the Danish Basin and the Fennoscandian Border Zone, southern Scandinavia. In: Ineson, J. R., Surlyk, F. (Eds.), The Jurassic of Denmark and Greenland. Geological Survey of Denmark and Greenland Bulletin, pp. 459-526.

Nielsen, B. L. & Friis, H. 1985: Diagenesis of Middle Jurassic Haldager Sand Formation sandstone in the Danish Subbasin, north Jutland. Bulletin of Geological Society of Denmark 33, 273-285.

Machemer, S. D. & Hutcheon, I. E.. 1988. Geochemistry of early carbonate cements in the Cardium Formation, Central Alberta. Journal of Sedimentary Petrology **58**, 136-147.

Marcussen, Ø., Maast, T. E., Mondol, N. H., Jahren, J, Bjørlykke, K. 2010: Changes in physical properties of a reservoir sandstone as a function of burial depth – The Etive Formation, northern North Sea. Marine and Petroleum Geology 27, 1725-1735.

Mansurbeg, H., Morad, S., Salem, A., Marfil, R., El-ghali, M.A.K., Nystuen, J.P., Caja, M.A. Amorosi, A., Garcia, D. & La Iglesia, A., 2008. Diagenesis and reservoir quality evolution of palaeocene deep-water, marine sandstones, the Shetland-Faroes Basin, British continental shelf. Marine and Petroleum Geology 25, 514-543.

Mathiesen, A., Kristensen, L., Bidstrup, T. & Nielsen, L. H. 2009: Vurdering af det geotermiske potentiale i Danmark. Danmark og Grønlands geolgosiek undersøgelse Rapport **2009/59**, 30p.

McBride, E. F. 1963: A classification of common sandstones. Journal of Sedimentary Petrology **33**, 664-669.

Michelsen, O. & Nielsen, L. H., 1991: Well records on the Phanerozoic stratigraphy in the Fennoscandian Border Zone, Denmark. Hans-1, Sæby-1, and Terne-1 wells. Geological Survey of Denmark **A 29**, 39 pp.

Michelsen, O. & Nielsen, L. H., 1993: Structural development of the Fennoscandian Border Zone, offshore Denmark. Marine and Petroleum Geology 10, 124-134.

Michelsen, O., Nielsen, L.H., Johannessen, P., Andsbjerg, J. & Surlyk 2003: Jurassic lithostratigraphy and stratigraphic development onshore and offshore Denmark. In: Ineson, J. R. & Surlyk, F. (eds): The Jurassic of Denmark and Greenland. Geological Survey of Denmark and Greenland Bulletin 1, 147–216.

Michelsen, O. & Clausen, O. R. 2002: Detailed stratigraphic subdivision and regional correlation of the southern Danish Triassic succession. Marine and Petroleum Geology 19, 563-587.

Morad, S., Bergen, M., Knarud, R., Nystuen, J.P., 1990. Albitization of detrital plagioclase in Triassic reservoir sandstones from the Snorre field, Norwegian North Sea. Journal of Sedimentary Petrology 60, 411-425

Nielsen, L. H. & Japsen, P., 1991: Deep wells in Denmark 1935-1990. Lithostratigraphic subdivision. Geological Survey of Denmark **A 31**, 179 pp.

Olsen, H. 1987: Ancient ephemeral stream deposits: a local terminal fan model from the Bunter Sandstone Formation (L. Triassic) in the Tønder-3, -4 and -5 wells, Denmark. In: Frostick, L., Reid, I. (Eds.), Desert Sediments: Ancient and Modern. Geological Society of London Special Publication, 35, 69-86.

Parcerisa, D., Thiry, M. & Schmitt, J. M. 2010: Albitisation related to the Triassic unconformity in igneous rocks of the Morvan Massif (France). International Journal of Earth Science 99, 527-549.

Pearce, J. M, Holloway, S. Wacker, H., Nelis, M. K., Rochelle, C. and Bateman, K. 1996. Natural occurrences as analogues for the geological disposal of carbon dioxide. Energy Conversion and Management 37, 1123-1128.

Pearce, J. M., Kemp, S. J. & Wetton, P. D. 1999: Mineralogical and petrographical characterisation of a 1 m core from the Utsira Formation, Central North Sea. British Geological Survey Technical Report, Mineralogy & Petrography Series, 17pp.

Priisholm, S. 1983: Gethermal reservoir rocks in Denmark. Geological Survey of Denmark and Greenland, Årbog 1982, 73-86.

Ramseyer, K., Boles, J. R., Lichtner, P. C. 1992: Mechanism of plagioclase albitization. Journal of Sedimentary Petrology 62, 349-356.

Rossi, C., Nielsen, B. L., Ramseyer, K. & Permanyer, A. 2001: Faceis-related diagenesis and multiphase siderite sementation an ddissolution in the reservoir sandstones of the Khatatba Formationm Egypt's Western Desert. Journal of Sedimentary Research 71, 459-472.

Saigal, G. C., Morad, S., Bjørlykke, K., Egeberg, P. K., Aagaard, P. 1988: Diagenetic albitization of detrital K-feldspar in Jurassic-Lower Cretaceous, and Tertiary clastic reservoir rocks from offshore Norway, I. Textures and origin. Journal of Sedimentary Petroloty 58, 1003-1013.

Schmid, V. and MacDonald, D. A. 1979: The role of secondary porosity in the course of sandstone diagenesis. In Scholle, A. P. & Schuldger, P. R. (eds.), Aspects of diagenesis. Soc. Econ. Paleont. Miner Spec. Publication 29, 175-207.

Spötl, C. and Pitman, J. K. (2009) Saddle (Baroque) Dolomite in Carbonates and Sandstones: A Reappraisal of a Burial-Diagenetic Concept. In: Morad, S. (ed.) Carbonate Cementation in Sandstones: Distribution Patterns and Geochemical Evolution, Blackwell Publishing Ltd., Oxford, UK.

Storvold, V., Bjørlykke, K., Karlsen, D., Saigal, G. 2002: Porosity preservation in reservoir sandstones due to grain-coating illite: a study of the Jurassic Garn Formation from the Kristin and Lavrans fields, offshore Mid-Norway. Marine and Petroleum Geology 19, 767-781.

Surdam, R. C., Boese, S.W. & Crossey, L.J. 1984: The chemistry of secondary porosity. In: McDonald, D.A. & Surdam, R.C. (Eds), Clastics Diagenesis, American Association of Petroleum Geologists Memoir **37,** 127–149.

Thyne, G. D. & Gwinn, C. J. 1994. Evidence for a paleoaquifer from early diagentic siderite of the Cardium Formation, Alberta, Canada. Journal of Sedimentary Research 64, 726-732.

Vejbæk, O. 1989: Effects of asthenospheric heat flow in basin modelling exemplified with the Danish Basin. Earth and Planetary Science Letters 95, 97-114.

Waugh, B. 1978: "Authigenic K-feldspar in British Permo-Triassic sandstones." Journal of Geological Society London 135, 51-56.

Weibel, R. 1998: Diagenesis in oxidising and locally reducing conditions – an example from the Triassic Skagerrak Formation, Denmark. Sedimentary Geology **121**, 259–276.

Weibel, R. 1999: Effects of burial on the clay assemblages in the Triassic Skagerrak Formation, Denmark. Clay Minerals **34**, 619–635.

Weibel, R. & Groberty, B. 1999: Pseudomorphous transformation of geothite needles into hematite in sediments of the Triassic Skagerrak Formation, Denmark. Clay Minerals **34**, 657–661.

Weibel, R. & Friis, H. 2004: Opaque minerals as keys for distinguishing oxidising and reducing diagenetic conditions in the Lower Triassic Bunter Sandstone, North German Basin. Sedimentary Gelogy **169**, 129–149.

Weibel, & Friis, H. 2007: Alteration of opaque heavy minerals as reflection of geochemical conditions in depositional and diagenetic environments. In: Mange, M. A. and Wright, D. T. (eds.) Heavy minerals in use. Developments in Sedimentology, Elsevier **58**, 305–333.

Wilkinson, M., Haszeldine, R. S., Fallick, A. E., Odling, N., Stoker, S. J., Gatliff, R. W. 2007. CO_2-mineral reaction in a natural analogue for CO_2 storage – implications for modeling. Journal of Sedimentary Research 79, 486-494.

Wright, V. P. 1990: Soil micromorphology: A basic and applied science. Developments in Soil Scien 19, Elsevier, Amsterdam, 401-407.

Appendix 1. Bulk rock XRD analyses

Bulk mineralogy of the investigated reservoir rocks.

Formation	Sample	Lab*	Quartz	K-feldspar	Plagioclase	Ankerite	Dolomite	Calcite	Siderite	Barite	Anhydrite	Analcime	Pyrite	Hematite	Clay minerals	Kaolinite	Chlorite	Illite
			%	%	%	%	%	%	%	%	%	%	%	%	%	%	%	%
Bunter Sandstone	TØ4-Bu166321	KU	48.3	11.6	21.5			4.7			5.0	4.6					2.1	2.1
	TØ4-Bu166331	KU	49.9	10.7	19.7			5.9				5.6					2.8	5.5
	TØ4-Bu166313	AU	54.3	13.4	20.5	1.8		5.3						1.9	2.8			
Skagerrak	VE1-Sk206487	KU	81.2	0.7	10.3	6.6										1.2		
	VE1-Sk206494	KU	73.2	2.2	13.7	7.1										3.8		
	VE1-Sk 206501	AU	66.6	4.1	14.9	7.0									7.4			
Gassum	ST18-Ga166240	KU	96.2	1.7	0.4			1.3					0.1			0.3		
	ST18-Ga166240	KU	96.2	1.2				1.3								1.3		
	ST18-Ga166245	AU	93.2	1.5	2.0	0.0		1.1	0.0	0.5			0.6	0.0	1.1			
	ST18-Ga166233	AU	89.0	2.7	1.4	0.0		1.9	1.7	0.6			0.8	0.0	2.0			
	ST18-Ga166264	AU	84.8	2.4	0.6	0.5		1.3	2.2	0.0			0.4	0.0	7.8			
	ST18-Ga167211	AU	85.5	1.4	3.8	0.0		1.3	6.5	0.0			0.6	0.0	1.0			
	ST18-Ga167245	AU	88.5	2.3	5.1	0.0		0.9	0.0	0.9			0.4	0.0	1.9			
	ST18-Ga167439	AU	78.3	7.9	1.9	0.6		1.4	4.1	0.0			0.3	0.0	5.5			
	ST18-Ga167811	AU	88.9	3.3	5.6	0.5		0.8	0.0	0.0			0.0	0.0	1.0			
	VE1-Ga201006	KU	80.3	4.1	10.4			0.1								3.9		1.2
	VE1-Ga201009	KU	81.6	4.8	9.2			0.8								3.8		
	VE1-Ga201010	AU	74.9	3.7	10.9	1.9			6.3						2.4			
	VE1-Ga201016	AU	76.6	6.0	3.3	0.8		0.0	5.2	0.0			2.0	0.0	6.0			
	VE1-Ga177566	AU	84.4	5.3	2.1	4.9		1.0	0.5	0.0			0.6	0.0	1.1			
	VE1-Ga200777	AU	56.7	6.6	7.7	0.0		0.6	7.8	0.0			0.0	0.0	20.6			
	VE1-Ga201010	AU	74.9	3.7	10.9	1.9		0.0	6.3	0.0			0.0	0.0	2.4			

Formation	Sample	Lab*	Quartz	K-feldspar	Plagioclase	Ankerite	Dolomite	Calcite	Siderite	Barite	Anhydrite	Analcime	Pyrite	Hematite	Clay minerals	Kaolinite	Chlorite	Illite
			%	%	%	%	%	%	%	%	%	%	%	%	%	%	%	%
Haldager Sand	VE1-Ha115083	KU	93.9	4.2												2.0		
	VE1-Ha115544	KU	91.9	5.8												2.3		
	VE1-Ha115550	AU	83.2	12.3	0.0	0.6		0.0	1.4	0.0			0.0	0.0	2.5			
	VE1-Ha115162	AU	87.4	8.3	0.0	1.2		0.0	1.8	0.0			0.0	0.0	1.3			
	FA1-Ha196816	AU	88.9	0.0	0.0	0.1		0.0	0.0	0.0			0.0	0.0	11.0			
	FA1-Ha196863	AU	91.1	0.0	0.0	0.0		0.0	0.0	0.0			0.0	0.0	8.9			
	FA1-Ha196660	AU	94.4	0.0	0.0	0.0		0.5	0.0	0.0			0.0	0.0	4.9			
	HA1-Ha122056	AU	76.5	0.0	1.8	0.0		0.4	0.0	0.0			0.0	0.0	21.3			
	HA1-Ha115450	AU	84.9	6.1	0.0	1.1		0.4	1.6	0.0			0.0	0.0	4.3			

* Two different methods of quantifying the XRD results have been attempted. Samples analysed at University of Aarhus (AU) has been semi-quantified by application of corrections factors determined for the applied X-ray diffractometer. Samples analysed at University of Copenhagen (KU) has been quantified by use of Rietveld refinement. The quantification method using corrections numbers it a relatively fast semi-quantitative method, but has its drawback when large amounts of poorly crystalline phases are present.

G E U S

Appendix 2. Microprobe analyses

Feldspar composition measured by microprobe.